ANA PAULA GOMES

OPTIMIZED REGULARIZATION OF INTERVAL S-WAVE VELOCITY ESTIMATION FROM SEISMIC SURFACE WAVE DATA

Undergraduate Project presented to the Polytechnic School of the University of São Paulo

SÃO PAULO

2019

ANA PAULA GOMES

OPTIMIZED REGULARIZATION OF INTERVAL S-WAVE VELOCITY ESTIMATION FROM SEISMIC SURFACE WAVE DATA

Undergraduate Project presented to the Polytechnic School of the University of São Paulo

Field of study: Geophysics

Supervisor: Prof. Dr. Cleyton de Carvalho Carneiro

Advisor: Prof. Dr. Laura Valentina Socco

SÃO PAULO

2019

Catalogação-na-publicação

GOMES, ANA PAULA
OPTIMIZED REGULARIZATION OF INTERVAL S-WAVE VELOCITY ESTIMATION FROM SEISMIC SURFACE WAVE DATA / A. P. GOMES -- São Paulo, 2019.
82 p.

Trabalho de Formatura - Escola Politécnica da Universidade de São Paulo. Departamento de Engenharia de Minas e Petróleo.

1.Geofísica 2.Ondas de Superfície 3.Regularização I.Universidade de São Paulo. Escola Politécnica. Departamento de Engenharia de Minas e Petróleo II.t.

To all women in science

ACKNOWLEDGMENTS

I would like to thank Dr. Socco for her expert advice and invitation to develop this project, as well as Farbod, for his extraordinary support in this thesis process. Also, to Dr. Vasquez Alvarez who did not participate directly during the development of this thesis, but tutored me since the beginning of my Bachelor's degree.

My most sincere gratitude to my parents, Vera and Marcos, who gave me everything, from my life to their extensive and unconditional support and encouragement; also, to my ~~terrible~~ beloved brothers and my fiancé Lucas, who has never let me down.

My deepest thanks and appreciation to Carol, Lucas and Micho, for their endless help and support throughout not just this project, but for all moments of joy and need. Also, for those who have touched my life, being my greatest gifts, you all know who you are, and I am truly grateful for sharing special moments of my life with you.

RESUMO

As ondas de superfície podem ser usadas para estimar modelos superficiais de velocidade de ondas de cisalhamento explorando sua natureza dispersiva: as curvas de dispersão locais (DCs, do inglês *dispersion curves*) estão sujeitas a uma dependência significativa da velocidade média quadrática ou de empilhamento Vsz. A relação entre o comprimento de onda da onda de superfície e a profundidade de investigação é usada para transformar diretamente DCs em Vsz, evitando o procedimento de inversão. Essa técnica, conhecida como método W/D, foi recentemente introduzida, mas a estimativa da velocidade intervalar de onda S (VS, do inglês *shear-wave velocity*) a partir de Vsz experimental, com ruídos de aquisição, usando uma equação do tipo DIX requer regularização dos dados. Um código MATLAB bem estruturado foi desenvolvido para simular VS em perfis sob diferentes níveis de ruído para testar e comparar o parâmetro de regularização que melhor se ajusta ao perfil de VS simulado com seu perfil original, na tentativa de correlacionar níveis de ruído e parâmetro de regularização.

Palavras-chave: Ondas de superfície, método W/D, parâmetro de regularização

ABSTRACT

Surface waves can be used to estimate near-surface shear wave velocity (VS) models due to their dispersive nature: local dispersion curves (DCs) are subjected to a significant dependency to time-average velocity (Vsz) and the relationship between the wavelength of surface waves and the investigation depth is used to directly transform DCs into Vsz, avoiding the inversion procedure. Such technique, known as W/D method, has been recently introduced but the estimation of the interval VS from noisy Vsz using a DIX type equation requires regularization of the data. A synthetic dataset of 1D VS models has been generated with a stochastic approach based on a Monte Carlo procedure. A well-structured MATLAB code was developed to simulate the interval VS under different noise levels to test and compare the regularization parameter that best fits the simulated VS with its original profile, in an attempt to correlate noise levels and regularization parameter.

Keywords: Surface Waves, W/D method, Regularization Parameter.

LIST OF FIGURES

LIST OF TABLES

TABLE OF CONTENTS

1 INTRODUCTION

The characterization of the subsurface is crucial for the modern oil and gas industry due to the fact that locating and producing oil demands a very good knowledge of the underground structure. The surface seismic data is measured in units of time, therefore good velocity models will convert successfully the data from time to depth domain, revealing structural and stratigraphic variations beyond the well locations, where the seismic data is originally acquired as a function of depth.

Though the most superficial part of the surface lacks information obtained by the use of refracted waves, surface waves propagates along the free surface interface, carrying more detailed information of the near-surface attributes. A proper characterization of the shallow onshore subsurface is important to avoid inconsistencies at the reservoir level caused by the weathered layers and also to avoid drilling hazards.

For a long time, surface waves have been filtered out from reflection data, but the interest in the plentiful information that they carry has been increasing recently, being used to interpreted and characterize the shallow near surface. Moreover, the spectral analysis of surface waves can be used for a wide variety of applications in engineering, e. g., pavement system analysis, identification of soft layers and seismic site assessment, among others.

In surface wave methods, after the acquisition phase, the data is processed to extract the dispersion curve and usually inverted to obtain the velocity model. The inversion process, however, does not ensure an unique solution, due to the fact that many models would fit the data to the same degree. The wavelength-depth (W/D) method is a new technique, first launched by SOCCO et al. (2015), that has been introduced recently for static corrections and time-average velocities estimation, avoiding extensive inversion processes by evaluating the time-average VS through simple data transform.

In addition, KHOSRO ANJOM et al. (2019) developed a method to transform the estimated Vsz to interval VS using a DIX-type equation and imposing regularization - such approach is necessary because of the noisy invariably present in the input data. Therefore, it is essential to optimize the regularization, that aims to smooth the data, acting to dampen the effects of noise. Furthermore, the degree of regularization is data driven and is strongly correlated to the noise level.

The regularization parameter is a component that determines the regularization level, which, in this case, have not been fixed and depends on the noise level. Acting as a tradeoff, this parameter will control how much the noise will be smoothed: the higher the noise, the higher the parameter is expected to be.

To define what would be ideal value of the regularization parameter, at a certain noise level, a set of parameters is tested on synthetic data, and the simulated shear wave velocity (VS) compared with the equivalent synthetic profile to determine the parameter that fits the best; at the end, after repeating it for a considerable number of synthetic profiles disturbed at a certain degree, the parameter with the highest occurrence is taken as the optimum value for that noise level.

In this study, we adopt the W/D and the Total-Variation Regularization methods (KHOSRO ANJOM et al., 2019) instead of the classic inversion, in order to estimate a relationship between the noise level and the regularization parameter. A stochastic approach has been adopted with the purpose to generate 1D VS synthetic profiles, in which different levels of noise are added to the dispersion curves.

2 THEORETICAL BACKGROUND

This chapter focus on the presentation of the core concepts applied along the development of this work.

2.1 MAIN TYPES OF ELASTIC WAVES AND THEIR PROPERTIES

Body waves and surface waves are two varieties of mechanical waves: the first travels through the earth's interior, while the second travels along the free-surface. Body waves are known as shear waves (S-waves) and compressional waves (P-waves) while Rayleigh and Love waves are the main types of surface waves.

2.1.1 Body Waves

S-waves are also known as transverse waves and do not travel through fluids due to the fact that shear stress and strain cannot occur. They are characterized by particle motion being perpendicular to the wave's motion (Figure 1).

Figure 1 - Particle motion during S-wave propagation

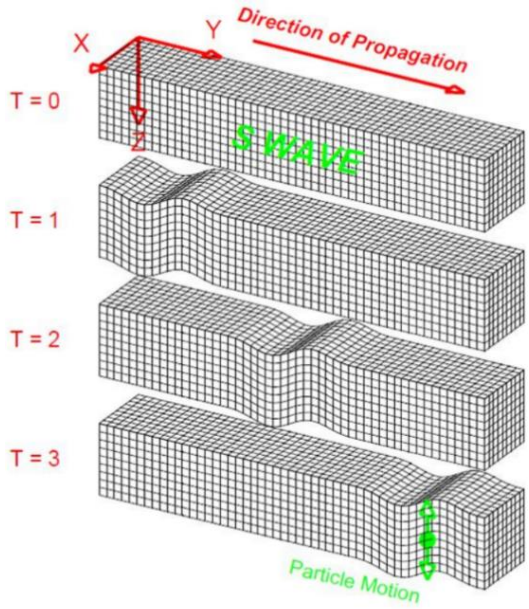

Source: BRAILE, 2006

P-waves are also called longitudinal waves and travel in both fluid and solid media. The particles move parallel to the direction that the wave moves, in a back and forth motion (Figure 2).

Figure 2 - Particle motion during P-wave propagation

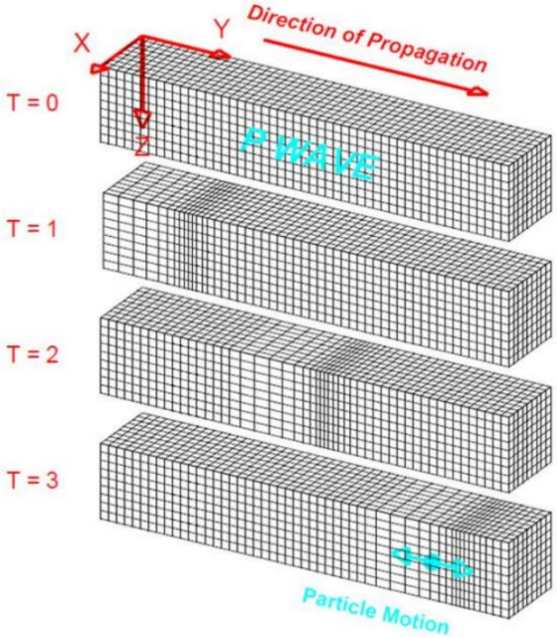

Source: BRAILE, 2006

2.1.2 Surface Waves

Only P-waves and S-waves can propagate in a homogeneous, isotropic and unlimited medium. If the medium is bounded, another type of waves, surface waves, can be guided along the surface of the medium (NOVOTNY, 1999). Love, Rayleigh, pseudo-Rayleigh and Scholte waves are different types of surface waves, being neither longitudinal nor transverse.

Scholte's waves are interface waves, presented at the interface of fluid-solid media. Most of the energy in this type of wave is presented in the interface and decays exponentially into the solid medium and fluid one (FLORES-MENDEZ et al, 2011).

Love waves only travel through one layer of the earth, not propagating in a homogenous half space, lying on top of another layer with a higher propagation velocity of S-waves (VS). The particle motion is transverse and parallel to the surface (Figure 3).

Figure 3 - Particle motion during Love wave propagation

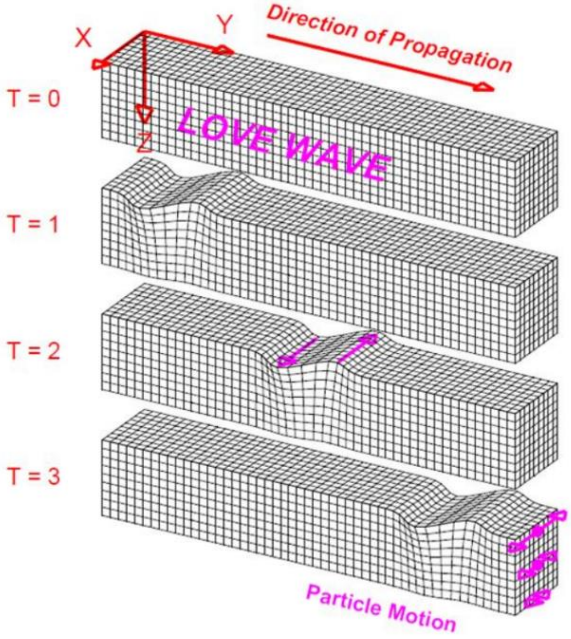

Source: BRAILE, 2006

Rayleigh waves propagate along the free surface of an infinite homogeneous isotropic elastic solid with a wavelength comparable to the propagation thickness (STRUTT, 2009), as a combination of P-waves and vertically polarized S-waves, with an elliptical motion, which consists of both vertical and horizontal particle motion, in a counter clockwise direction at the surface, with decrescent amplitudes (Figure 4). The amplitudes of the Rayleigh wave motion decrease with distance away from the surface (BRAILE, 2006).

These waves are called Pseudo-Rayleigh when the medium is heterogeneous – as encountered in seismic exploration. Even though the waves captured in seismic exploration may include modes other than a pure Rayleigh wave, they are usually merely labeled a Rayleigh wave. They propagate close to the surface, affecting a limited depth depending on the wavelength (SOCCO and STROBBIA, 2004).

The propagation velocity depends mainly on the S-wave velocity: in a homogeneous half-space the Rayleigh-wave velocity (VR) is slightly lower than VS ($0.87VS<VR<0.96VS$, depending on Poisson's ratio (RICHART et al., 1970)). Considering a point source, a high percentage of the radiated energy is transmitted as Rayleigh waves, making them prevalent in traces recorded on the surface. This makes the surface wave methods a powerful tool for near-surface characterization.

Even though Rayleigh waves carry information related to the media they travel through and represent a great portion of the radiated energy of the source, they are labeled ground roll, a sort of coherent noise to be identified and canceled out.

Figure 4 - Particle motion during Rayleigh wave propagation

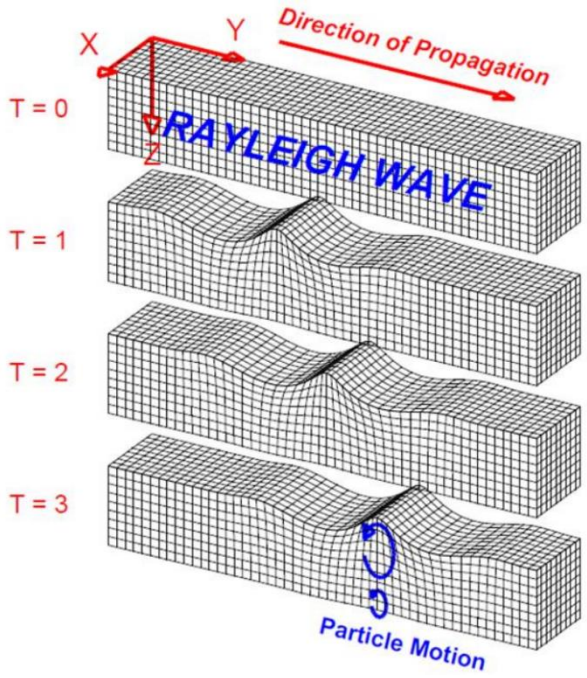

Source: BRAILE, 2006

2.1.3 Dispersion of Waves

Dispersion is a phenomenon of a wave in which its velocity varies with frequency. If each frequency component travels at its phase velocity, which is a product of the frequency and wavelength of that component, then shallow layers will be affected by short wavelengths while deeper layers by large wavelengths. The dispersive nature of Rayleigh-type surface waves in layered medium provides key information regarding the properties of near-surface materials (ÓLAFSDÓTTIR, 2014).

Whereas surface waves are dispersive, body waves are not. Dispersion is indicated if the wave velocity depends on frequency (Figure 5c) or wavelength (Figure 5b) – A dispersion curve depicts the distribution of phase velocities as a function of frequency or wavelength. High frequencies are equivalent to short

wavelengths, therefore, the lower the frequency, the deeper the extension of wavelength in depth (Figure 5a). This phenomenon can be used to study the medium through which the waves have propagated (NOVOTNY, 1999).

Figure 5 –(a) Representation of the geometric dispersion of surface waves in a layered, heterogeneous media. (b) Dispersion curve: phase velocity (V) vs Wavelength (λ). (c) Dispersion curve: phase velocity vs frequency (f).

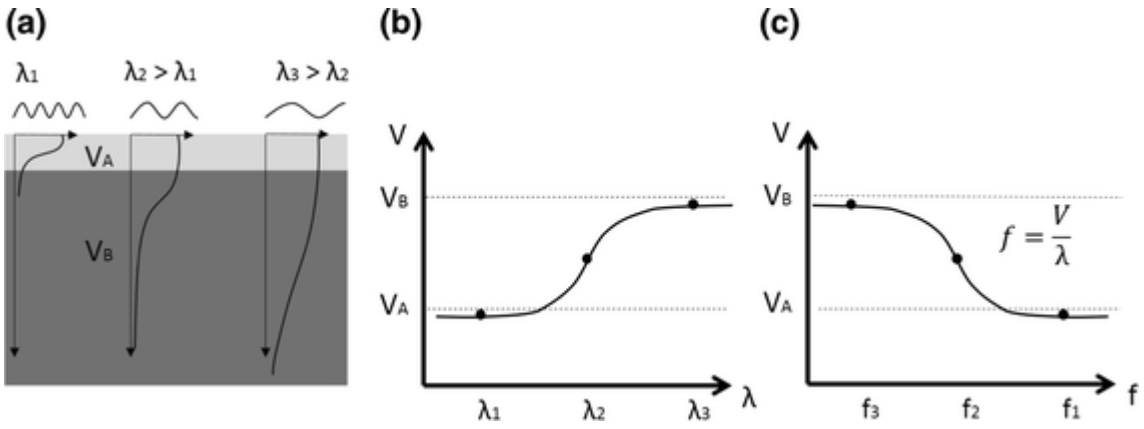

Source: FOTI et al., 2017

Propagation of surface waves is a multi-modal phenomenon in vertically heterogenous media: different phase velocities (or wavelengths) may relate to the same frequency, creating modes of propagation (Figure 6). The first mode is also known as fundamental mode, being characterized by being the slowest one, being followed by ‘faster’ modes, which only exist above a cut-off frequency. The cut-off frequency corresponds to the lowest frequency for which a mode will propagate in it.

Figure 6 - Dispersion Curve for the first 4 modes

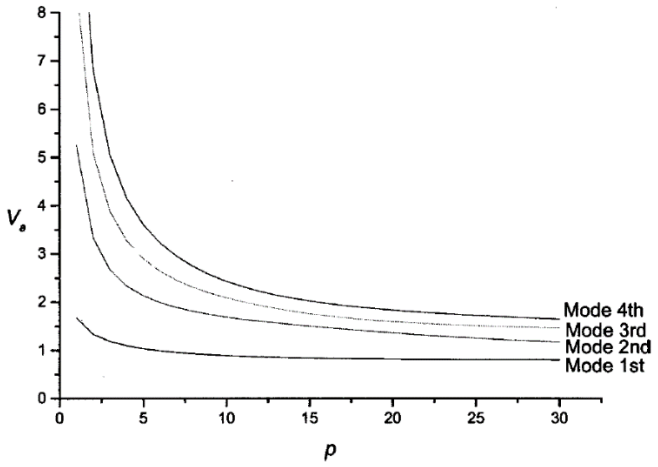

Source: WANG, 2002

2.2 FREQUENCY-WAVENUMBER METHOD

The frequency-wavenumber (f-k) is a processing method employed to quantify the DC given the acquired raw data using multichannel analysis of surface waves, from both passive and active surveys. Another common approach is the Spatial Correlation (SPAC) method.

According to FOTI (2000), the application of a discrete Fourier transform along time domain leads to frequency domain, while a straight line in space leads to the wavenumber domain. Therefore, through a 2D Fourier transform (i. e., two successive applications of the 1D transform, one over each domain), a series of time histories recorded along a straight line in space can be transformed in its f-k spectrum, and consequently a DC is retrieved, with no loss of information.

Still according to FOTI (2000), working in the f-k domain is noteworthy due to the fact that unlike in the spectral analysis of surface waves, it is possible to get DCs

for different modes, giving smoother results and allowing more robust inversion processes or clustering the data for the W/D method.

2.3 INVERSION

The inversion process is aimed at searching the best subsurface model whose forward response fits well the experimental data (FOTI et al., 2017). Even though the inversion of surface wave DCs is used as a convenient way to estimate local 1D velocity profiles (SOCCO and COMINA, 2015), its solution is not unique, non-linear and mathematically ill-posed (FOTI et al., 2017; OLDENBURG, 2015). Different approaches have been investigated with varying degrees of complexity, from deterministic to stochastic strategies for better assessing the non-uniqueness of this reconstruction problem (KHOSRO ANJOM et al., 2019).

Due to its poor sensitivity to VP, the DC is often inverted assuming an a priori value for Poisson's ratio (or VP) and density, and only layer thickness and VS are kept as inversion unknowns. (SOCCO et al. 2017). Furthermore, inversion problems based on wave propagation theory cannot be solved in a direct way due to their non-linearity. Thus, iterative methods where a theoretical dispersion curve is determined for a given layer model and compared to the previously obtained experimental dispersion curve must be used (RYDEN et al., 2006).

The forward model computed for the inversion analysis assumes a horizontally layered linear elastic medium (Figure 7), establishing values for VS, VP, density and thickness of each layer.

Figure 7- Horizontally layered medium for inversion analysis. The parameters of the model are VS, VP, mass density, ρ, and thickness of layers, h. The last layer is assumed to be a half-space.

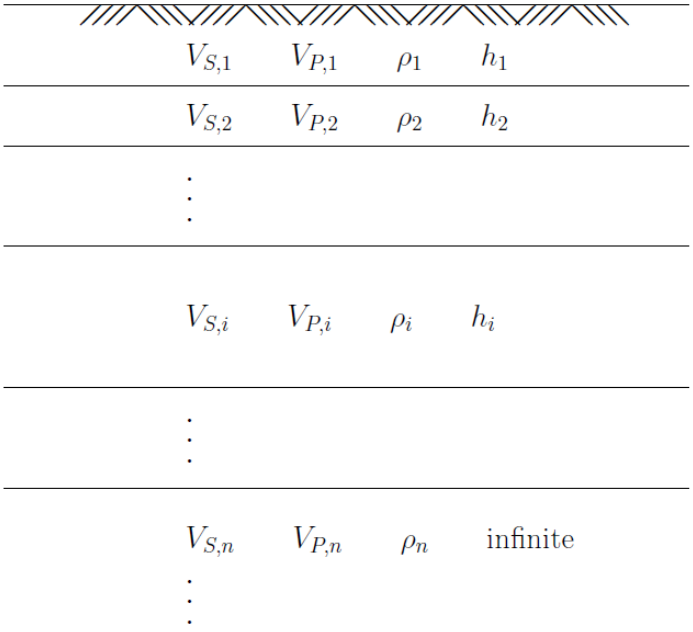

Source: ÓLAFSDÓTTIR, 2014

Local and global search procedures are two categories of possible inversion processes. The division is based on how model parameters are updated between iterations during search for the most probable set of parameters (OROZCO, 2003).

For a local inversion algorithm, the first step is to provide a fair initial guess. Based on this initial set of parameters, a convergence is expected, and a theoretical solution is determined: whenever the disparity between the theoretical solution and the real data is acceptable, the process is finished. If the method does not converge, the initial set of model parameters must be changed (OROZCO, 2003).

For global inversion algorithms, the conventional methodology consists in produce, randomly, parametric sets within a pre-determined range. Such methods, that both involve iteration and a random generator, are referred to as Monte Carlo methods (SOCCO and BOIERO, 2008). The selected solution will be the one, as in

local algorithms, the one who presents the best fit among all the tested theoretical curves.

The main advantage of local methods is considerably better computational speed as compared to global methods. However, solutions obtained by local methods are generally strongly biased by the initial guess (ÓLAFSDÓTTIR, 2014). The risk of finding a local minimum instead of the global minimum is thus substantial when local search methods are applied (SOCCO and BOIERO, 2008).

2.4 WAVELENGTH-DEPTH RELATIONSHIP

Although approximate relationships between investigation depth and wavelength of surface waves had been proposed before by ABBIS (1981) and BROWN et al. (2000), the wavelength to depth (W/D) was first launched by SOCCO et al. (2015) as a method to calculate approximately time-average S-wave velocity (Vsz) models at any depth without the need to invert the data: a linear correlation is assessed to connect depth and wavelength, where Vsz is given by:

$$V_{sz} = \frac{\sum_n h_i}{\sum_n {h_i}/{V_i}}, \quad (1)$$

n is the number of layers above the depth z, h_i and V_i are the thickness and the velocity of the i^{th} layer, respectively.

Such technique is possible due to the fact that DCs are sensible to Vsz – even more than they are sensible to layered velocity models (KHOSRO ANJOM et al., 2019).

Mathematically speaking, according to KHOSRO ANJOM et al. (2019), it initially requires a known Vsz profile for one of the DCs, which could be estimated through inversion or known from other independent surveys.

This single profile is then used as a calibration velocity model for all the other dispersion curves: for each velocity value, the depth from the Vsz model is associated with the wavelength from the phase velocity model (Figure 8a), allowing to collect points to develop the W/D relationship (Figure 8b). Then, the W/D relationship can be used to transform all DCs to Vsz.

Figure 8 - (a) Initial S-wave velocity data model (Vs model), Dispersion curve with wavelength domain (DC), true and estimated time average velocities (True V_{sz} and est V_{sz} respectively). (b) Wavelength vs Depth

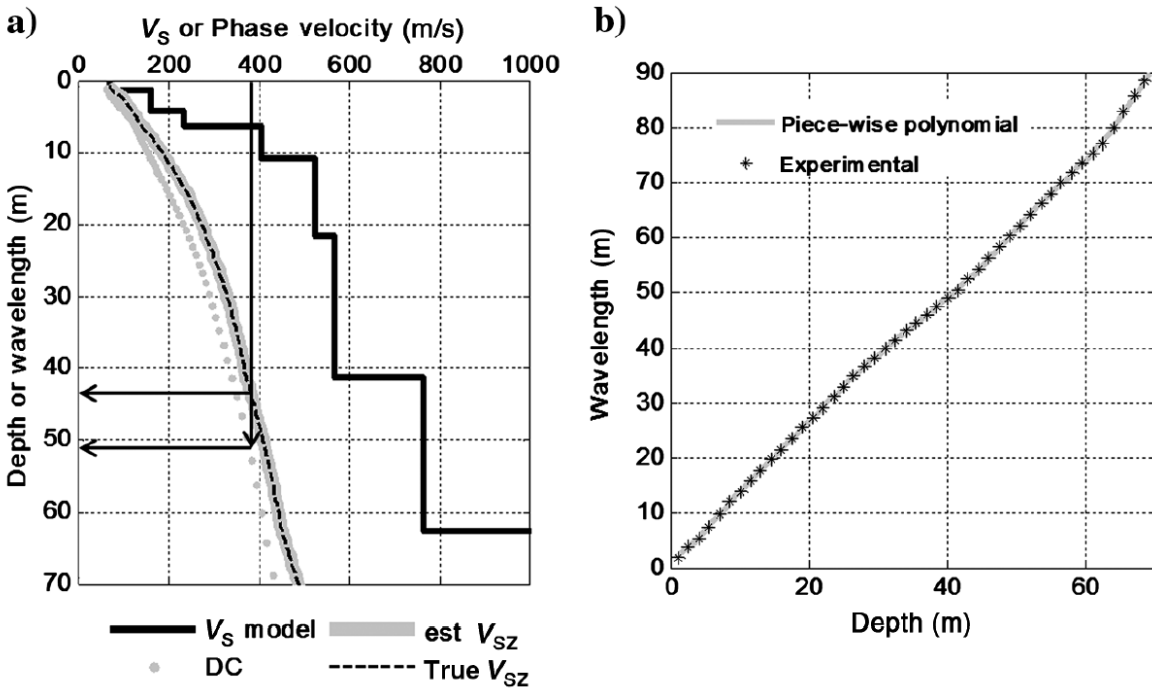

Source: SOCCO et al. 2017

The performance of the W/D method has been explored in real data, proving itself to be successful. SOCCO et al. (2017) have improved the estimation through a polynomial fitting and tested it in two field cases, proving the approach to be effective on sites with lateral variations in near-surface velocities on synthetic field data.

However, using a unique reference curve for the whole line becomes problematic when sharp lateral variations or zones with different velocities are present (KHOSRO ANJOM et al., 2017). To overcome such restriction, hierarchical clustering algorithm was developed by KHOSRO ANJOM et al. (2017) in order to select ensembles of DCs that can be interpreted using the same reference W/D relationship.

In addition to that, SOCCO and COMINA (2017) demonstrated that while the DC is not particularly sensitive to the Poisson's ratio, the W/D relationship is – they utilized this sensitivity to estimate also the time-average VP profile.

Once the Vsz values are known, it is possible to transform them into interval VS (V) models - V stands for the continuous local velocity profile. Starting from the Equation 1, KHOSRO ANJOM et al. (2019) developed a stable approach to transform Vsz into interval velocities (V_t), that led ultimately to the expression:

$$V_t = V_{sz} + t.\frac{dV_{sz}}{dt} \quad (2)$$

where t represents the one-way travel time. The derivative term dV_{sz} can be discretized at each depth and divided by the stepwise dt to find a numerical value of the derivative; however, small perturbations in the time-average velocity lead to large relative changes in the derivative estimation (KHOSRO ANJOM et al., 2019). Consequently, the derivative term must be evaluated through a different technique, mainly for noisy data.

Methods as least-squares polynomial approximation, Tikhonov regularization and total-variation regularization are presented in literature for such derivative estimation of noisy data. For a detailed mathematical review, refer to KNOWLES and RENKA (2014).

2.5 REGULARIZATION

Regularization is an optimization methodology that controls the misfit between real and estimated values, reaching an optimum tradeoff through a term defined as regularization parameter, and, according to FOMEL (2007), it is a required component of geophysical estimation problems that operate with insufficient data.

Total-variation regularization was introduced by RUDIN et al. (1992) with the purpose of removing noise from images without smearing the edges. And later, it was utilized by CHARTRAND (2011) to differentiate noisy data. It has been chosen for this project due to the fact that unlike typical regularizations, it allows for discontinuities in the derivative, not smoothing it excessively while it suppresses the noise. The derivative is approximated by the solution u of the minimization of the following function (Equation 3):

$$F(u) = \alpha \int_0^T |u(t)'|dt + 0.5 \int_0^T |Au(t) - V_z(t)|^2 dt, \qquad (3)$$

where $Au(t)$ defines the smoothed V_z and α is the regularization parameter, the terms controlling the balance between the two terms: the total variation of the first derivative u and the second term, which aims to minimize the distance between the smoothed and the input function, as a desirable balance between damping the oscillations while adjusting to the data.

3 METHOD

In a forward modelling, a synthetic 1D layered VS profile (Figure 9a) is the starting point, and from it, the theoretical DC (Figure 1b) can be computed, according to the method and MATLAB routine provided by MARASCHINI (2008), for a fixed frequency band, using essential model parameters for each layer: thickness, density, Poisson's ratio. Such computation method was proposed by HASKELL (1953). The adopted frequency band for this project was from 5 to 200 Hz.

Figure 9 – (a) 1D layered VS profile (b) DC correspondent to the Figure 1a

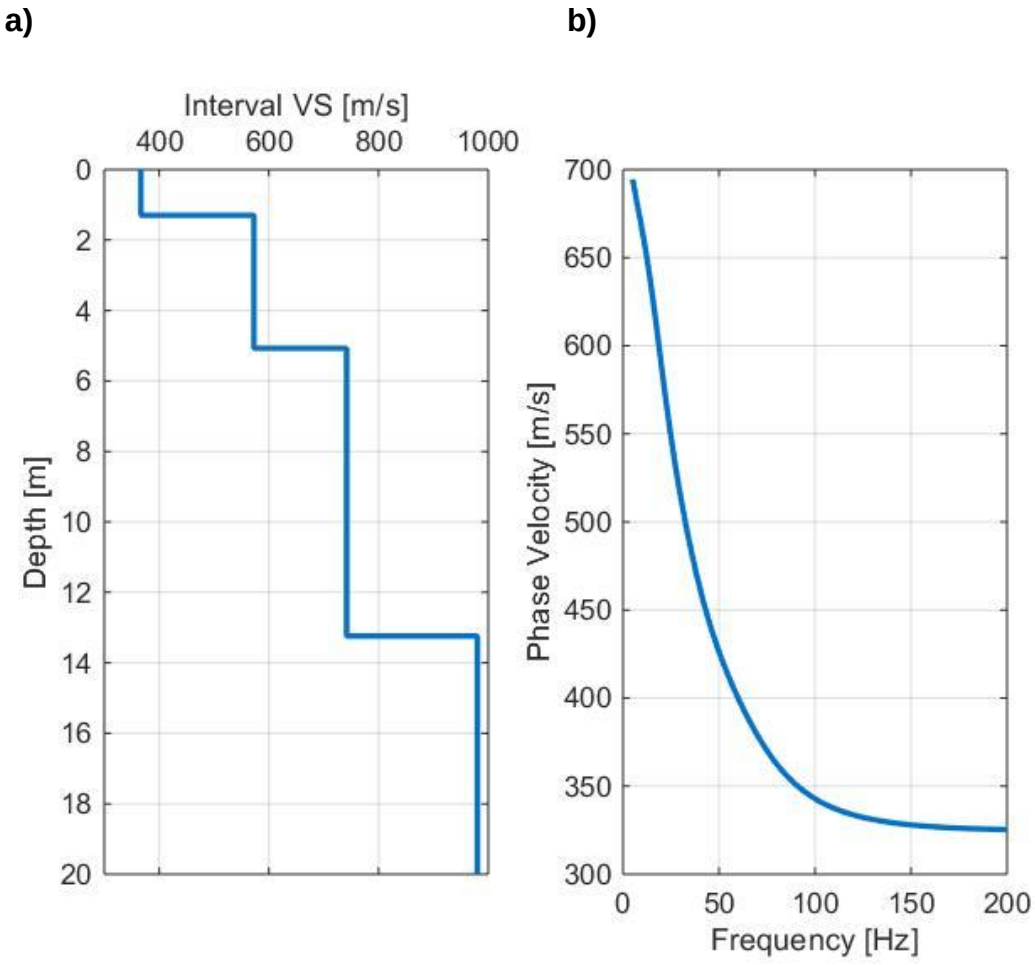

Source: Prepared by the author

For a noise free synthetic case, a DIX type equation can be utilized to perfectly transform the time-average velocity into interval velocity. In order to make the synthetic case realistic, it is necessary to disturb the data. Since for real data the DCs are estimated from f-k domain, the DC will be transformed to the f-k domain, with the intention of adding the noise directly to it, as in real data.

The wavenumber (k), or wavelength number is the spatial frequency of a wave, measured in cycles per unit distance or radians per unit distance; it is given by the following expression:

$$k = \frac{2\pi}{\lambda}, \tag{4}$$

where λ stands for the wavelength.

Considering that the phase velocity (V_r) and the frequency (f) are correlated as it follows,

$$v_r = \lambda . f, \tag{5}$$

after combining both equations, k can be determined using the following expression:

$$k = \frac{2\pi f}{v_r}, \tag{6}$$

the f-k relationship regarding the 1D layered model introduced in the Figure 1a, is depicted in the Figure 10a.

Random normal noise is added to the wavenumber, where the mean parameter is k and the standard deviation is proportional to the intended noise intensity. It can be seen in the Figure 10b the effect of the added noise.

Figure 10 - (a) Noise-free f-k (b) F-k with 2% noise added

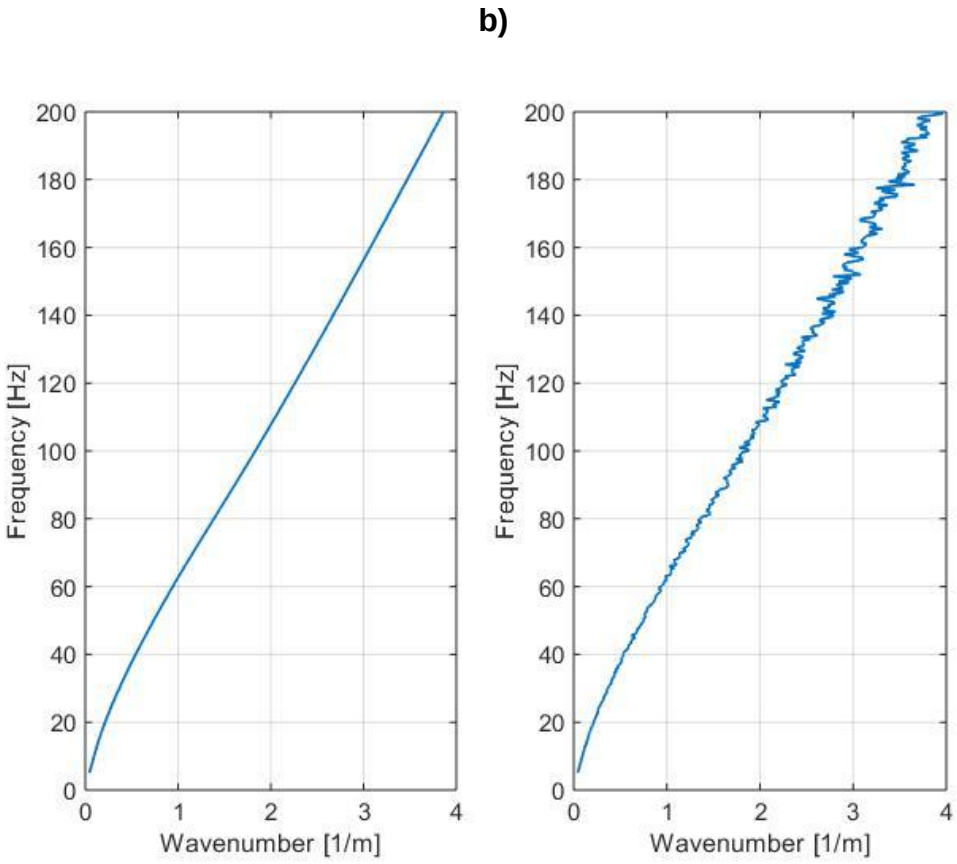

Source: Prepared by the author

Later on, a noisy DC is retrieved, representing a DC retrieved from f-k, in real acquired data: the noisy phase velocity (vr_{noisy}) can be assessed rearranging the Equation 4, where k_{noisy} stands for the noisy wavenumber:

$$vr\_noisy = \frac{2\pi f}{k\_noisy} \tag{7}$$

the result can be seen below (Figure *11*).

Figure 11 - True and Noisy DC (2% noise added)

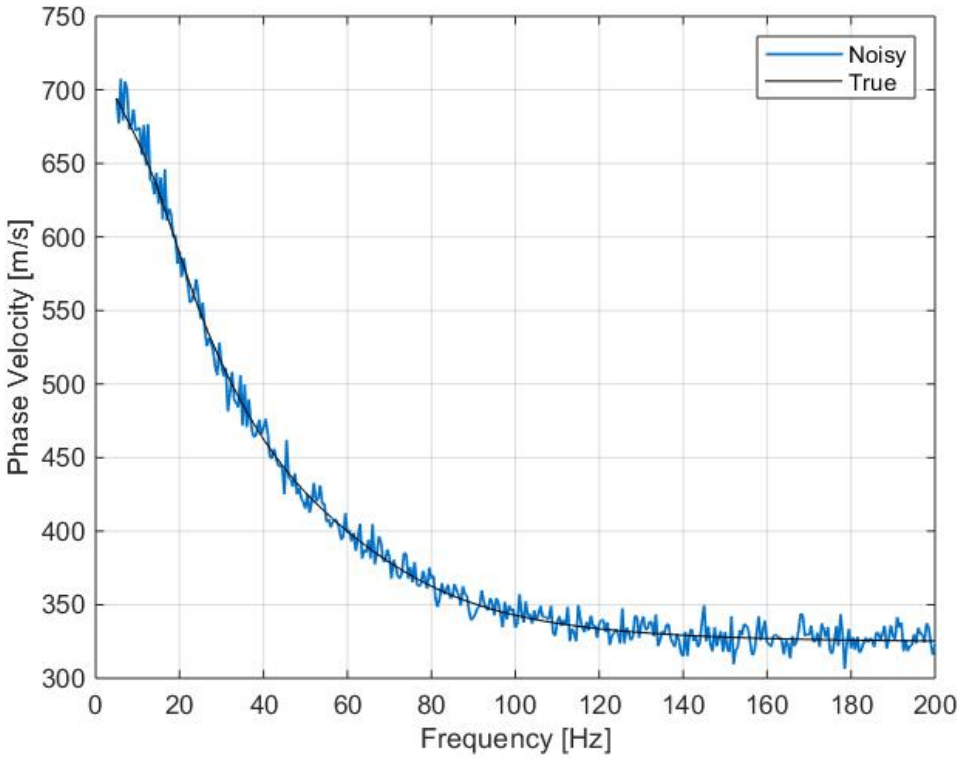

Source: Prepared by the author

The true Vsz is calculated using the VS profile. Therefore, the next step consists in assessing the W/D relationship, estimated using the true Vsz and noise-free DC, which is absolutely fundamental for this process in order to evaluate the noisy Vsz without the necessity to perform an inversion. To estimate it, the DC is interpolated using a piece-wise polynomial, correlating the Vsz with the v_r.

The W/D relationship (Figure 12b), is then used in the noisy DC in wavelength domain (Figure 12a) in order to retrieve the noisy Vsz (Figure 13). Since the bottom layer has no fixed thickness, the W/D is calculated up to certain depth, defined as investigation depth.

Figure 12 - (a) Noisy DC in the wavelength domain (b) W/D relationship

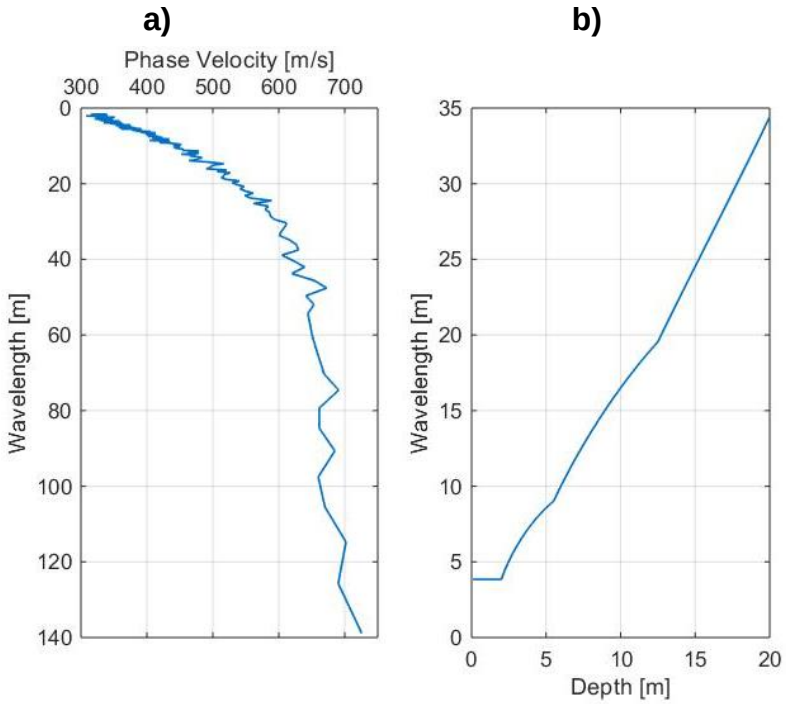

Source: Prepared by the author

Figure 13 - Vsz true and estimated

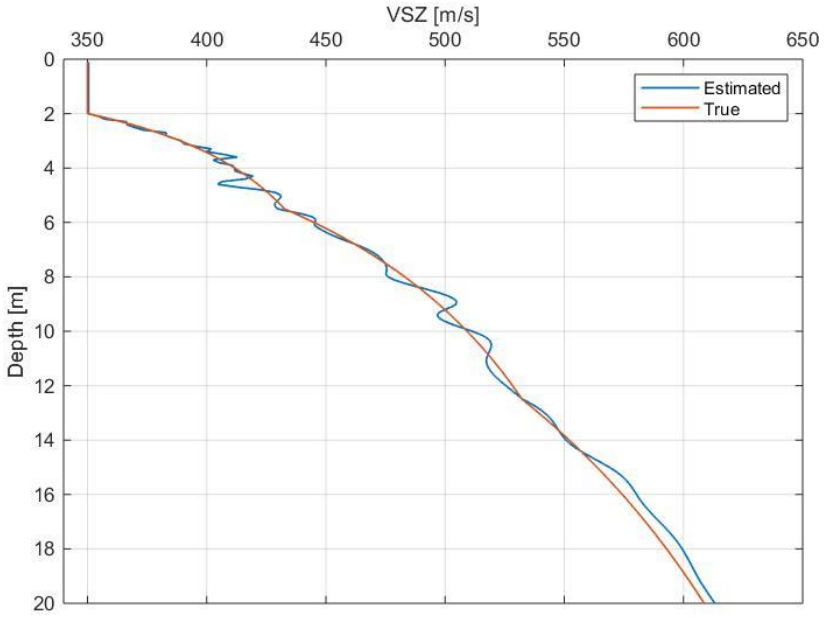

Source: Prepared by the author

The next stage comprises the interval velocity estimation. Non-regularized VS interval is computed by discretizing the derivative term at each depth dividing it by the correspondent time interval. As a consequence, when calculated using the noisy Vsz, its value presents a strong variation: a small perturbation in Vsz leads to a large variation in the derivative estimation, while the noise-free Vsz has an excellent match with the VS model (Figure 14).

Figure 14 - Non regularized Interval VS

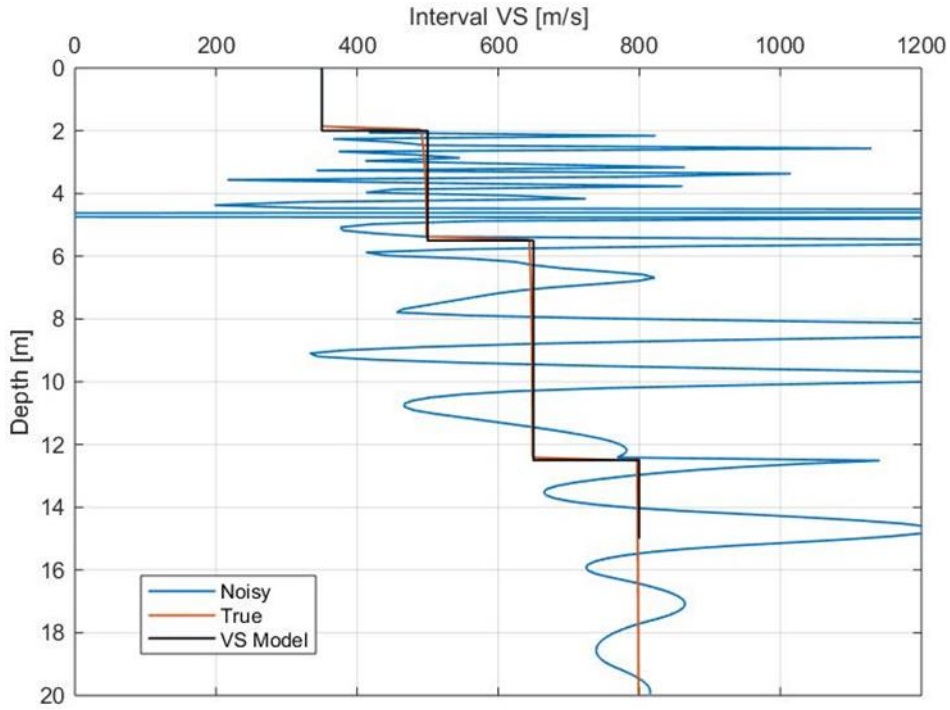

Source: Prepared by the author

Since noise is the source of such variations, and it is invariably present in any acquired dataset, regularization must be applied - the chosen method is the Total Variation Regularization, since it provides a good approximation, avoiding too excessive smoothing, allowing for discontinuities. The MATLAB routine used to calculate the derivative was provided by CHARTRAND (2011).

Regularization applied in an inversion or in an W/D process is a pretty straightforward, iterative concept: it controls the misfit between the model and the

real one, in such a way that through the regularization term a certain error threshold can be achieved, being the error given by:

$$\text{Error} = \frac{\sum \frac{|VS - VS\_est|}{VS}}{number\ of\ points}, \tag{8}$$

where VS is the real velocity at a certain depth and $VS_{\_est}$ is the estimated VS, for a certain regularization parameter (α), at the same depth. Therefore, the α is directly linked with the fitting quality of the VS estimation, which means that for the minimum attainable error value, the correspondent α will be taken as the optimum one.

The derivative trends are depicted in (Figure 15a) – the regularized curve is smoothed but still follows the overall trend of the true curve, while the not regularized is completely unstable. For this proposed VS model, the α which minimizes the error is equal to 5, generating an estimated interval VS (Figure 15b) with an average error equal to 3.2% - the minimum value that could be achieved through this method.

Figure 15 – Optimum scenario: (a) True, Regularized and Non-Regularized derivative trends (b) Interval VS – True and Simulated

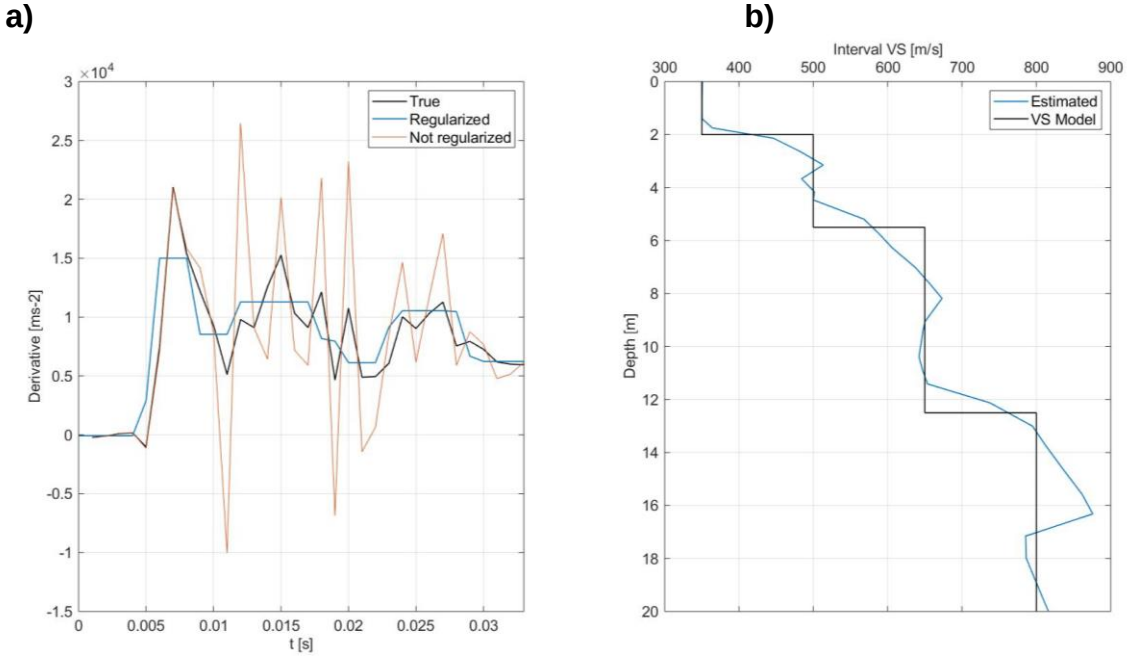

Source: Prepared by the author

As α increases, the smoothness increases dramatically, compromising the results. This is due to the fact that the α acts as tradeoff between the derivative term and the term controlling the smoothed and real functions (Equation 3). If α is too little, the differentiation will not be efficient, but if it is too big, the regularized derivative (Figure 16a) will be flatten causing the VS interval to become over-regularized, its profile losing definition (Figure 16b).

Figure 16 – Over-regularized scenario: (a) True, Regularized and Non-Regularized derivative trends (b) Interval VS – True and Simulated

a) **b)**

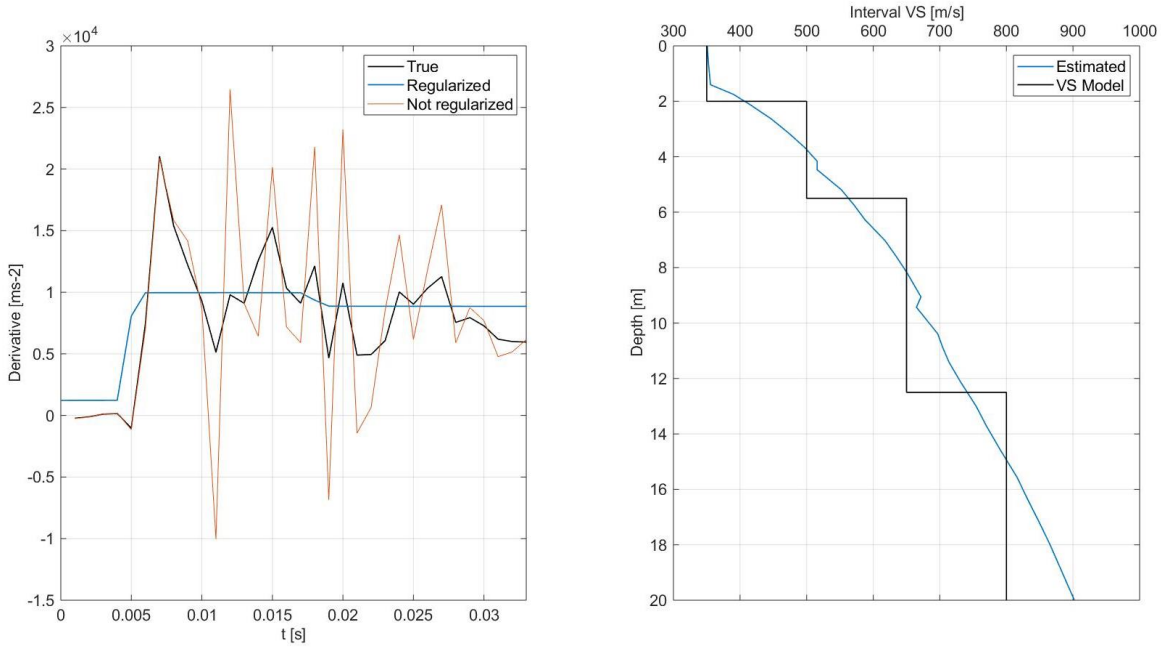

Source: Prepared by the author

Although it is essential to select the best α for each noise level, it is unlikely that a first guess for α will result in the desired value, i. e., in this case, the number which minimizes the error (Equation 8). That being said, a code to search the best α was implemented in MATLAB, and for each single profile, the best α value is retrieved.

So far, the process has been described for a single 1D VS profile. However, in order to depict a set of acquired data, a stochastic approach has been adopted with the purpose to generate a substantial number of profiles in order to depict a set

of acquired data (Figure 17). A MATLAB routine provided by SOCCO and BOIERO (2008) generates random models in a specified model space for VS, and thickness of each layer given values of mass density, Poisson's ratio and number of layers.

Figure 17 - Generated models

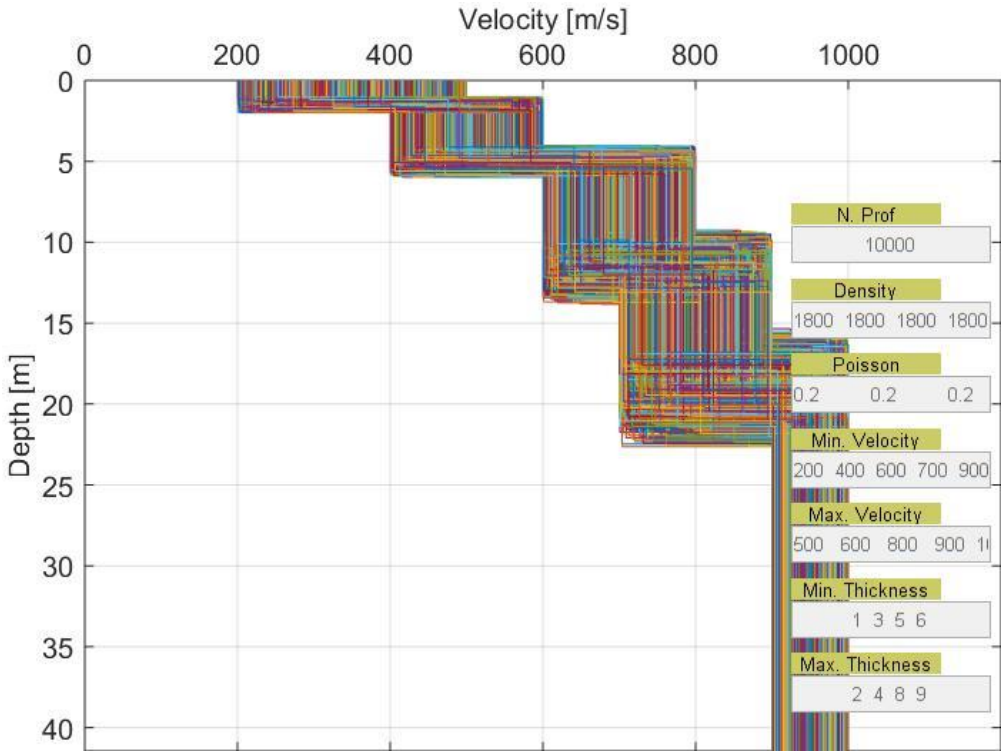

Source: Prepared by the author

For a specific noise level, the program finds the α that best optimizes the interval VS for each random VS profile generated. The distribution of the best α corresponding to the random models is plotted (Figure 18), and the α value with the most occurrence is recorded as the best α that optimizes the interval VS estimation for that specific noise level in the DCs. This recorded α is then applied to all profiles, the average error measured, and the simulated profiles plotted to be compared with the synthetic ones.

This procedure is repeated for different noise levels, from 0 to 10% in steps of 0.5%, and for each stage, the optimum α recorded. The α values were discretized in a logarithmic scale, from 1 to 10,000.

Figure 18 - Regularization Parameter Distribution – Noise = 3.5%

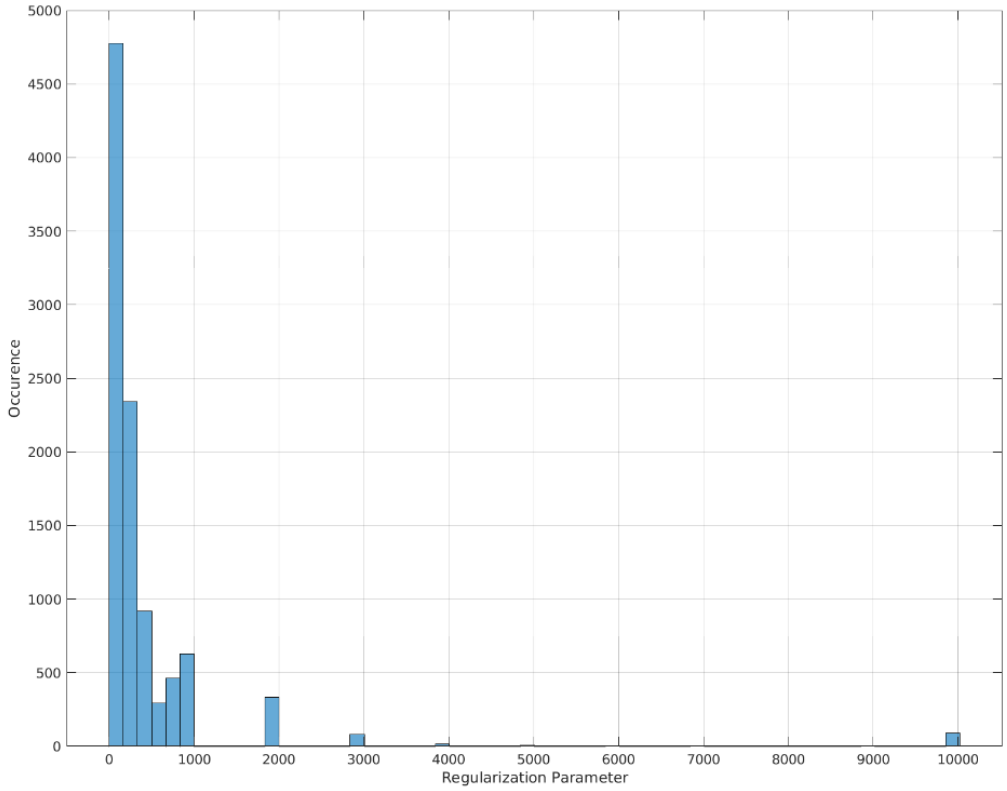

Source: Prepared by the author

4 RESULTS

4.1 THE SYNTHETIC DATASET

The adopted dataset is composed by 10,000 1D VS models, generated with a stochastic approach based on a Monte Carlo procedure. Each single model was assumed to have 4 layers with constant mass density, being the 5th layer limited by an investigation depth, set at a depth of 30m. Table 1 summarizes the model parameters and their maximum and minimum adopted values.

Table 1 - Properties of the synthetic dataset: thickness, S-wave velocities, Poisson's ratio and mass density

		VS [m/s]		**Thickness [m]**		**Poisson's Ratio**		**Mass Density**
		min	max	min	max	min	max	**[kg/m^3]**
Layer	**1**	200	500	1	2	0.2	0.4	1800
	2	400	600	3	4			
	3	600	800	5	8			
	4	700	900	6	9			
	5	900	1000	n/a				

Source: Prepared by the author

The VS of the generated models and their upper and lower boundaries are plottled in the Figure 19.

Figure 19 - Sampled models: upper and lower boundaries (in black)

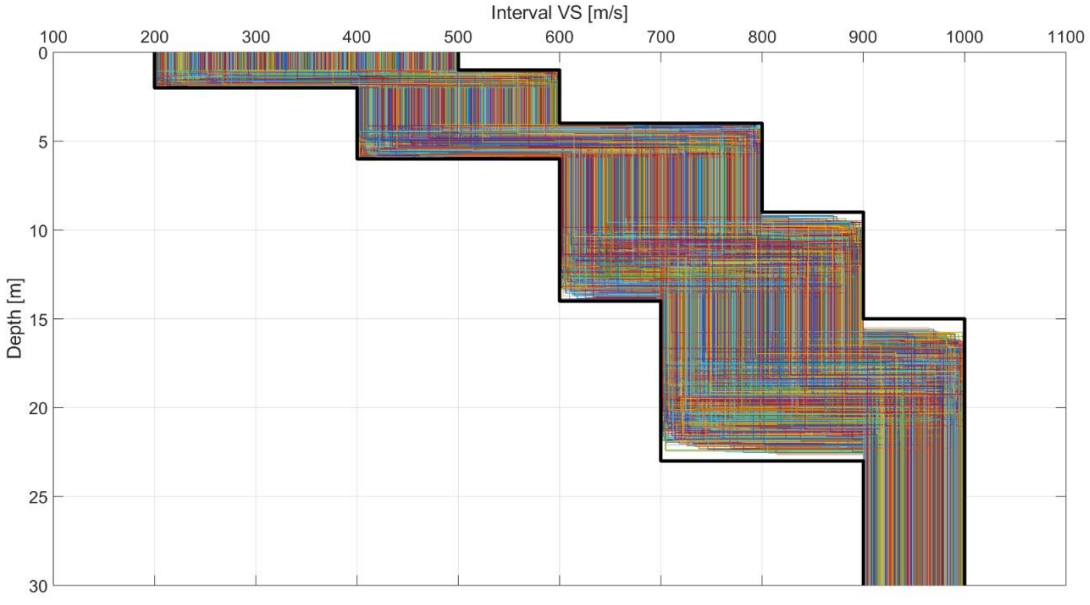

Source: Prepared by the author

4.2 THE OUTLIERS

Even though broad band DCs (5 to 200Hz, discretized in steps of 0.5Hz) were adopted to avoid extrapolation in the W/D method, a number of profiles exhibited a strong misfit in the noisy Vsz, with unrealistic values being generated (Figure 20).

Figure 20 - Interpolation irregularities in the Vsz estimation

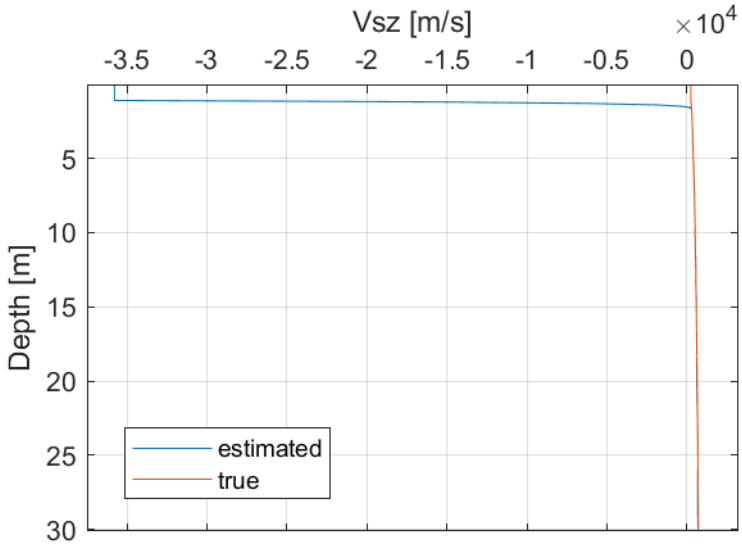

Source: Prepared by the author

Those profiles exhibiting such a strong misfit (outliers) had to be tracked and filtered. The quantity of models was initially 10,000, but even with the exclusion of a number of profiles (Figure 21), a representative amount was still being sucessfuly transformed into interval VS estimations.

Figure 21 - Number of Deleted Profiles vs Noise Level

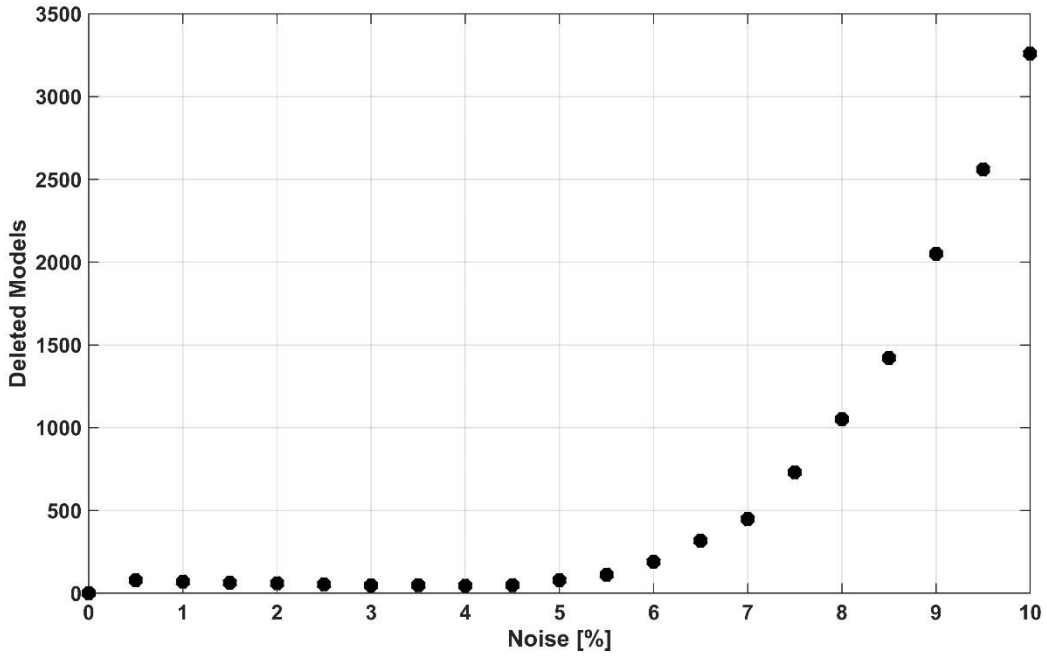

Source: Prepared by the author

4.3 THE OUTCOME

The established procedure was implemented for the whole data set. Noise levels from 0 to 10%, in steps of 0.5%, were added to the data at each turn. The α range was kept constant, from 1 to 10,000 in logarithmic steps.

4.3.1 No-noise

When no noise was applied (Figure 22a and Figure 22b), the optimum regularization parameter was 1 (Figure 23), i. e., the value with the highest occurrence among the tested values. The synthetic profiles (Figure 24a) and the estimated interval

VS (Figure 24b) were quite similar: the average error was 2.2%. For this case, from the initial 10,000 profiles not even a single one had been deleted due to misfit in the Vsz interpolation.

Figure 22 - No noise (a) True and Noisy DC (b) True and Noisy f-k

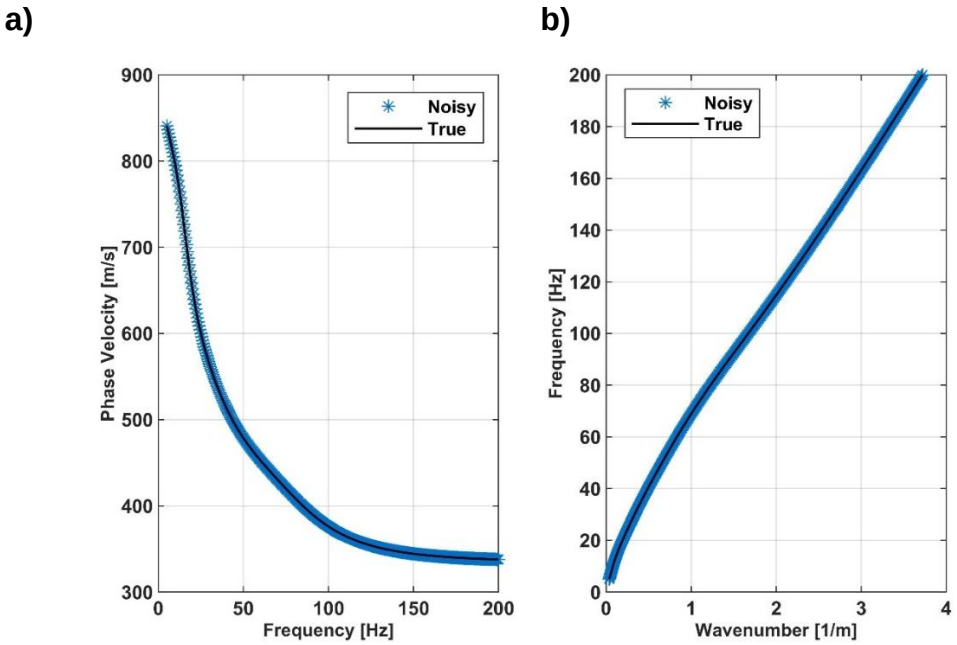

Source: Prepared by the author

Figure 23 - Distribution of α - No noise

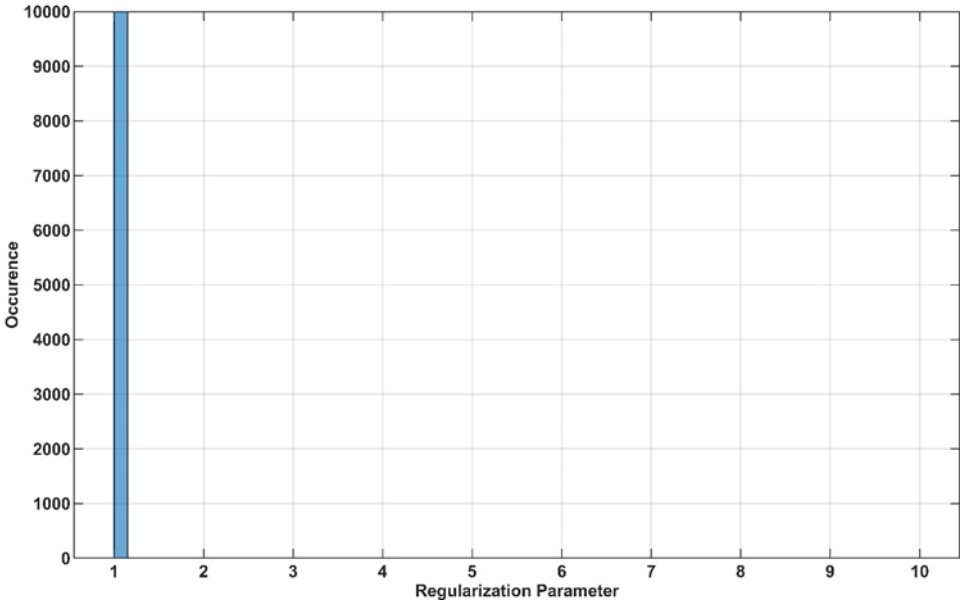

Source: Prepared by the author

Figure 24 - (a) Synthetic Profiles (b) Simulated Profiles - No noise

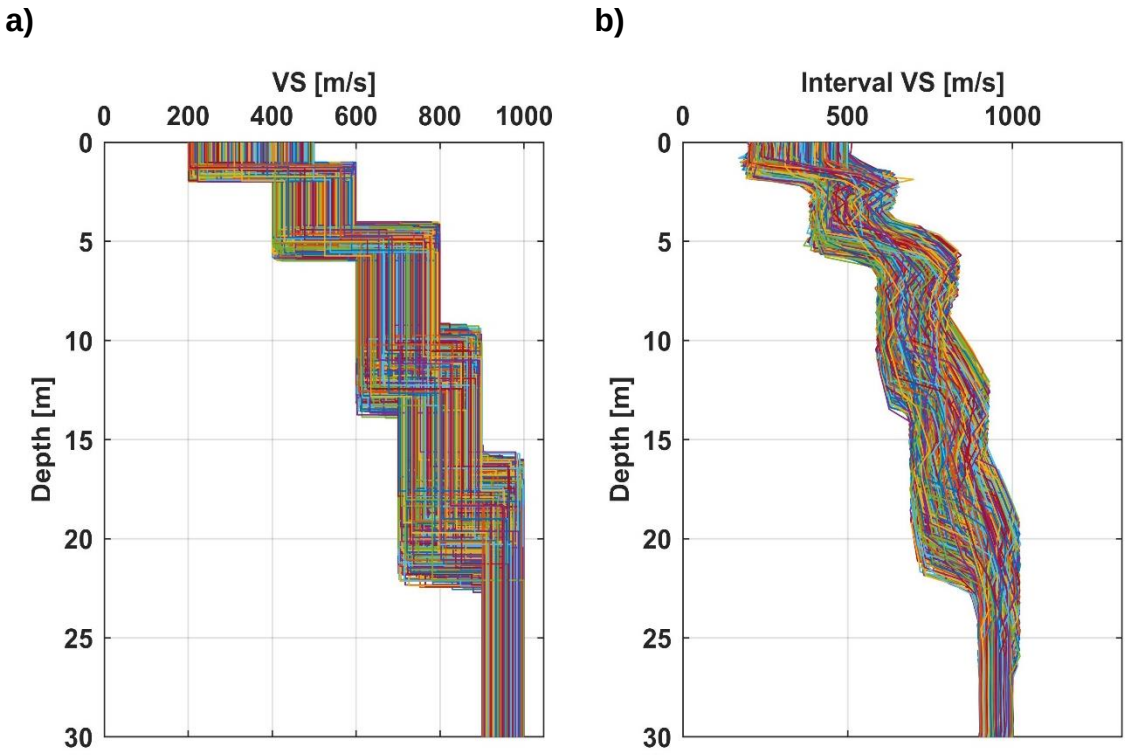

Source: Prepared by the author

4.3.2 Noise Level: 0.5%

When 0.5% noise was applied (Figure 25a and Figure 25b), the optimum regularization parameter was 1 (Figure 26). The synthetic profiles (Figure 27a) and the estimated interval VS (Figure 27b) were quite similar: the average error was 3.7%, presenting an excellent of the layers

As a small perturbance level is added, the distribution of α has increased, but being by far dominated by small values.

Figure 25 - 0.5% noise (a) True and Noisy DC (b) True and Noisy f-k

a) **b)**

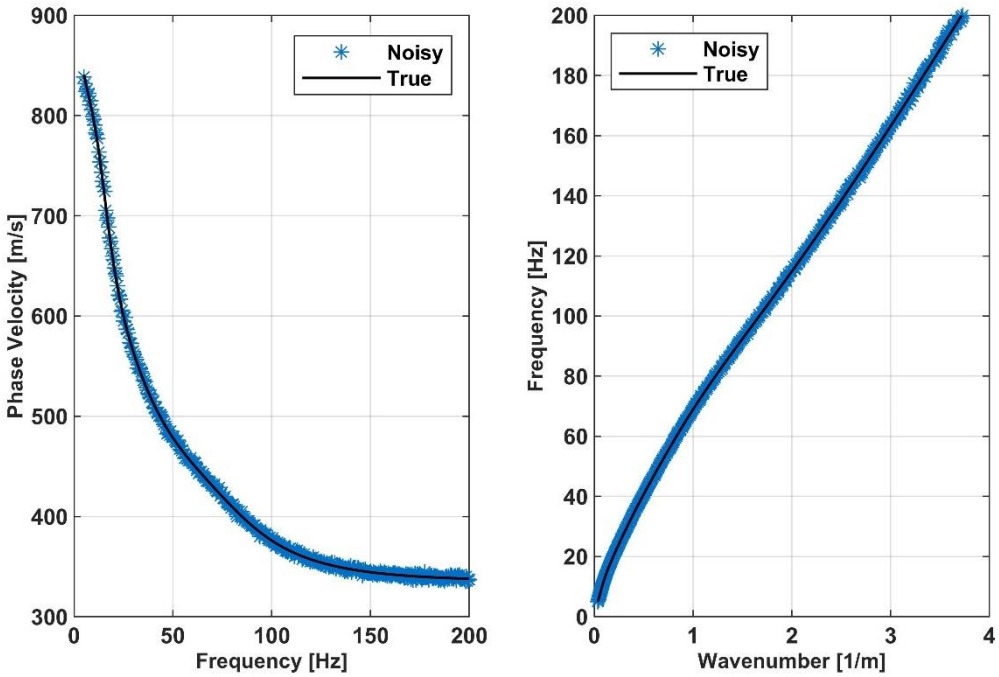

Source: Prepared by the author

Figure 26 - Distribution of α – 0.5% noise

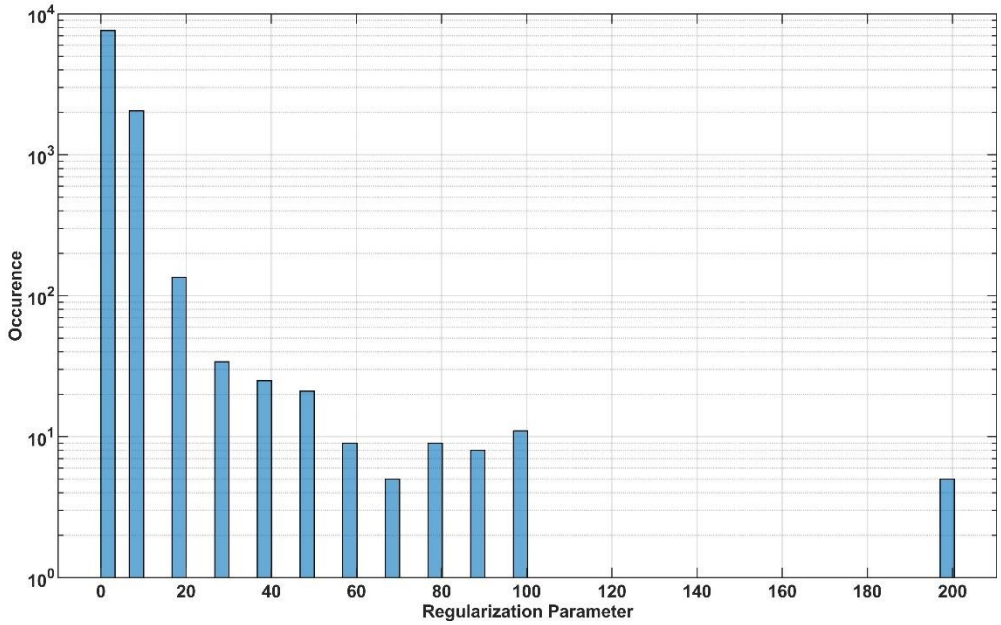

Source: Prepared by the author

Figure 27 – (a) Synthetic Profiles (b) Simulated Profiles – 0.5% noise

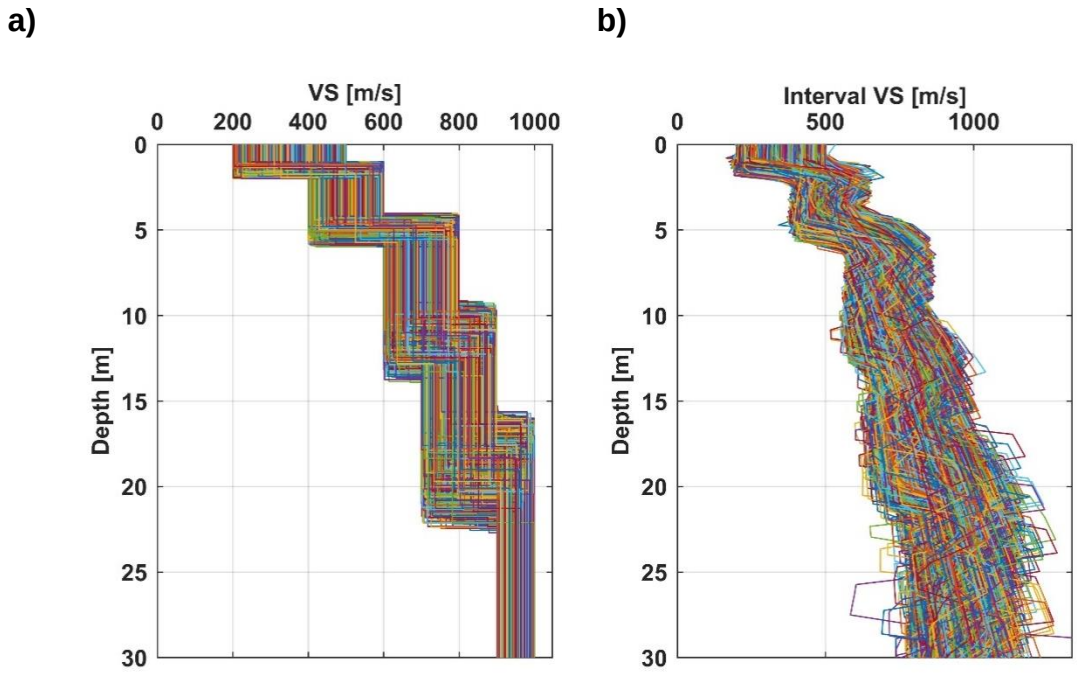

Source: Prepared by the author

4.3.3 Noise Level: 1%

When 1% noise (Figure 28a and Figure 28b) was applied, the optimum regularization parameter selected was 10 (Figure 29). The synthetic profiles (Figure 30a) and the estimated interval VS (Figure 30b) were quite similar: the average error was 4.8%, still with a good resolution of the layers.

As the perturbance level added increased, the distribution of α has also increased, reaching higher values in comparison with the previous noise level, but still being dominated by values lower than 1000.

Figure 28 - 1% noise (a) True and Noisy DC (b) True and Noisy f-k

a) **b)**

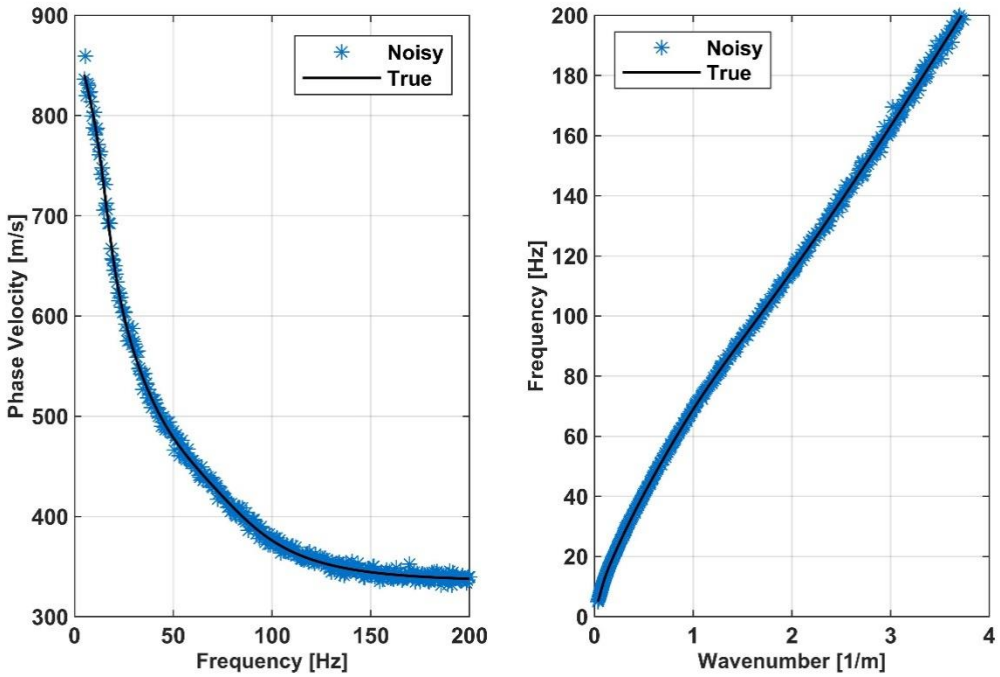

Source: Prepared by the author

Figure 29 - Distribution of α – 1% noise

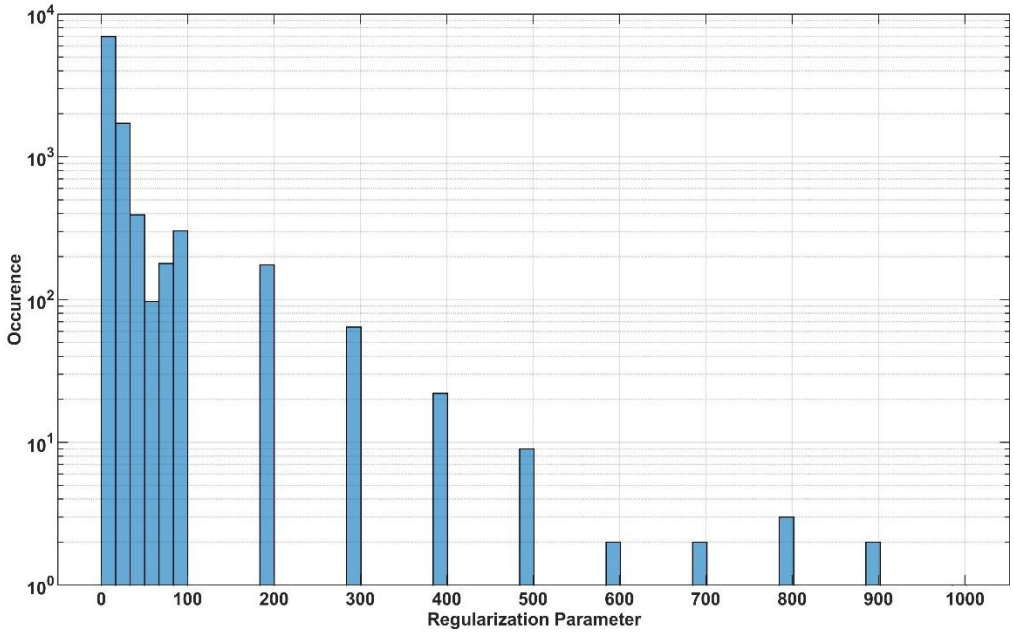

Source: Prepared by the author

Figure 30 - (a) Synthetic Profiles (b) Simulated Profiles – 1% noise

a) **b)**

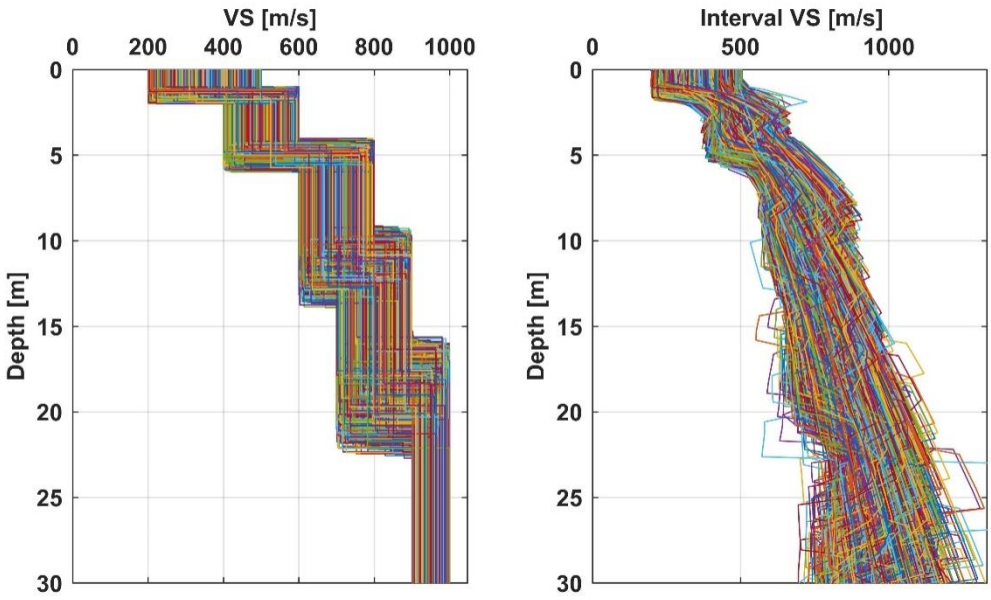

Source: Prepared by the author

4.3.4 Noise Level: 1.5%

When 1.5% noise was applied (Figure 31a and Figure 31b), the optimum regularization parameter was 10 (Figure 32). The synthetic profiles (Figure 33a) and the estimated interval VS (Figure 33b) were quite similar for the first layers, but the definition for the deeper ones starts to fade out: the average error was 5.7%, with tangled bottom layers.

As the perturbance level added increased, although the distribution of α has remained similar to the previous noise level (1%), higher values were selected even more frequently, but still being dominated by values lower than 1000.

Figure 31 - 1.5% noise (a) True and Noisy DC (b) True and Noisy f-k

a) **b)**

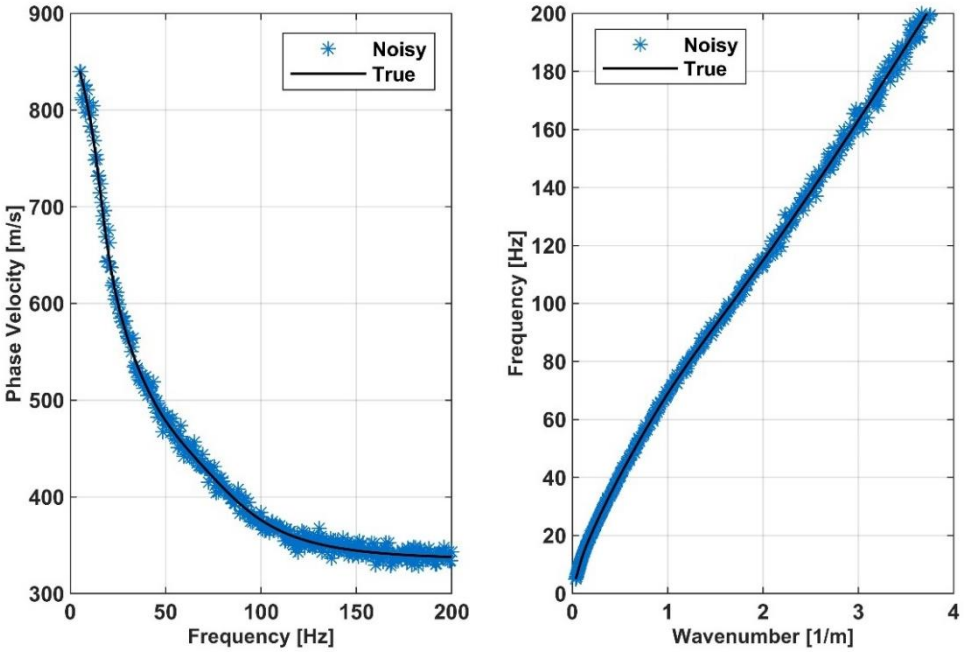

Source: Prepared by the author

Figure 32 - Distribution of α – 1.5% noise

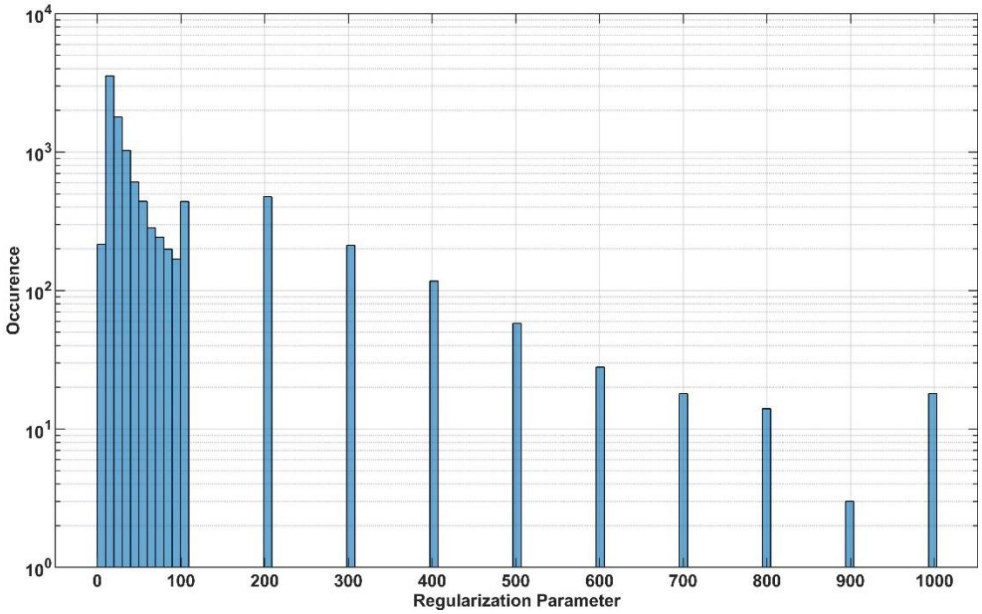

Source: Prepared by the author

Figure 33 - (a) Synthetic Profiles (b) Simulated Profiles – 1.5% noise

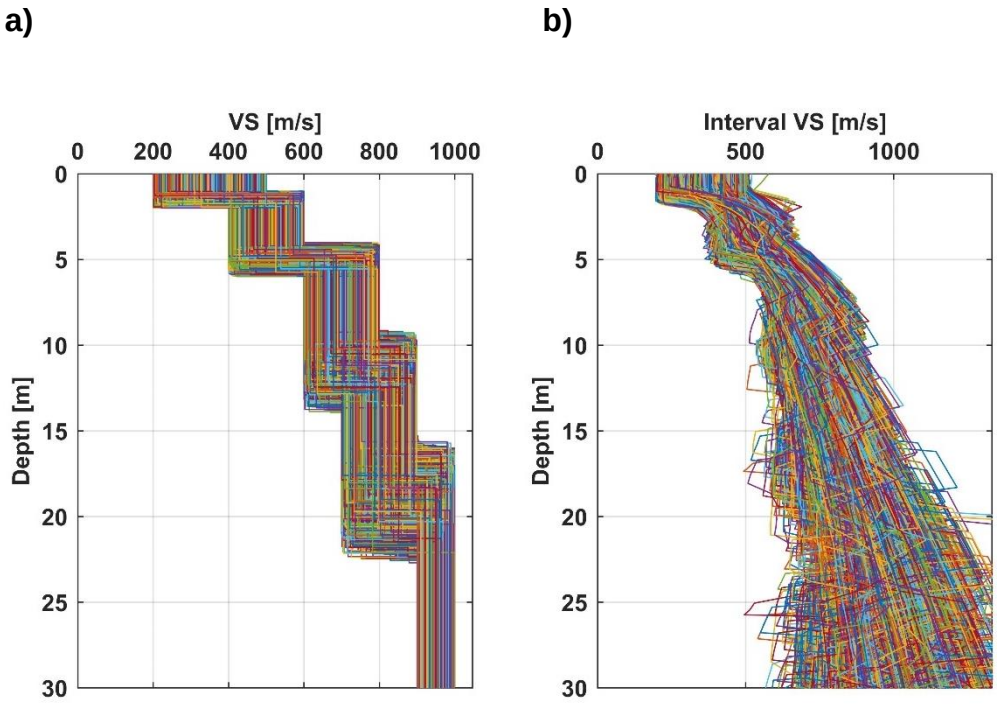

Source: Prepared by the author

4.3.5 Noise Level: 2%

When 2% noise was applied (Figure 34a and Figure 34b), the optimum regularization parameter was still 10 (Figure 35) . The synthetic profiles (Figure 36a) and the estimated interval VS (Figure 36b) had still a good definition for the top layers, but the bottom ones turned into a chaotic fan-like shaped, with an average error of 7.1%.

The α distribution has spread to all its range, reaching for the first time the maximum value, but only for an insignificant amount of profiles. With the noise increase and the α being kept constant, the simulated profiles started to lose resolution also for the middle layers.

Figure 34 - 2% noise (a) True and Noisy DC (b) True and Noisy f-k

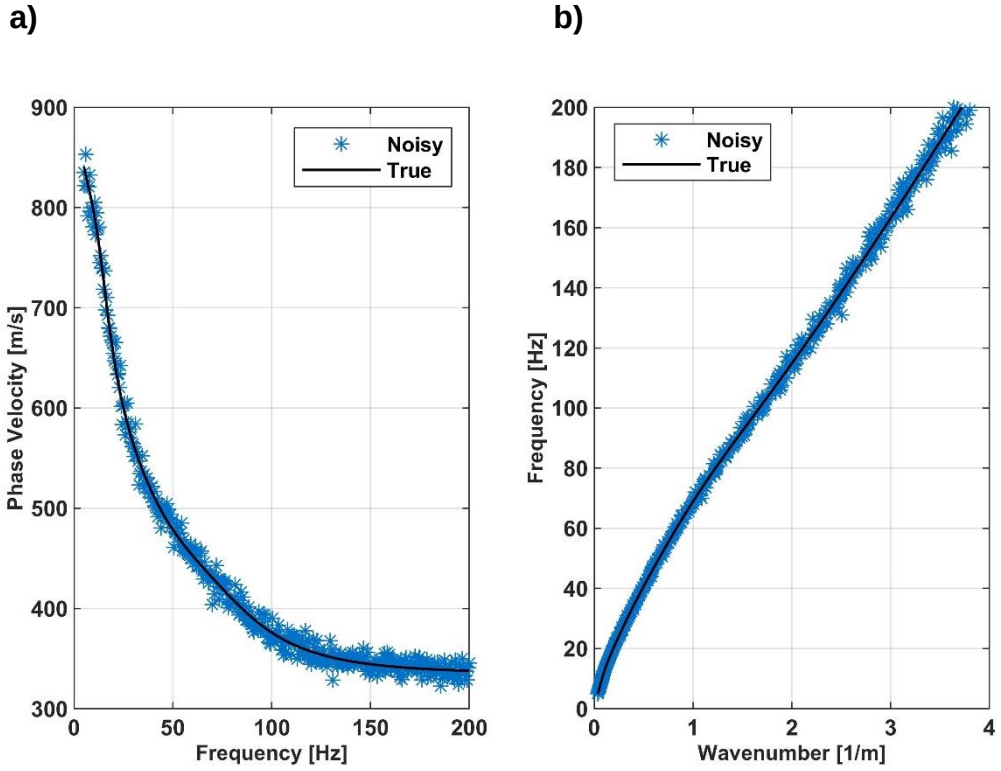

Source: Prepared by the author

Figure 35 - Distribution of α – 2% noise

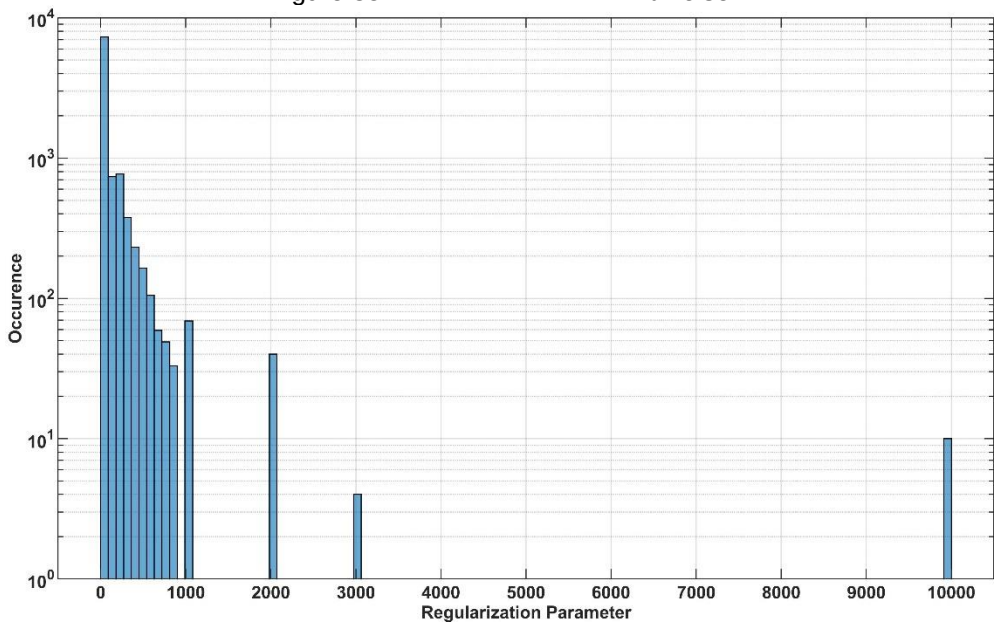

Source: Prepared by the author

Figure 36 - (a) Synthetic Profiles (b) Simulated Profiles – 2% noise

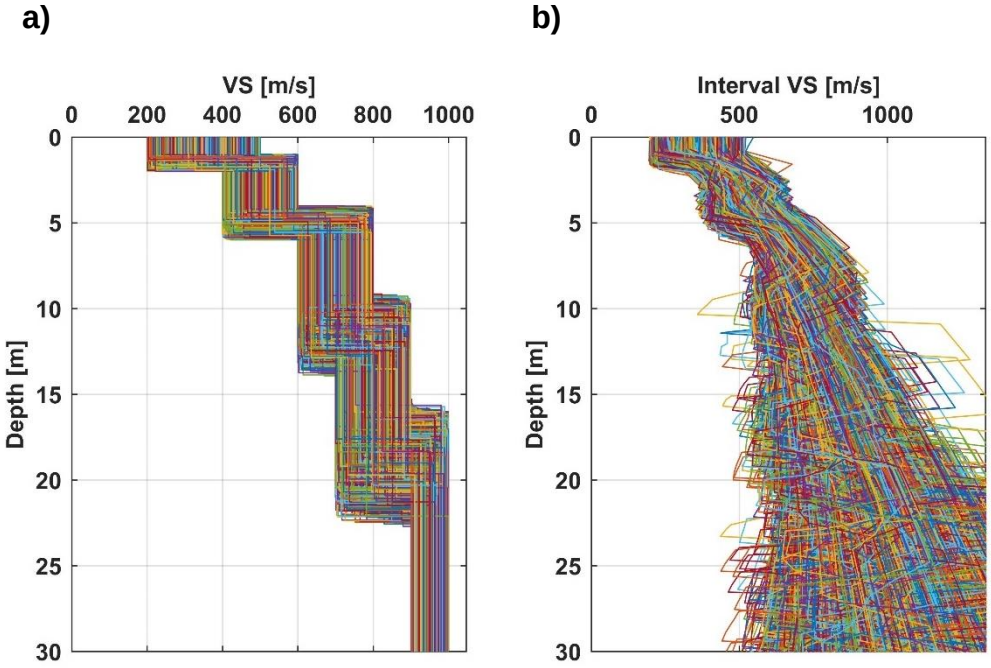

Source: Prepared by the author

4.3.6 Noise Level: 2.5%

When 2.5% noise (Figure 37a and Figure 37b) was applied, the optimum regularization parameter had jumped to 200 (Figure 38). As the α value has increased, the estimated interval VS (Figure 39b) got slimmer than in (Figure 36b), as in the synthetic profiles (Figure 39a), but with definition only for the shallower layers. The average error was 6.2%.

Figure 37 - 2.5% noise (a) True and Noisy DC (b) True and Noisy f-k

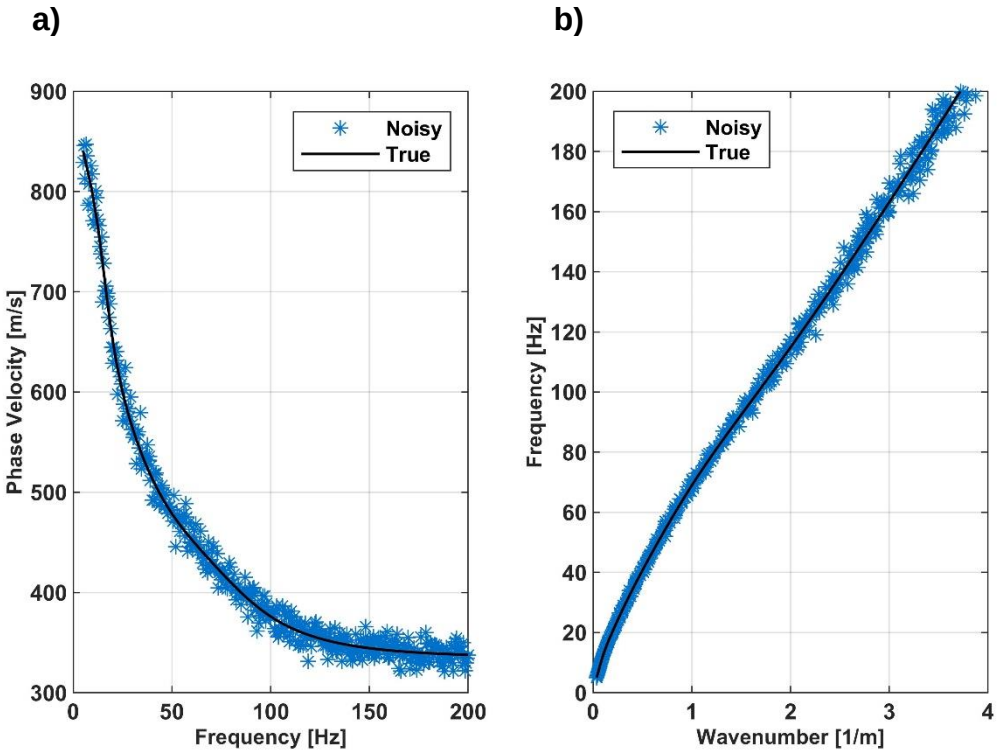

Source: Prepared by the author

Figure 38 - Distribution of α – 2.5% noise

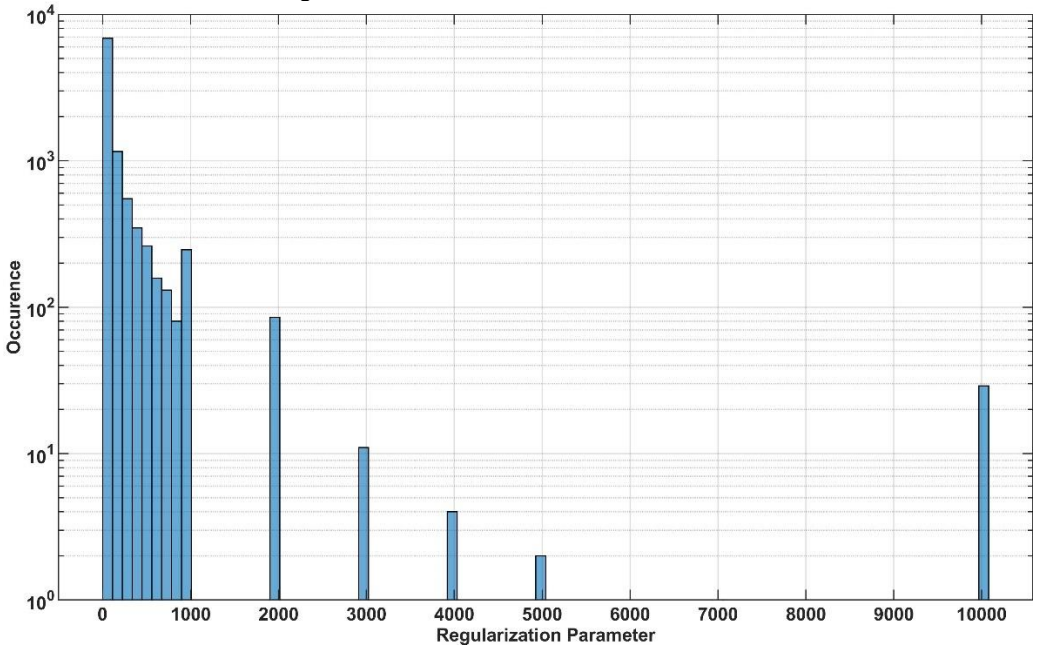

Source: Prepared by the author

Figure 39 - (a) Synthetic Profiles (b) Simulated Profiles – 2.5% noise

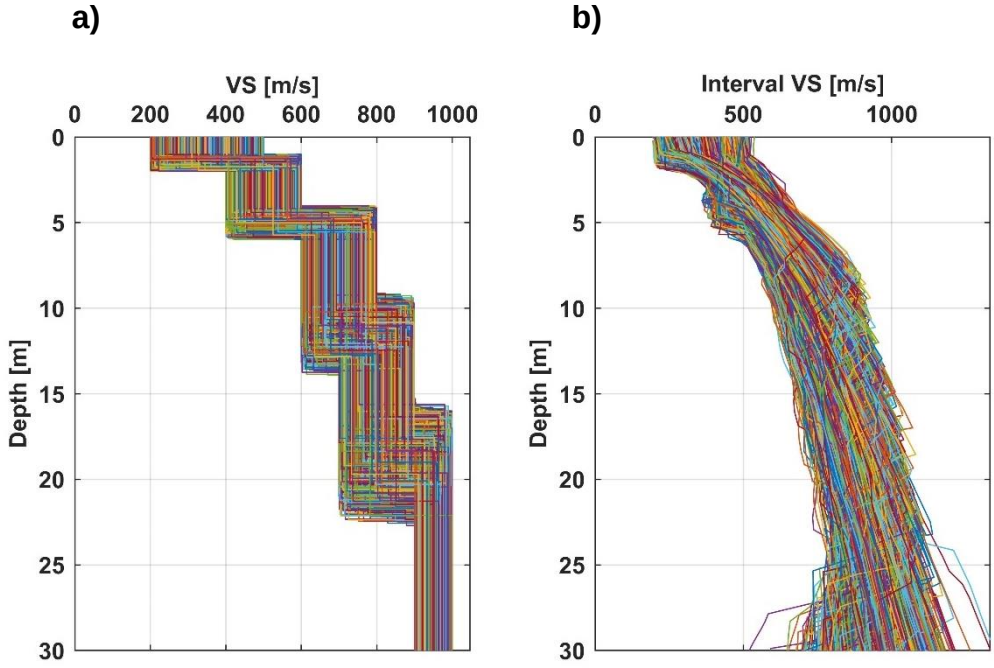

Source: Prepared by the author

4.3.7 Noise Level: 3%

When 3% noise (Figure 40a and Figure 40b) was applied, the optimum regularization parameter was also 200 (Figure 41). The estimated interval VS (Figure 42b) has definition only in the first shallower layers in respect to the synthetic profiles (Figure 42a). The average error was 6.4%.

As the noise increases, the number of profiles which best α had larger values increased as well, tendency being observed all over the simulation results.

Figure 40 - 3% noise (a) True and Noisy DC (b) True and Noisy f-k

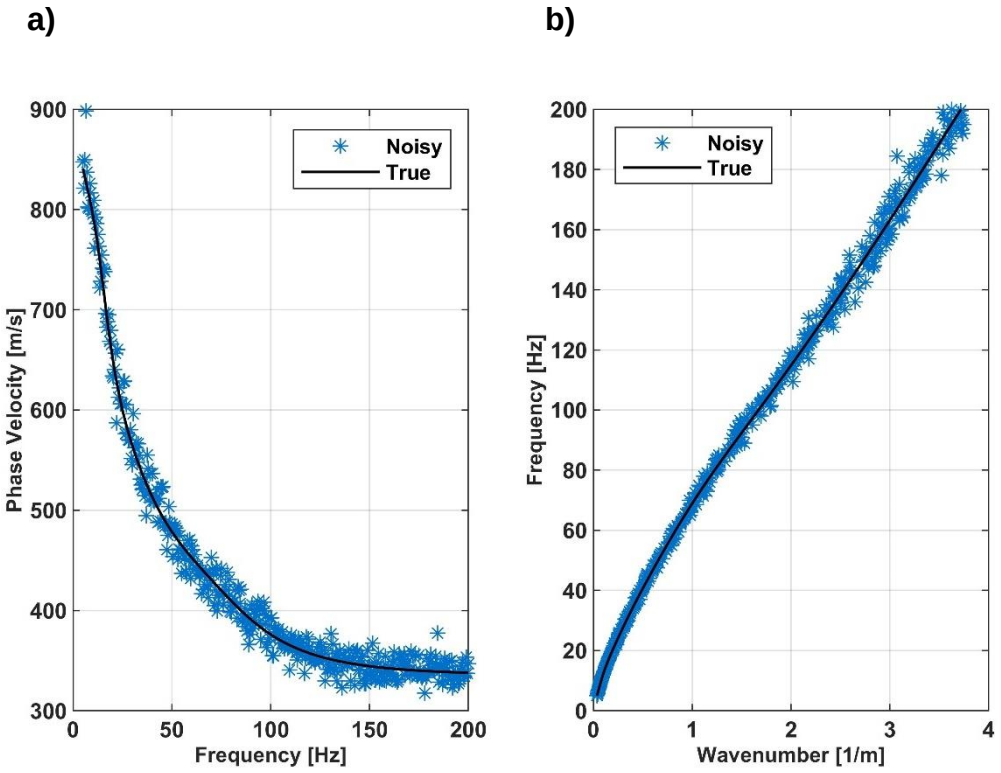

Source: Prepared by the author

Figure 41 - Distribution of α – 3% noise

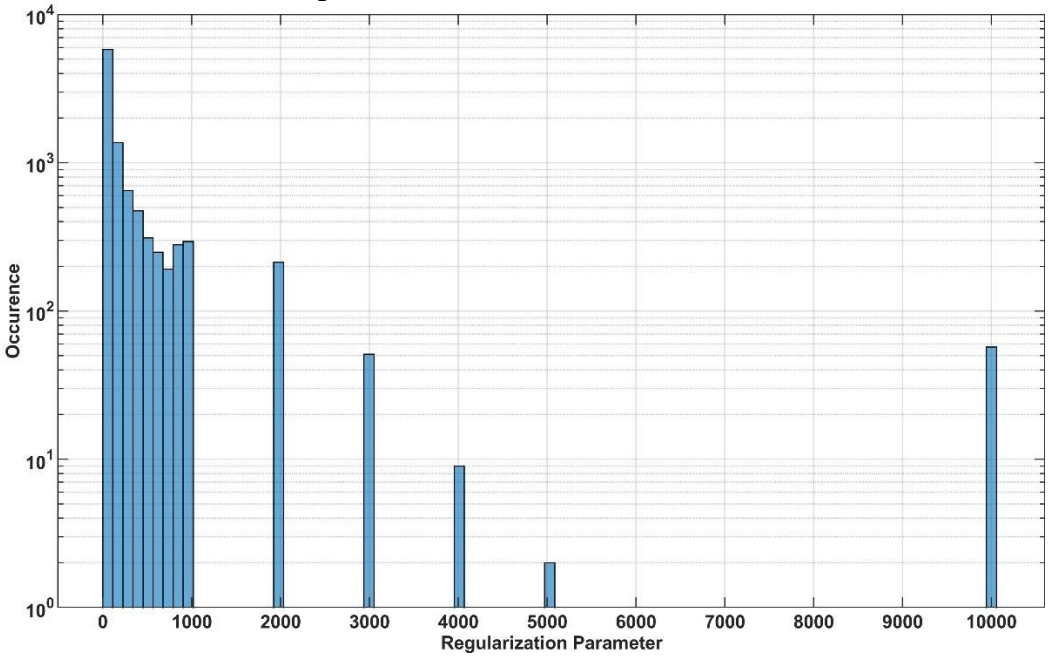

Source: Prepared by the author

Figure 42 - (a) Synthetic Profiles (b) Simulated Profiles – 3% noise

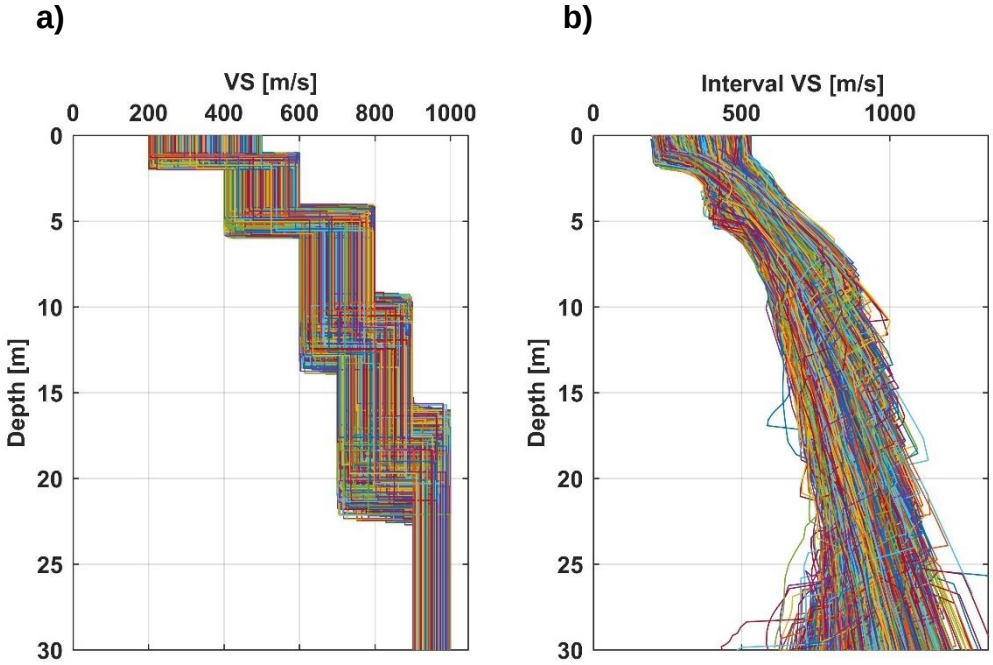

Source: Prepared by the author

4.3.8 Noise Level: 3.5%

When 3.5% noise was applied (Figure 43a and Figure 43b), the optimum regularization parameter was 200 (Figure 44). In comparison with the synthetic profiles (Figure 45a), the estimated interval VS (Figure 45b) is quite similar to the previous noise level (Figure 42b). The average error was 6.8% number that had been increasing steadily with the disturbance in the dataset.

Figure 43 - 3.5% noise (a) True and Noisy DC (b) True and Noisy f-k

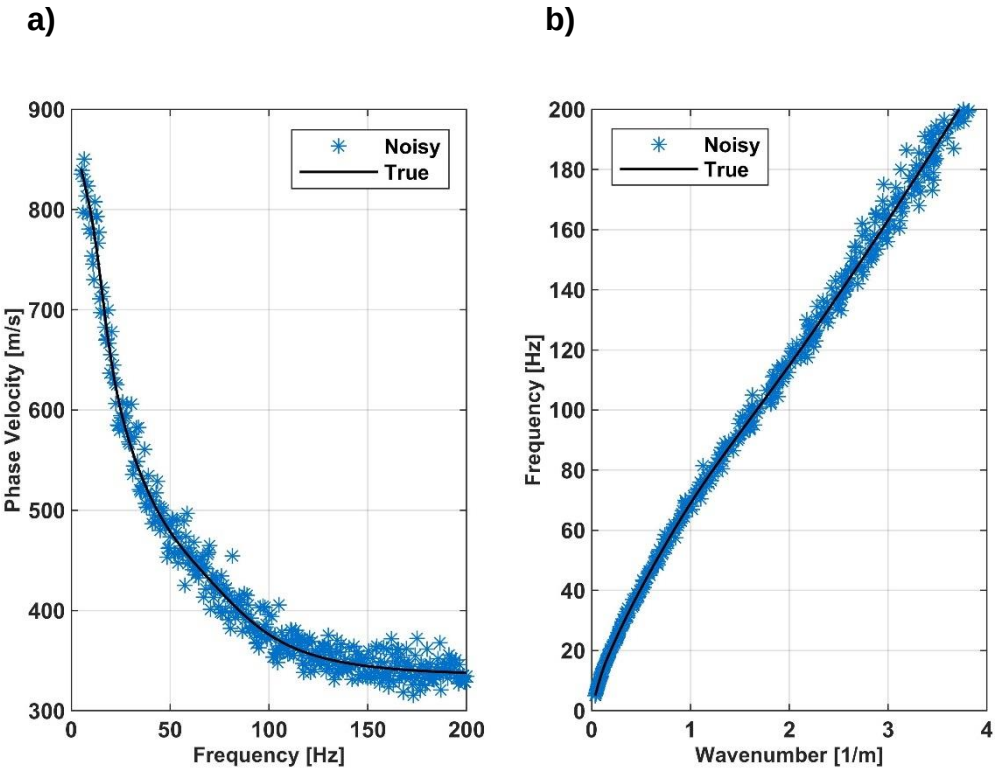

Source: Prepared by the author

Figure 44 - Distribution of α – 3.5% noise

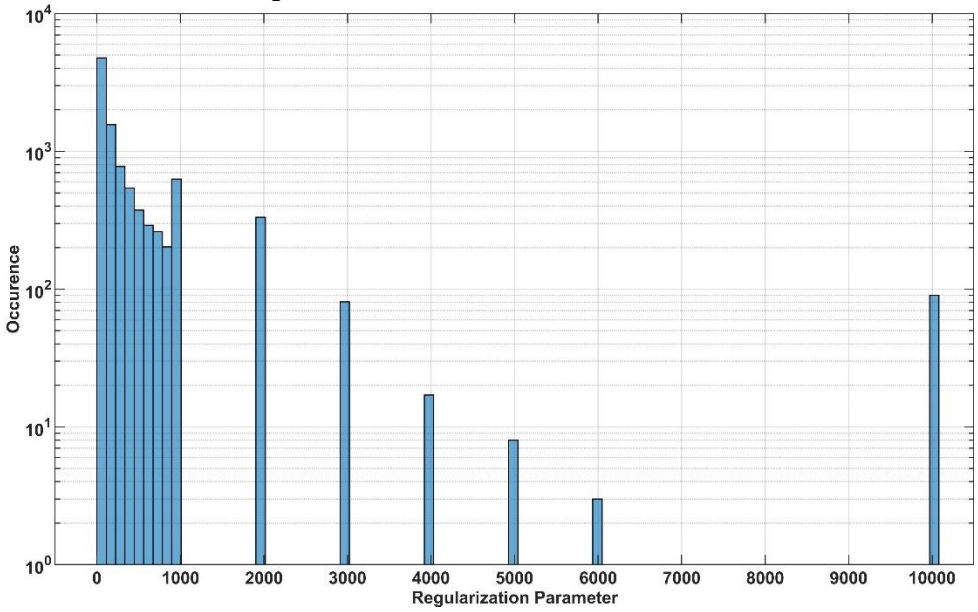

Source: Prepared by the author

Figure 45 - (a) Synthetic Profiles (b) Simulated Profiles – 3.5% noise

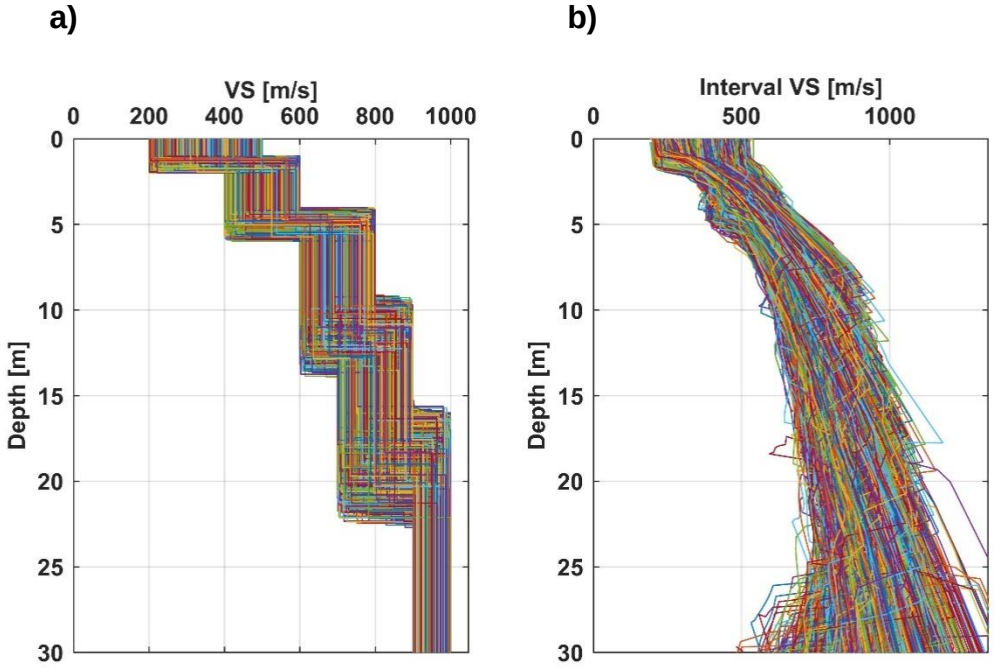

Source: Prepared by the author

4.3.9 Noise Level: 4%

When 4% noise was applied (Figure 46a and Figure 46b), the optimum regularization parameter was 200 (Figure 47). The synthetic profiles (Figure 48a) and the estimated interval VS (Figure 48b) present an the average error of 7%, with very close results to the previous noise level.

Figure 46 - 4% noise (a) True and Noisy DC (b) True and Noisy f-k

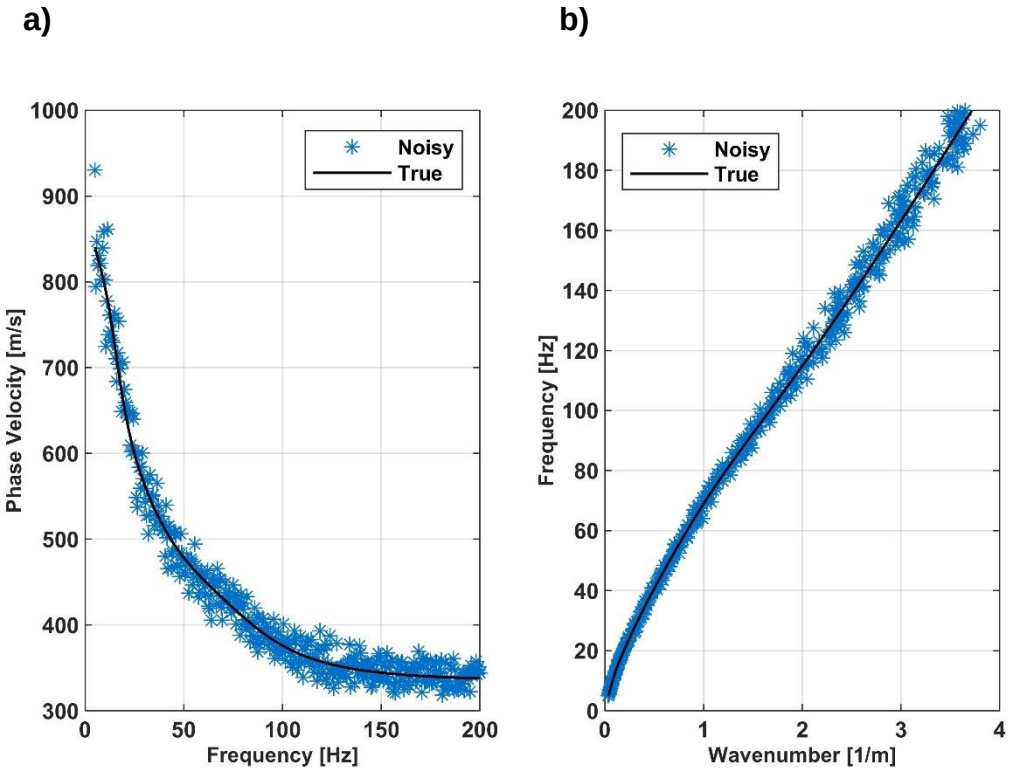

Source: Prepared by the author

Figure 47 - Distribution of α – 4% noise

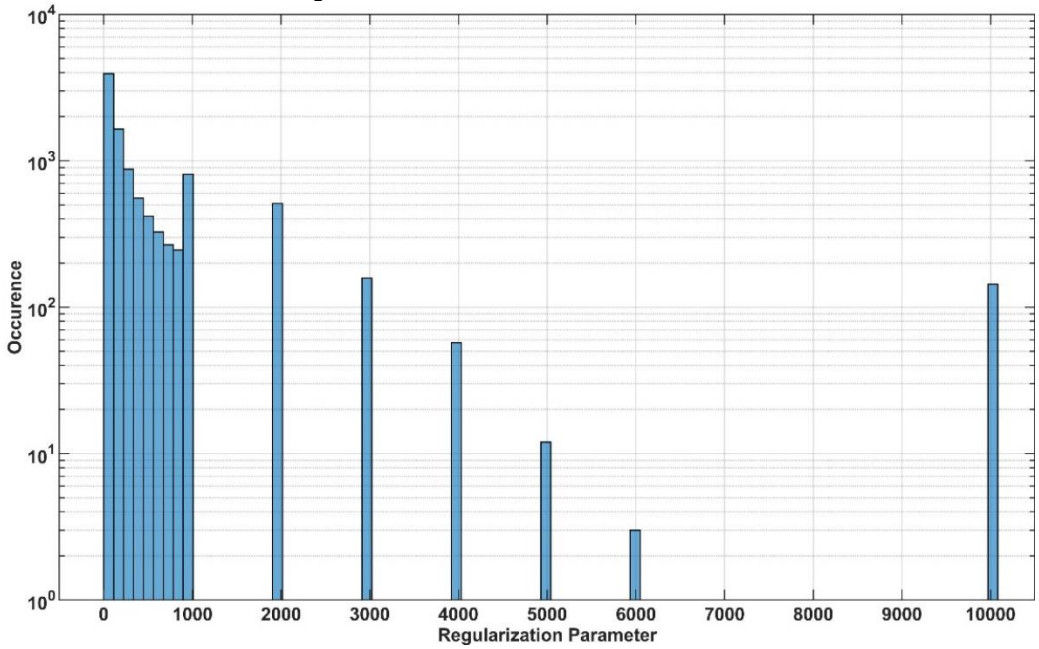

Source: Prepared by the author

Figure 48 - (a) Synthetic Profiles (b) Simulated Profiles – 4% noise

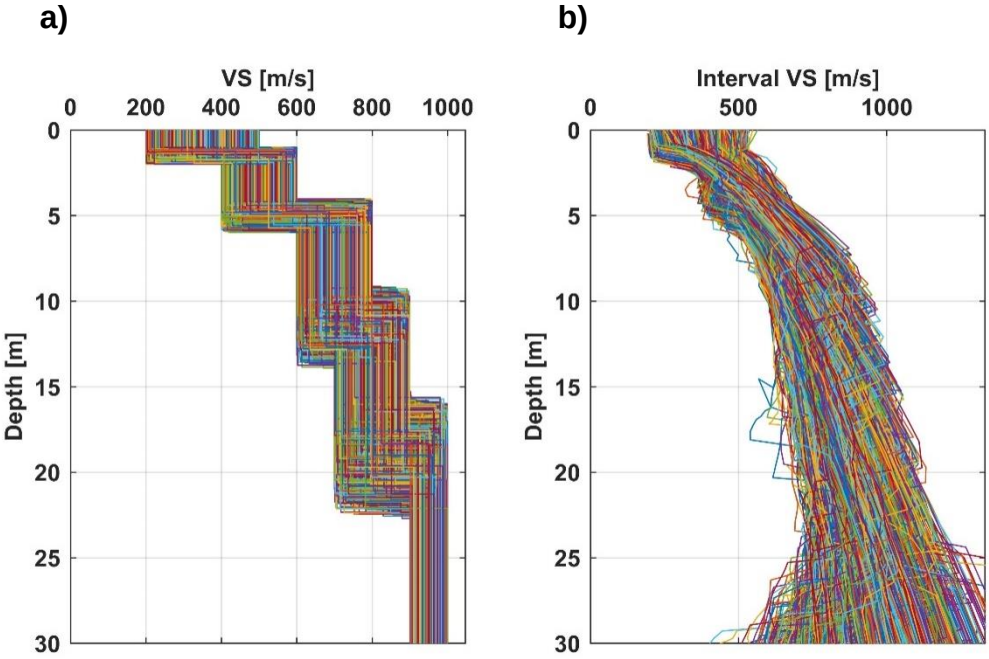

Source: Prepared by the author

4.3.10 Noise Level: 4.5%

When 4.5% noise was applied (Figure 49a and Figure 49b), the optimum regularization parameter was 200 (Figure 50). The synthetic profiles (Figure 51a) and the estimated interval VS (Figure 51b) had an average error of 8%, with the bottom layers once more becoming fan-like shaped.

The α frequency distribution has tended to higher values. Even though the vast majority of models are concentrated with values lower than 1000, a considerable amount had 2000 as the best parameter.

Figure 49 - 4.5% noise (a) True and Noisy DC (b) True and Noisy f-k

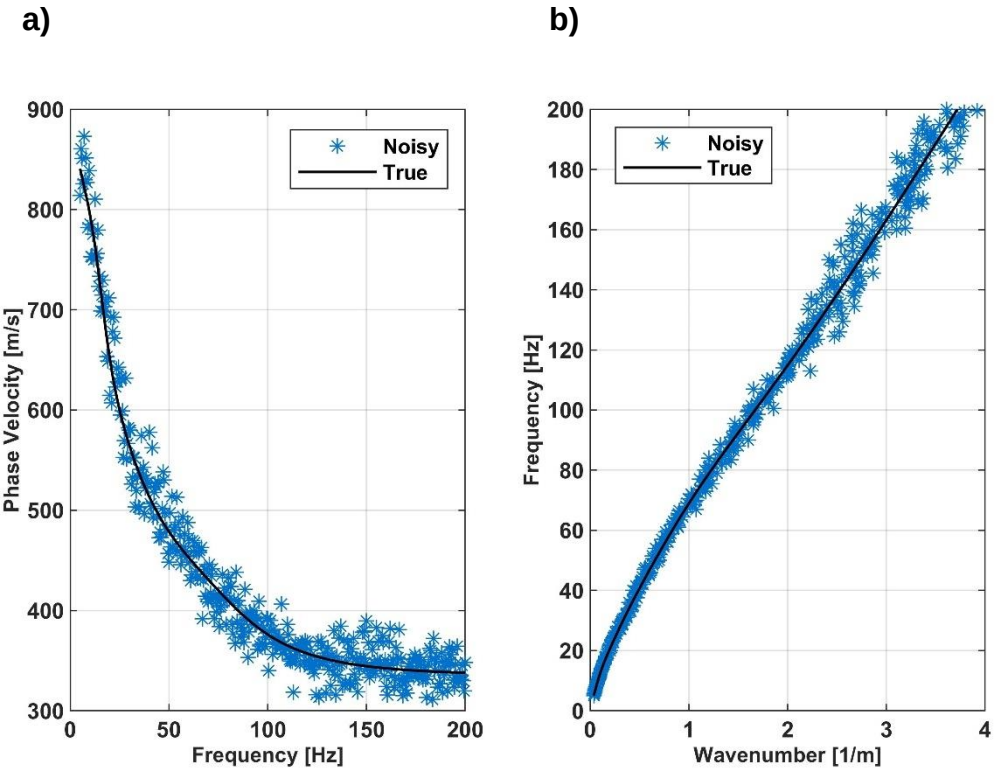

Source: Prepared by the author

Figure 50 - Distribution of α – 4.5% noise

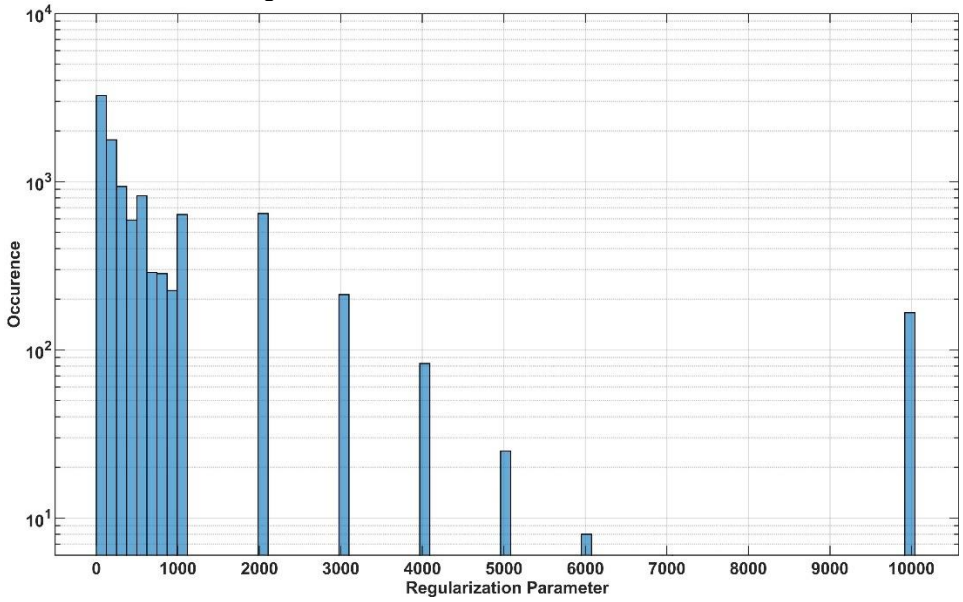

Source: Prepared by the author

Figure 51 - (a) Synthetic Profiles (b) Simulated Profiles – 4.5% noise

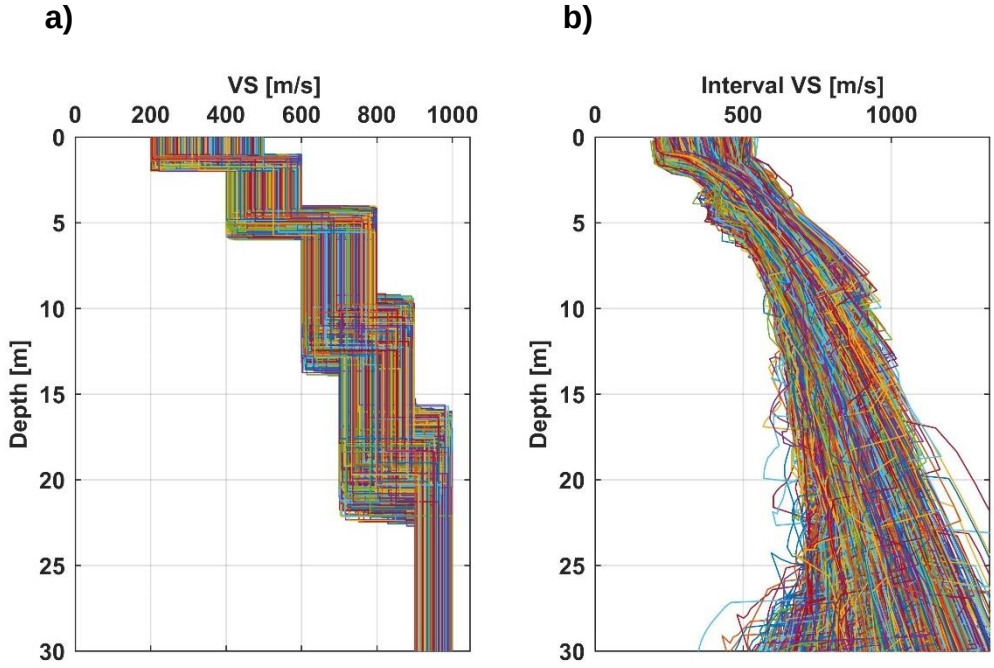

Source: Prepared by the author

4.3.11 Noise Level: 5%

When 5% noise (Figure 52a and Figure 52b) was applied, the optimum regularization parameter was 200 (Figure 53). The synthetic profiles (Figure 54a) and the estimated interval VS (Figure 54b) had an average error of 7.5%. The estimated models, apart from the first two, have lost the resolution, starting to look tangled and widespread.

The α occurrence distribution continued to increase: more models had their best α 10,000, but the distribution remains concentrated for 2,000 or less.

Figure 52 - 5% noise (a) True and Noisy DC (b) True and Noisy f-k

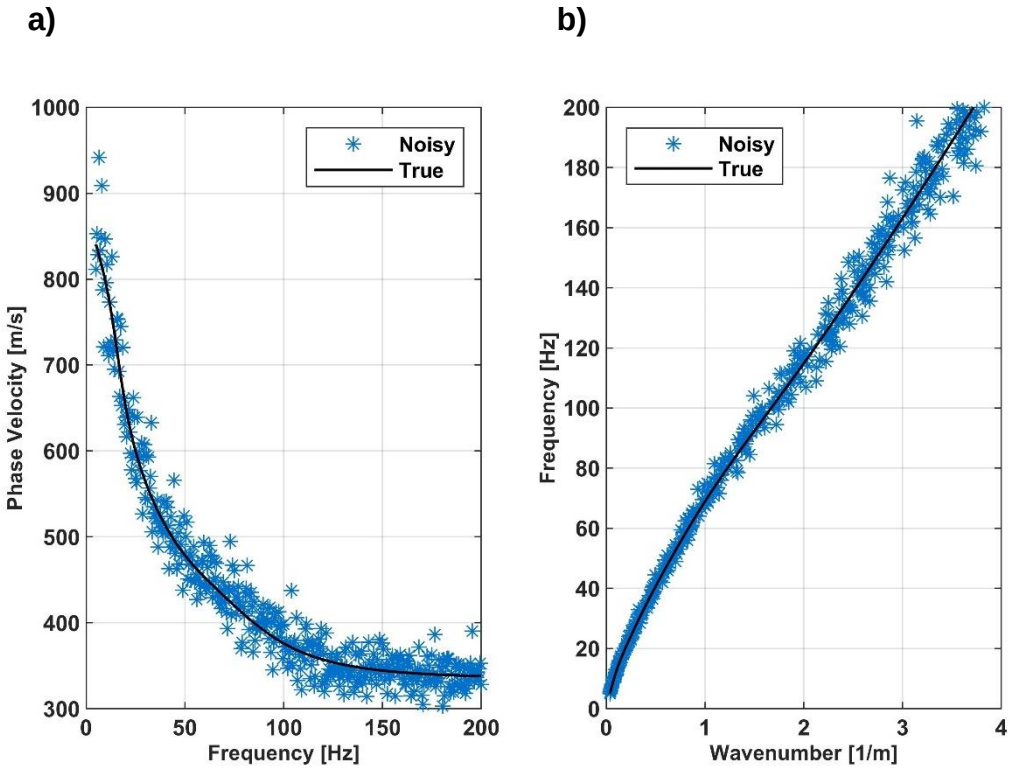

Source: Prepared by the author

Figure 53 - Distribution of α – 5% noise

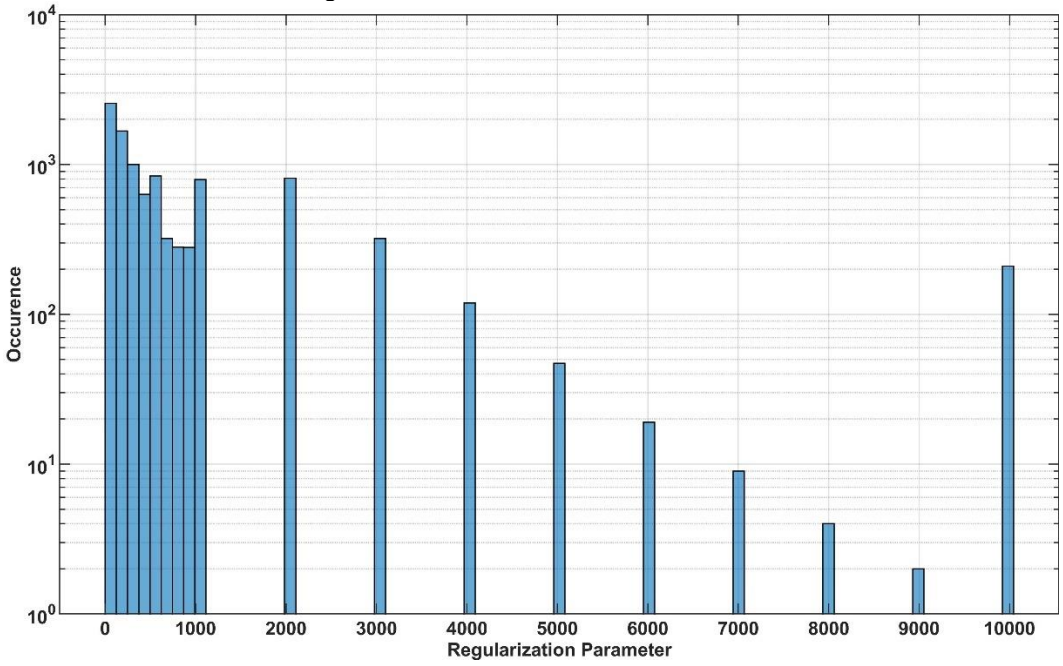

Source: Prepared by the author

Figure 54 - (a) Synthetic Profiles (b) Simulated Profiles – 5% noise

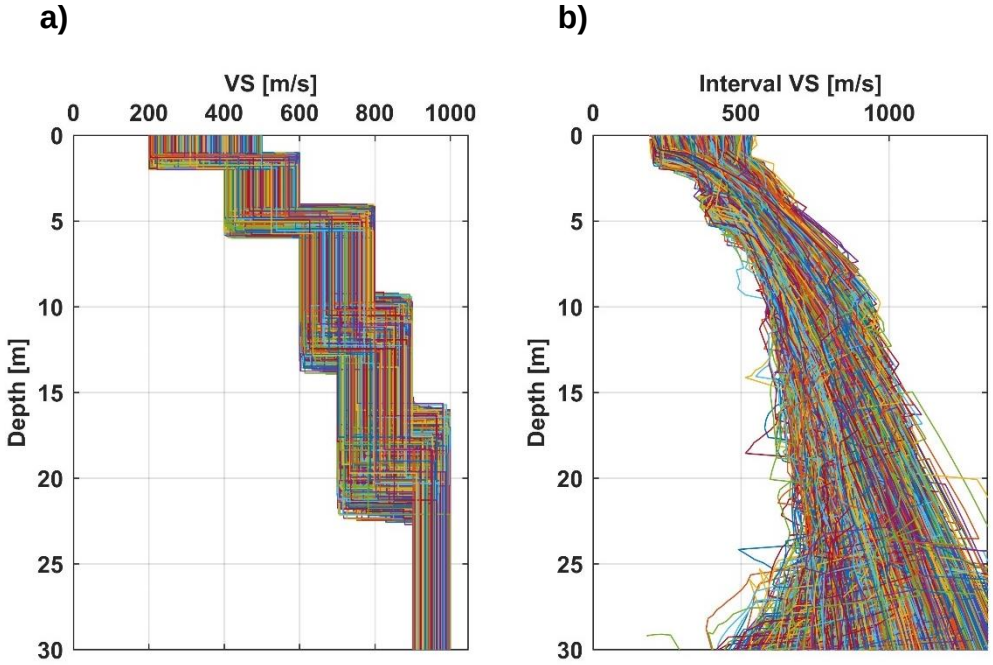

Source: Prepared by the author

4.3.12 Noise Level: 5.5%

When 5.5% noise was applied (Figure 55a and Figure 55b), the optimum regularization parameter was 200 (Figure 56). The synthetic profiles (Figure 57a) and the estimated interval VS (Figure 57b) had an average error of 8.6%.

The number of models with higher α values continue to increase with the noise, and since the optimum α has been constant, the simulated profiles do not have a slim-shape anymore.

Figure 55 - 5.5% noise (a) True and Noisy DC (b) True and Noisy f-k

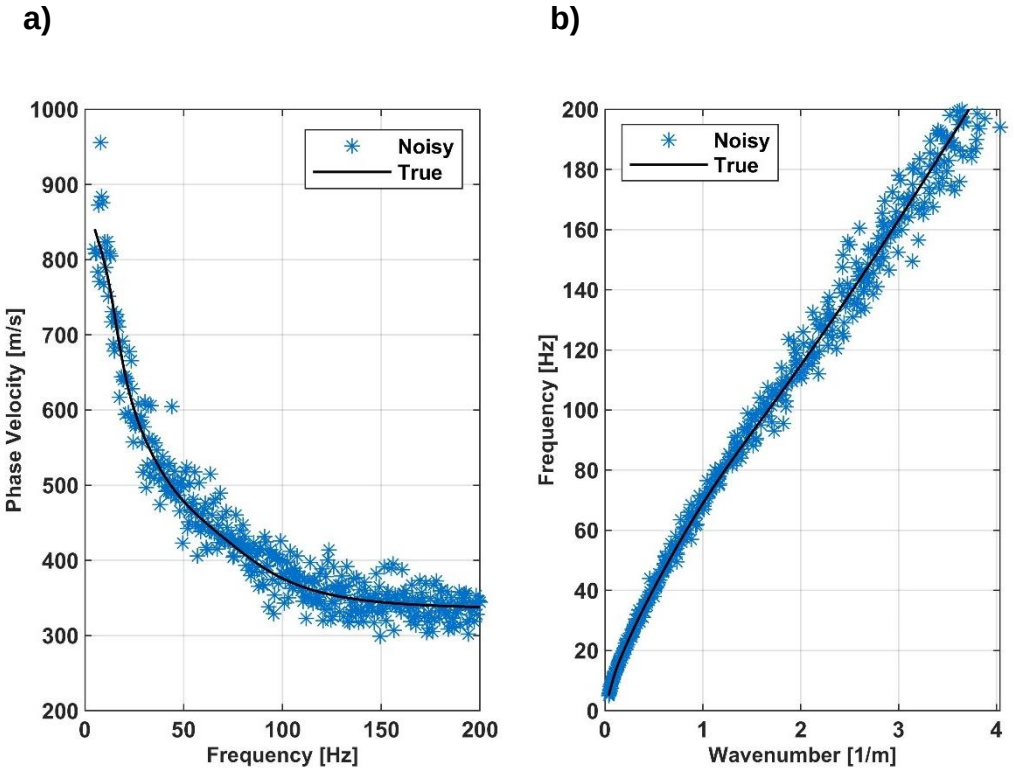

Source: Prepared by the author

Figure 56 - Distribution of α – 5.5% noise

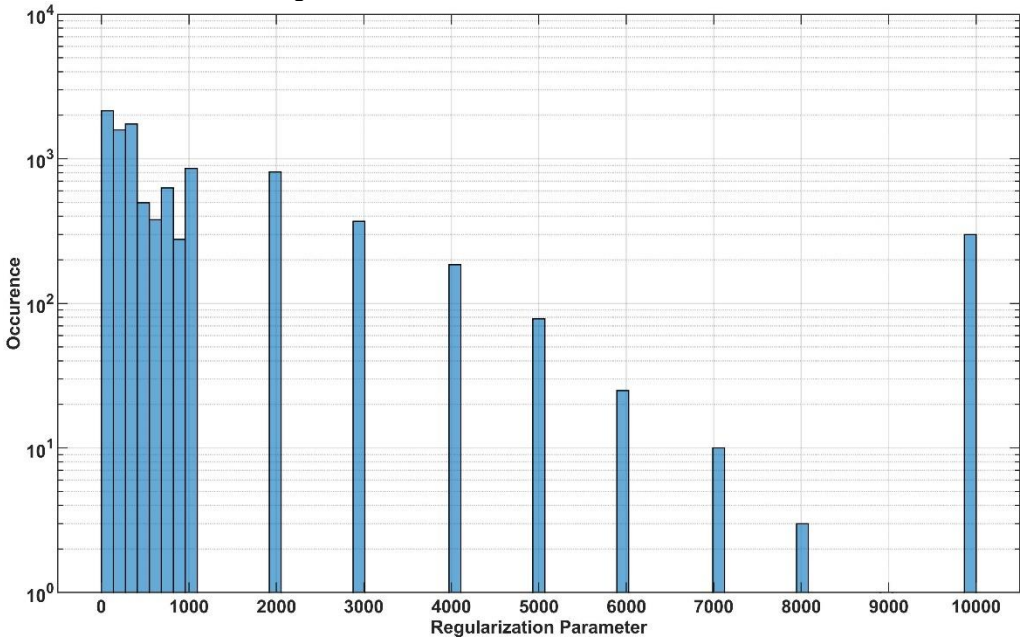

Source: Prepared by the author

Figure 57 - (a) Synthetic Profiles (b) Simulated Profiles – 5.5% noise

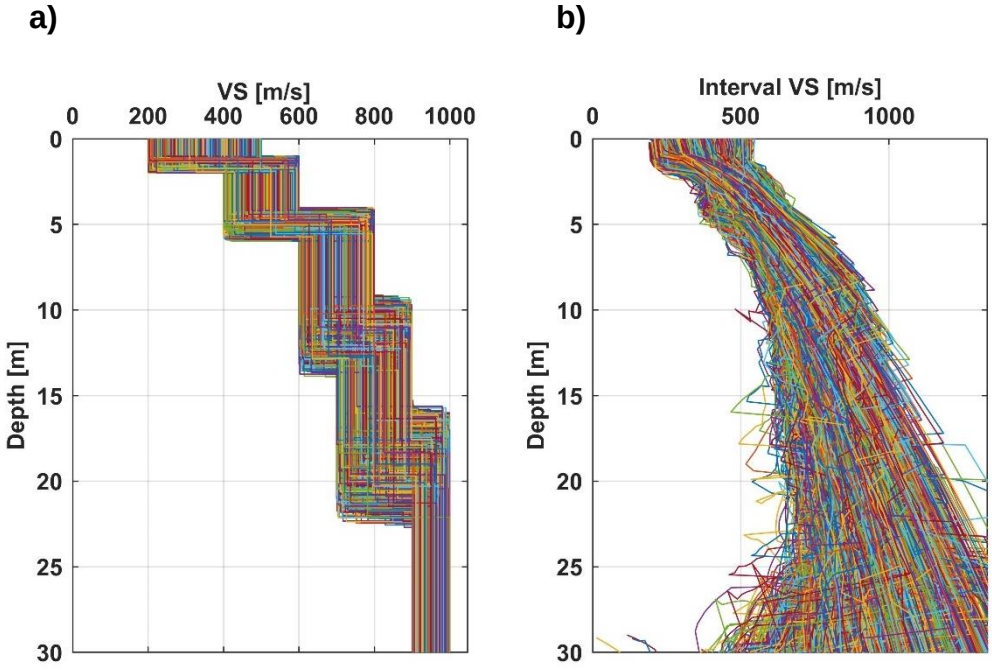

Source: Prepared by the author

4.3.13 Noise Level: 6%

When 6% noise was applied (Figure 58a and Figure 58b), the optimum regularization parameter was 200 (Figure 59). The synthetic profiles (Figure 60a) and the estimated interval VS (Figure 60b) had an average error of 8.1%.

Figure 58 - 6% noise (a) True and Noisy DC (b) True and Noisy f-k

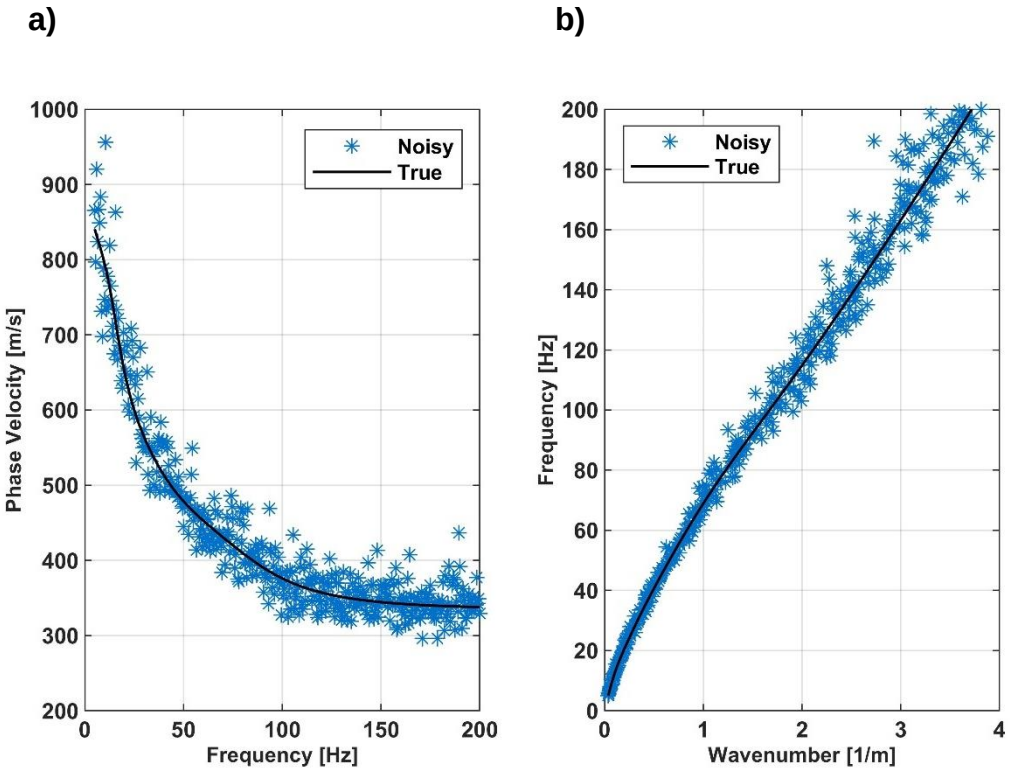

Source: Prepared by the author

Figure 59 - Distribution of α – 6% noise

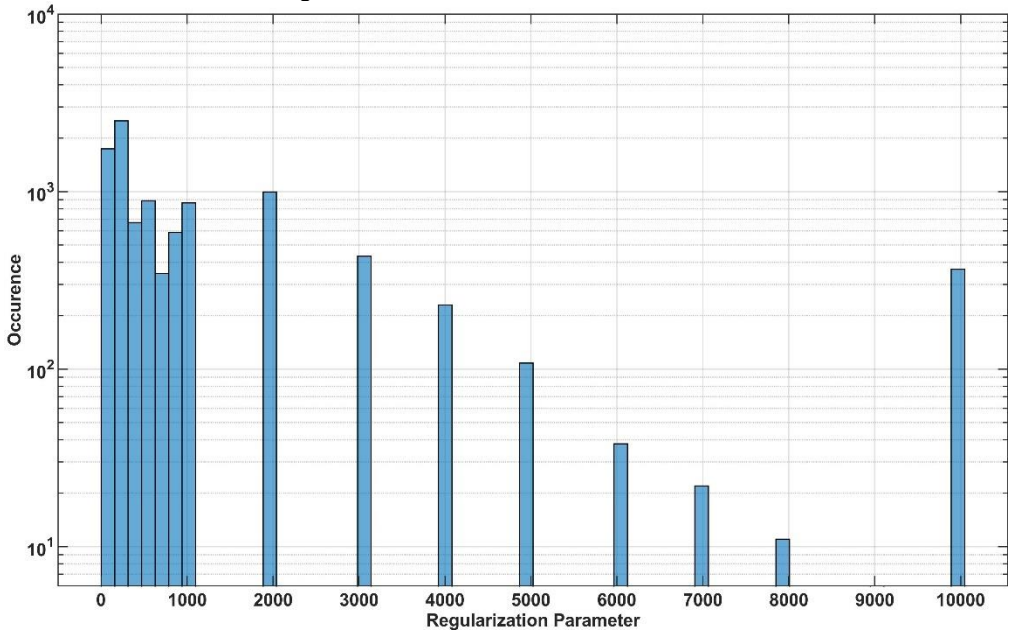

Source: Prepared by the author

Figure 60 - (a) Synthetic Profiles (b) Simulated Profiles – 6% noise

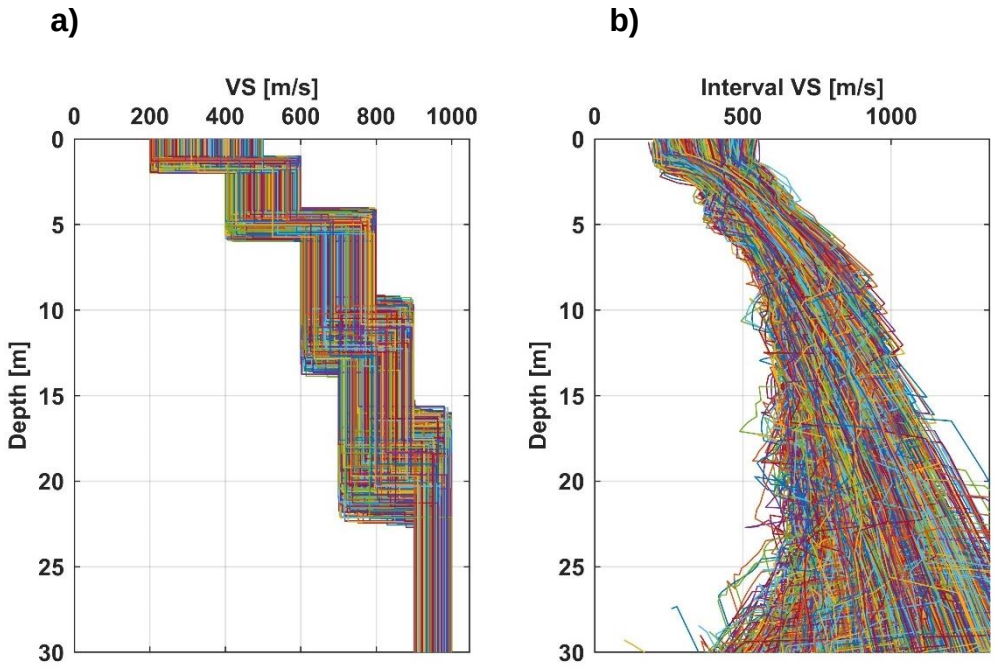

Source: Prepared by the author

4.3.14 Noise Level: 6.5%

When 6.5% noise was applied (Figure 61a and Figure 61b), the optimum regularization parameter was 200 (Figure 62). The synthetic profiles (Figure 63a) and the estimated interval VS (Figure 63b) had an average error of 8.4%, with a tangled, fan-like shape. A representative amount of profiles started to select high α values as their best parameter.

Figure 61 - 6.5% noise (a) True and Noisy DC (b) True and Noisy f-k

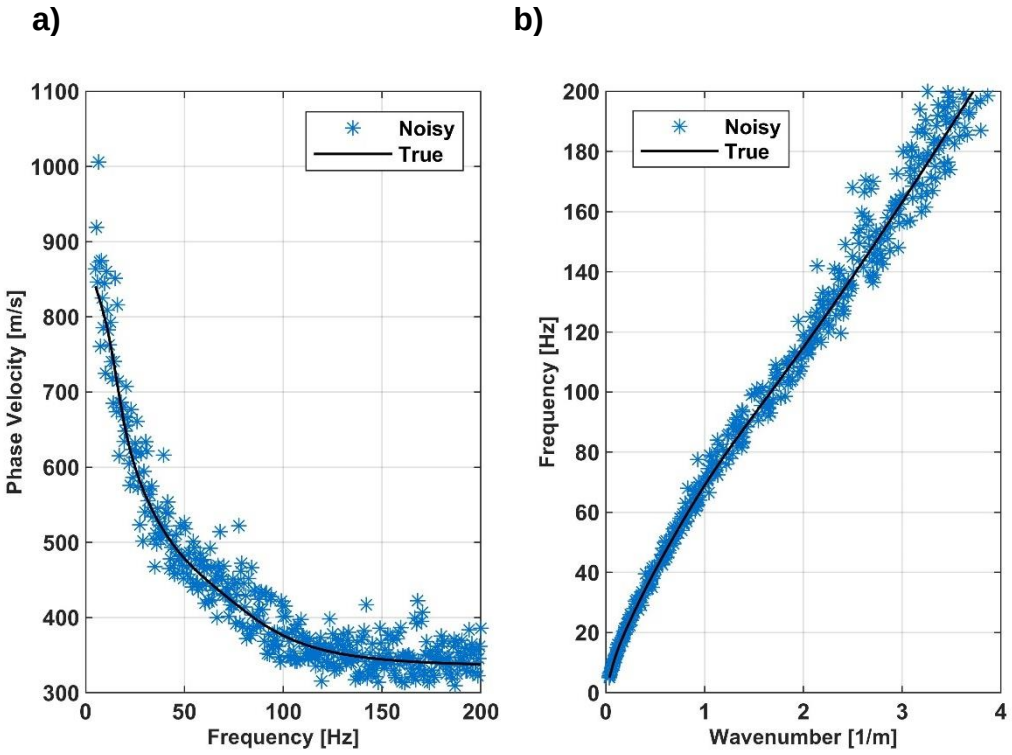

Source: Prepared by the author

Figure 62 - Distribution of α – 6.5% noise

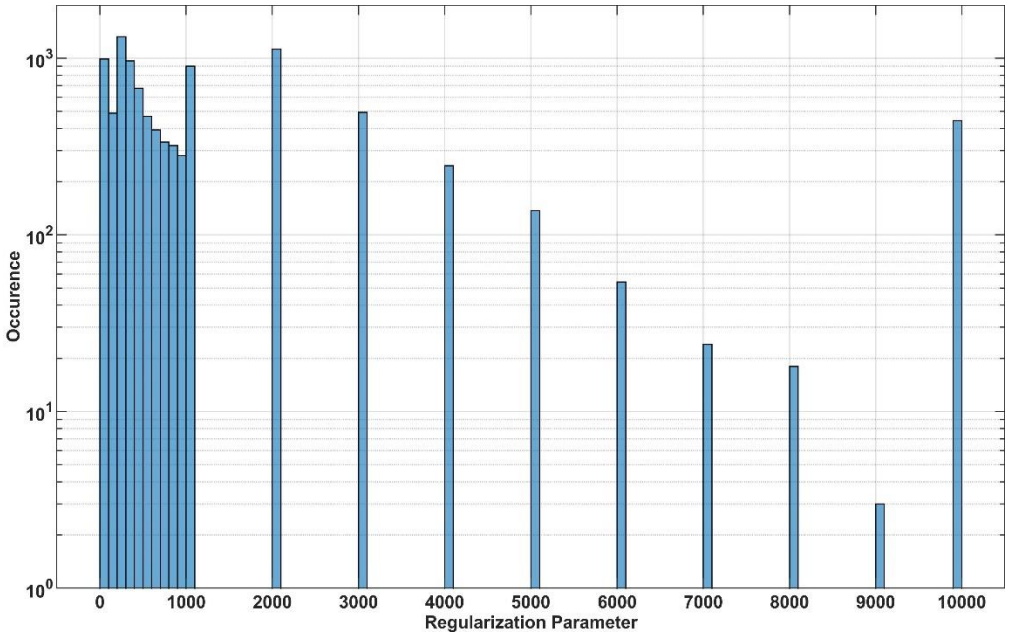

Source: Prepared by the author

Figure 63 - (a) Synthetic Profiles (b) Simulated Profiles – 6.5% noise

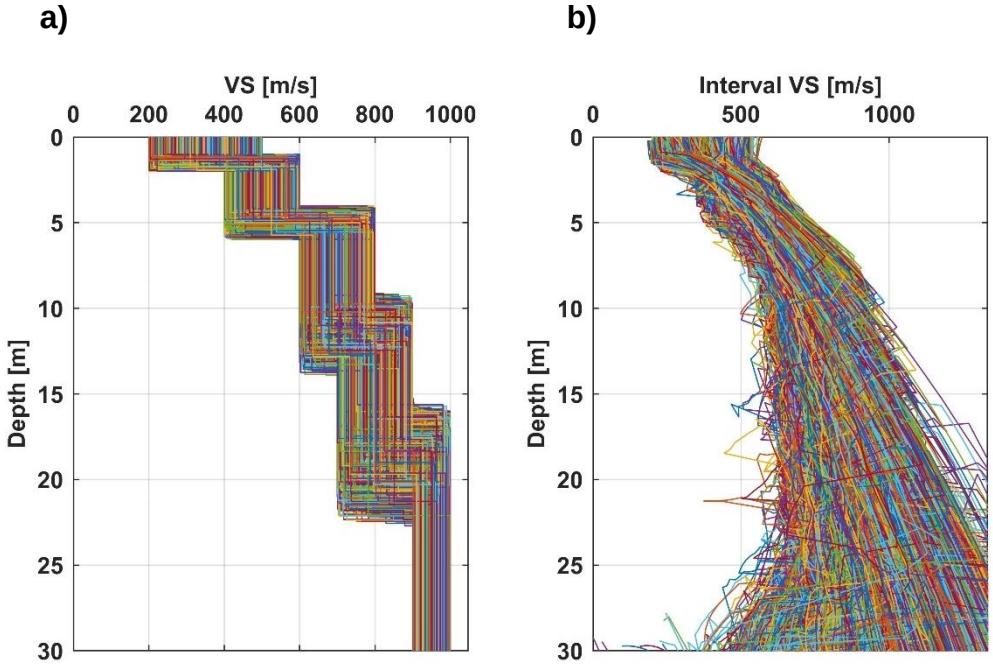

Source: Prepared by the author

4.3.15 Noise Level: 7%

When 7% noise was applied (Figure 64a and Figure 64b), the optimum regularization parameter was still 200 (Figure 65). The synthetic profiles (Figure 66a) and the estimated interval VS (Figure 66b) had an average error of 8.8%, with an intricate overall look, exhibiting no definition.

As the simulated profiles got more widespread with the constant increase of the noise, the α distribution got wider, signalizing that the optimum α was about to change.

Figure 64 - 7% noise (a) True and Noisy DC (b) True and Noisy f-k

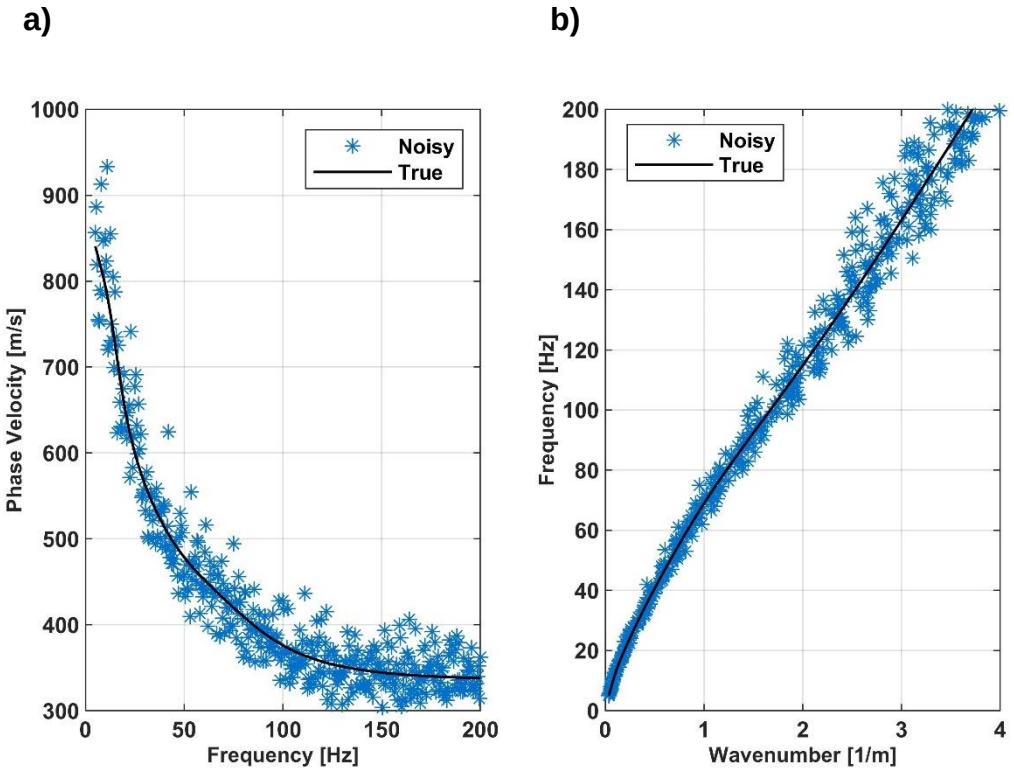

Source: Prepared by the author

Figure 65 - Distribution of α – 7% noise

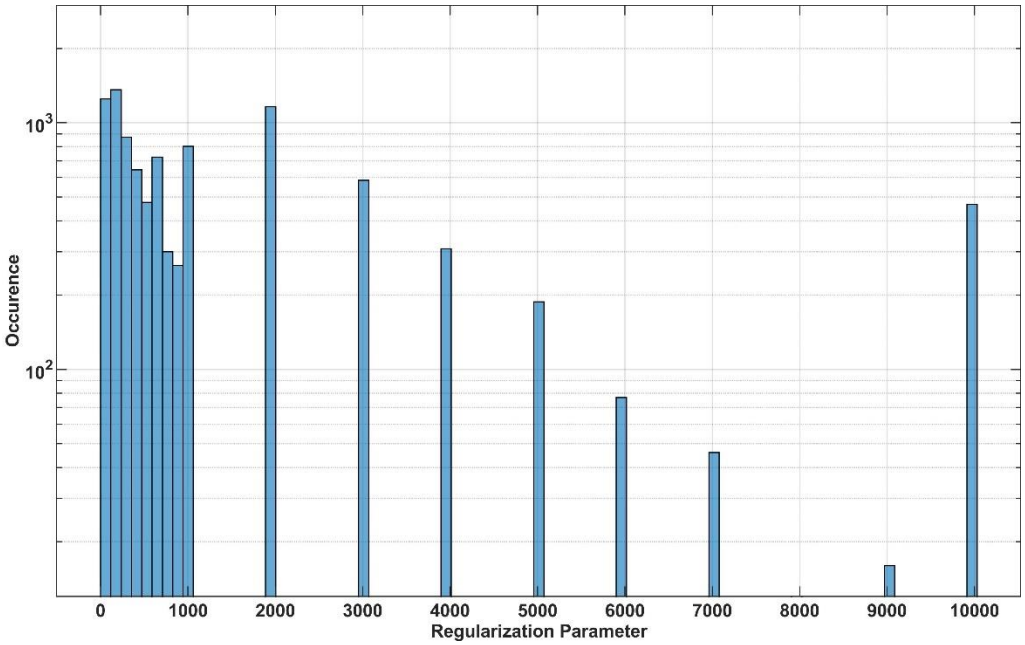

Source: Prepared by the author

Figure 66 - (a) Synthetic Profiles (b) Simulated Profiles – 7% noise

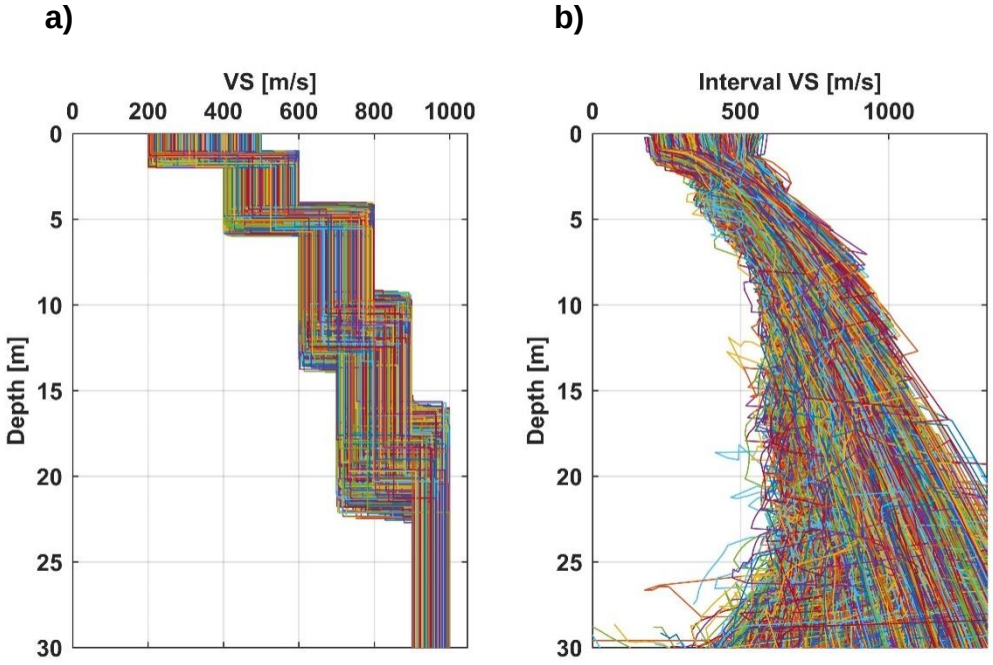

Source: Prepared by the author

4.3.16 Noise Level: 7.5%

When 7.5% noise was applied (Figure 67a and Figure 67b), the optimum regularization parameter jumped to 2000 (Figure 68). The synthetic profiles (Figure 69a) and the estimated interval VS (Figure 69b) had average error of 8.5%.

As the α value has increased, the simulated profiles got once more slim-shaped, but the layers resolution was lost.

Figure 67 - 7.5% noise (a) True and Noisy DC (b) True and Noisy f-k

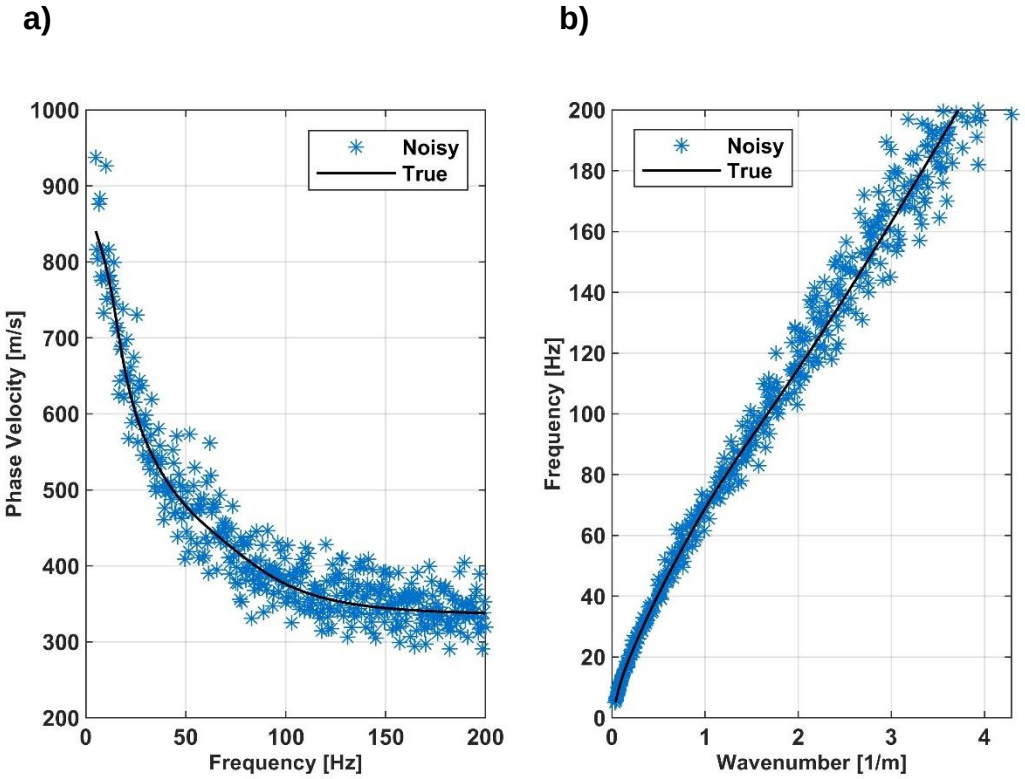

Source: Prepared by the author

Figure 68 - Distribution of α – 7.5% noise

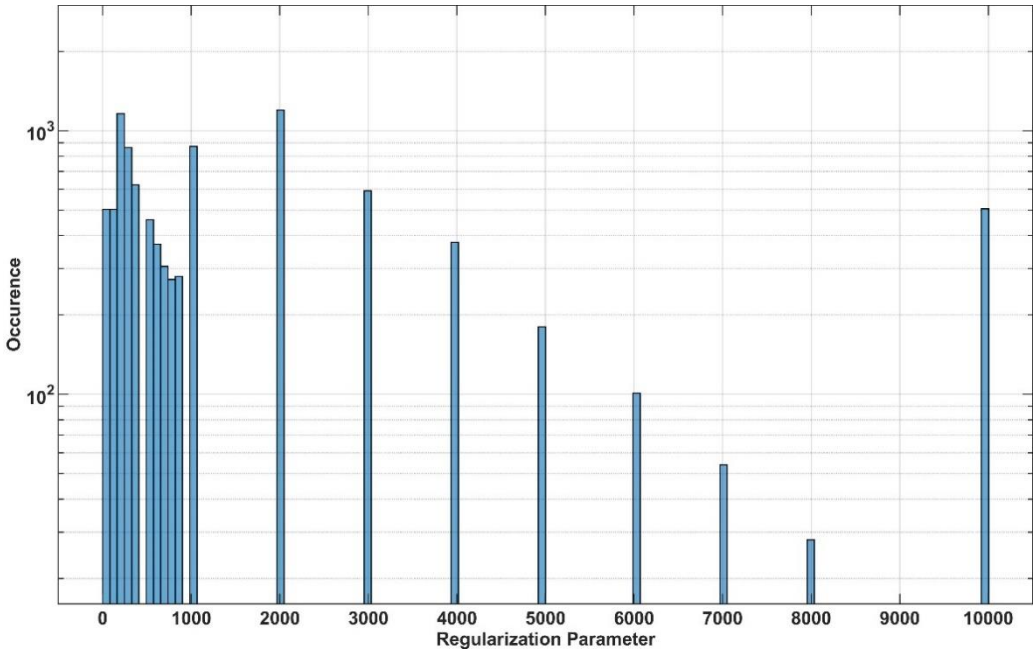

Source: Prepared by the author

Figure 69 - (a) Synthetic Profiles (b) Simulated Profiles – 7.5% noise

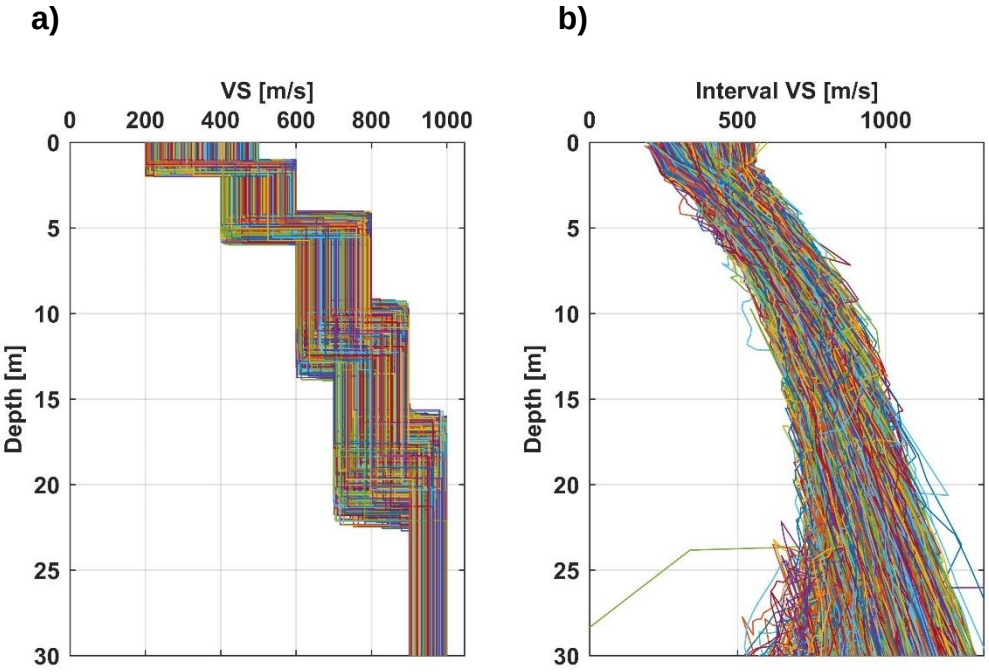

Source: Prepared by the author

4.3.17 Noise Level: 8%

When 8% noise was applied (Figure 70a and Figure 70b), the optimum regularization parameter has remained 2000 (Figure 71). The synthetic profiles (Figure 72a) and the estimated interval VS (Figure 72b) had an average error of 8.6%.

Figure 70 - 8% noise (a) True and Noisy DC (b) True and Noisy f-k

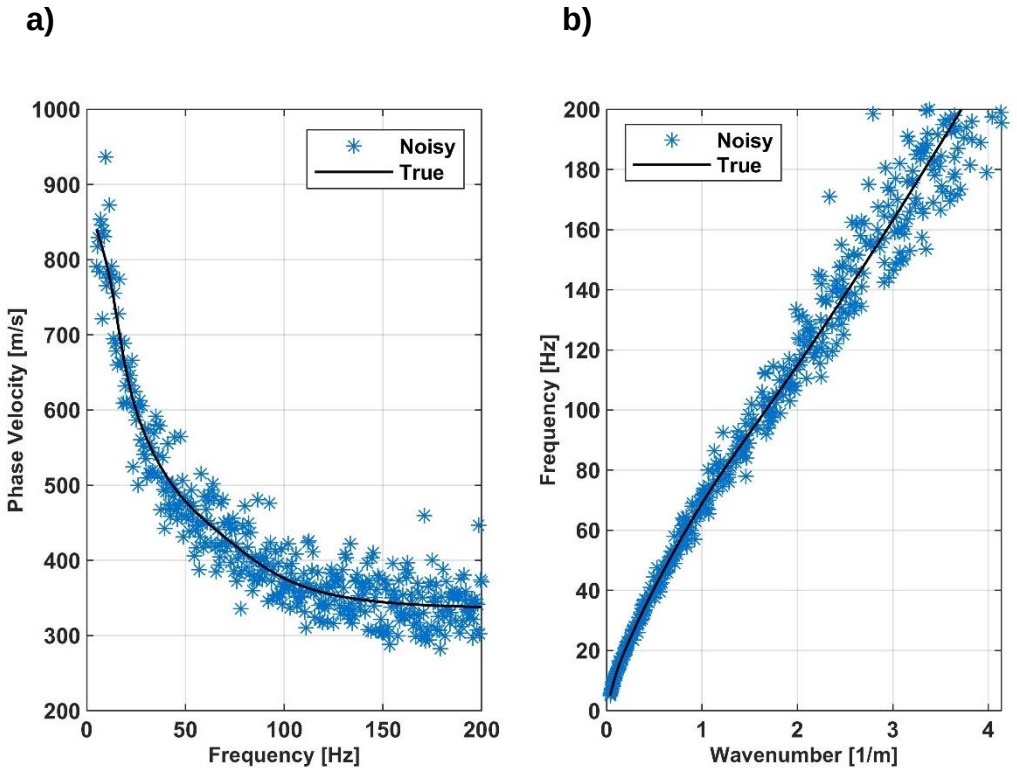

Source: Prepared by the author

Figure 71 - Distribution of α – 8% noise

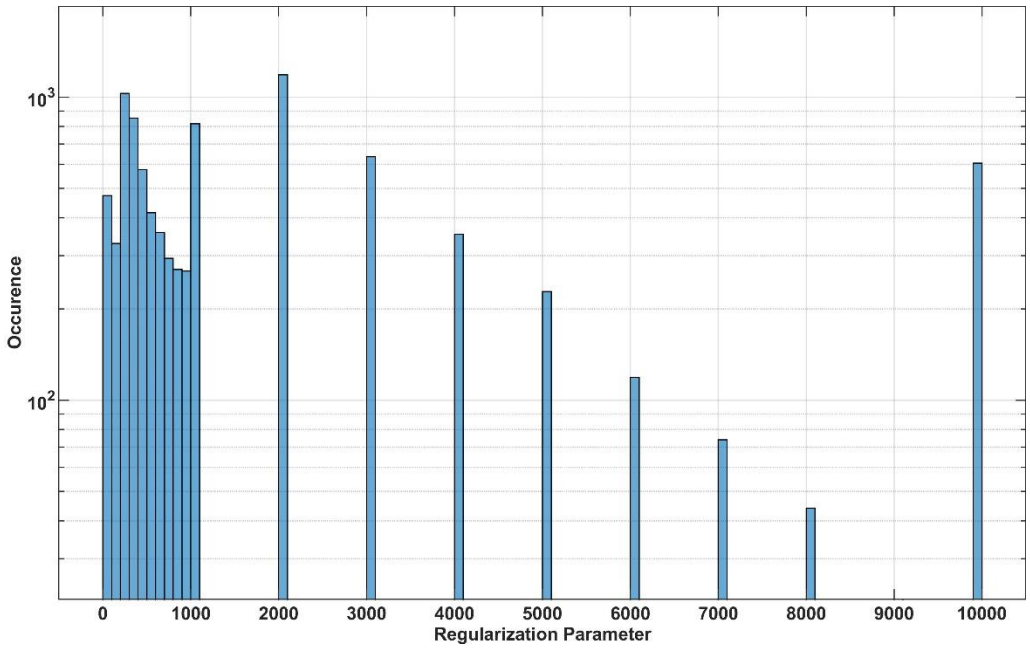

Source: Prepared by the author

Figure 72 - (a) Synthetic Profiles (b) Simulated Profiles – 8% noise

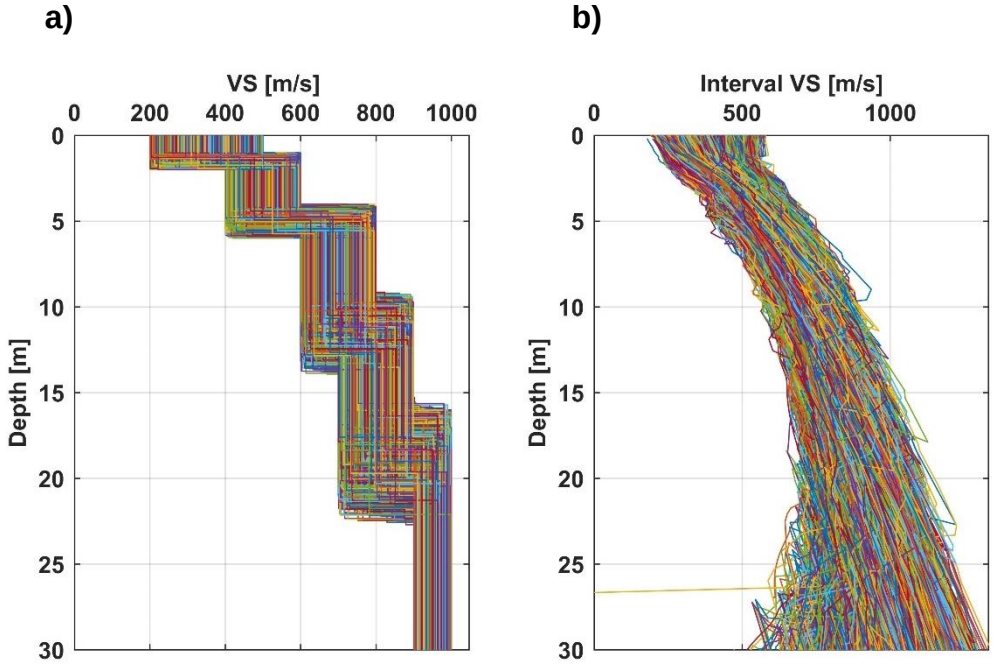

Source: Prepared by the author

4.3.18 Noise Level: 8.5%

When 8.5% noise was applied (Figure 73a and Figure 73b), the optimum regularization parameter was 2000 (Figure 74). The synthetic profiles (Figure 75a) and the estimated interval VS (Figure 75b) had an average error of 8.7%.

Regarding the α distribution, the number of models with best α equal to 10,000 had been increasing steadily.

Figure 73 - 8.5% noise (a) True and Noisy DC (b) True and Noisy f-k

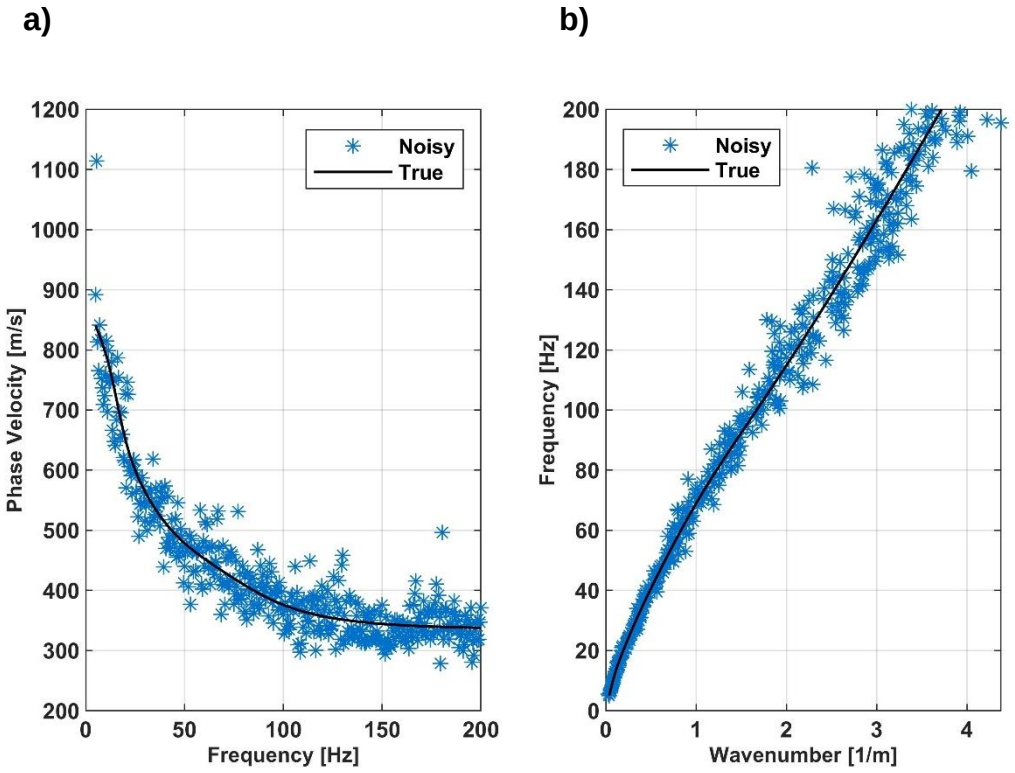

Source: Prepared by the author

Figure 74 - Distribution of α – 8.5% noise

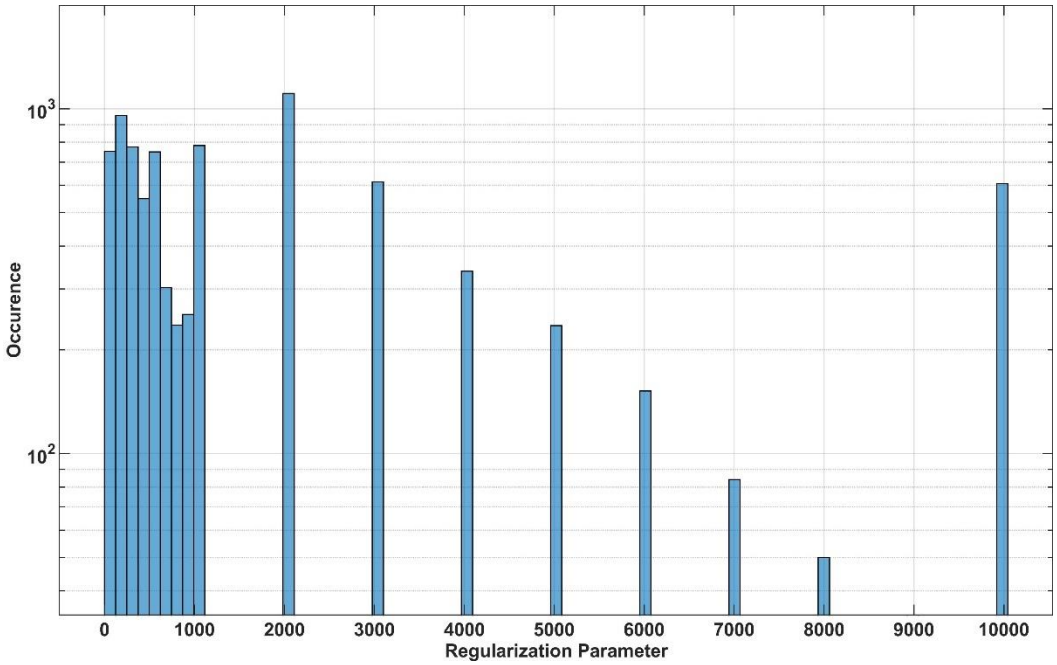

Source: Prepared by the author

Figure 75 - (a) Synthetic Profiles (b) Simulated Profiles – 8.5% noise

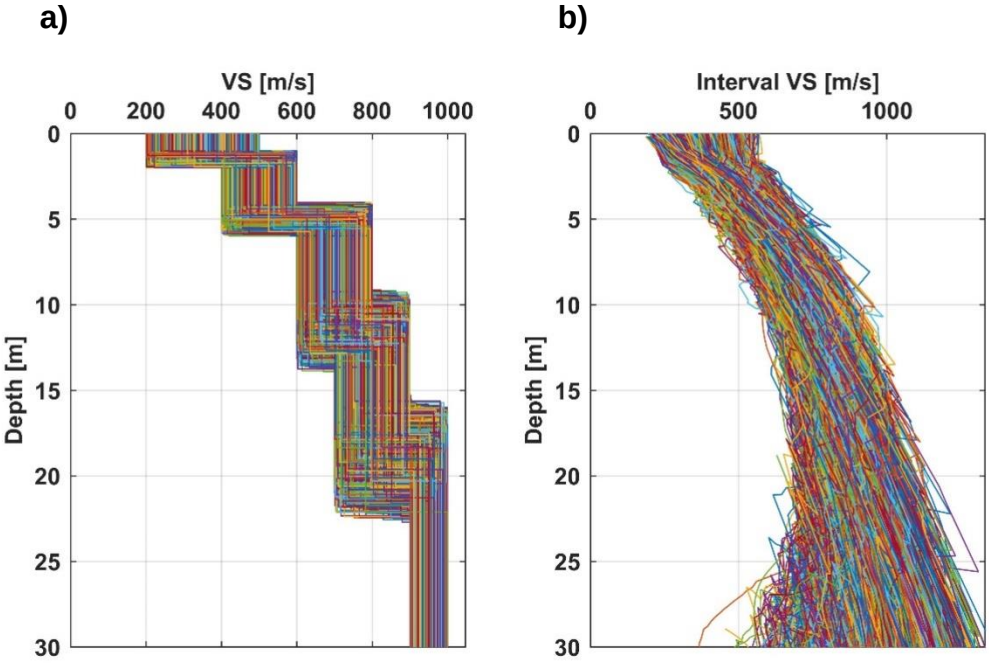

Source: Prepared by the author

4.3.19 Noise Level: 9%

When 9% noise was applied (Figure 76a and Figure 76b), the optimum regularization parameter was 2000 (Figure 77). The synthetic profiles (Figure 78a) and the estimated interval VS (Figure 78b) had an average error of 8.9%.

Figure 76 - 9% noise (a) True and Noisy DC (b) True and Noisy f-k

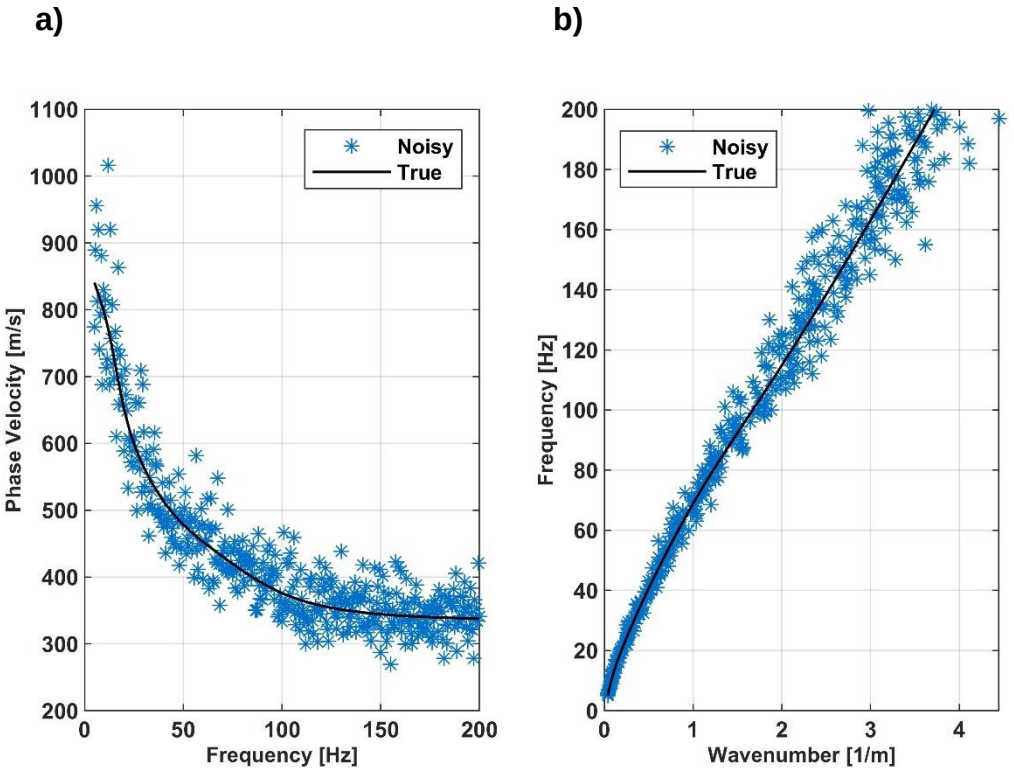

Source: Prepared by the author

Figure 77 - Distribution of α – 9% noise

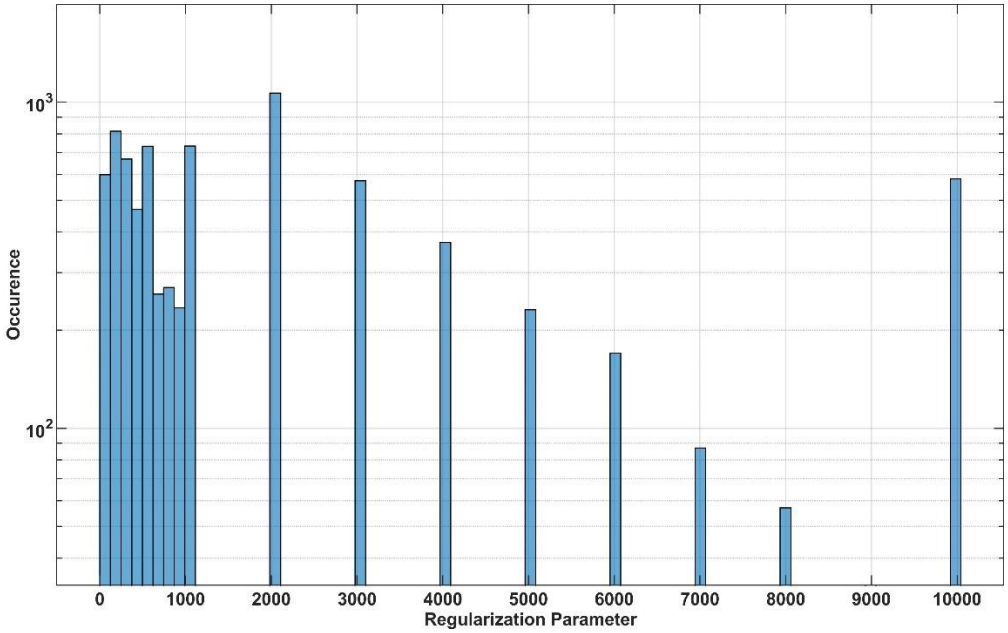

Source: Prepared by the author

Figure 78 - (a) Synthetic Profiles (b) Simulated Profiles – 9% noise

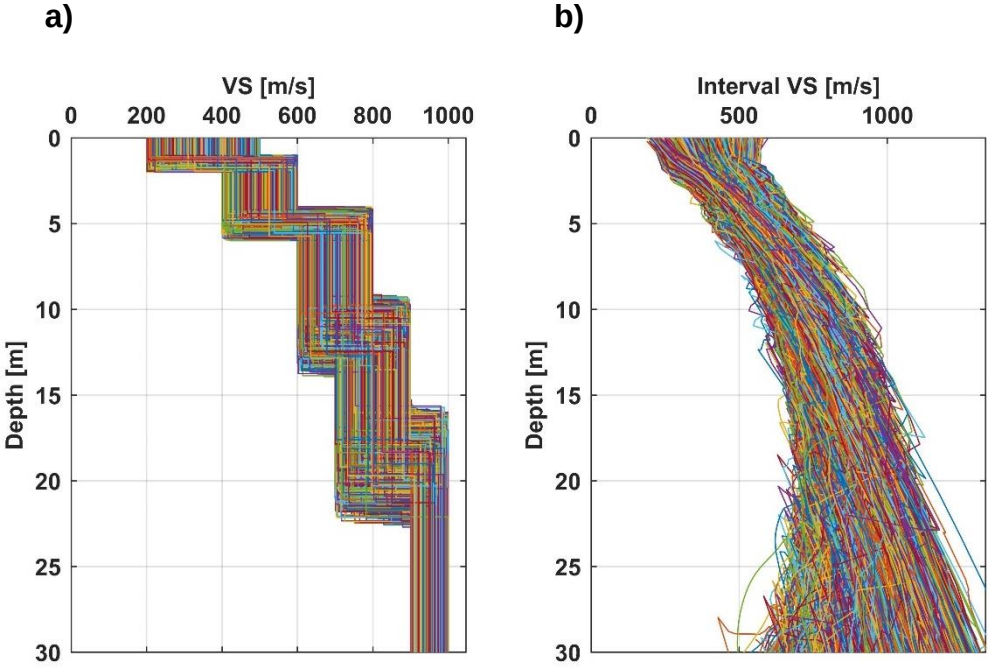

Source: Prepared by the author

4.3.20 Noise Level: 9.5%

When 9.5% noise was applied (Figure 79a and Figure 79b), the optimum regularization parameter was 2000 (Figure 80). The synthetic profiles (Figure 81a) and the estimated interval VS (Figure 81b) had an average error of 9.1%.

Figure 79 - 9.5% noise (a) True and Noisy DC (b) True and Noisy f-k

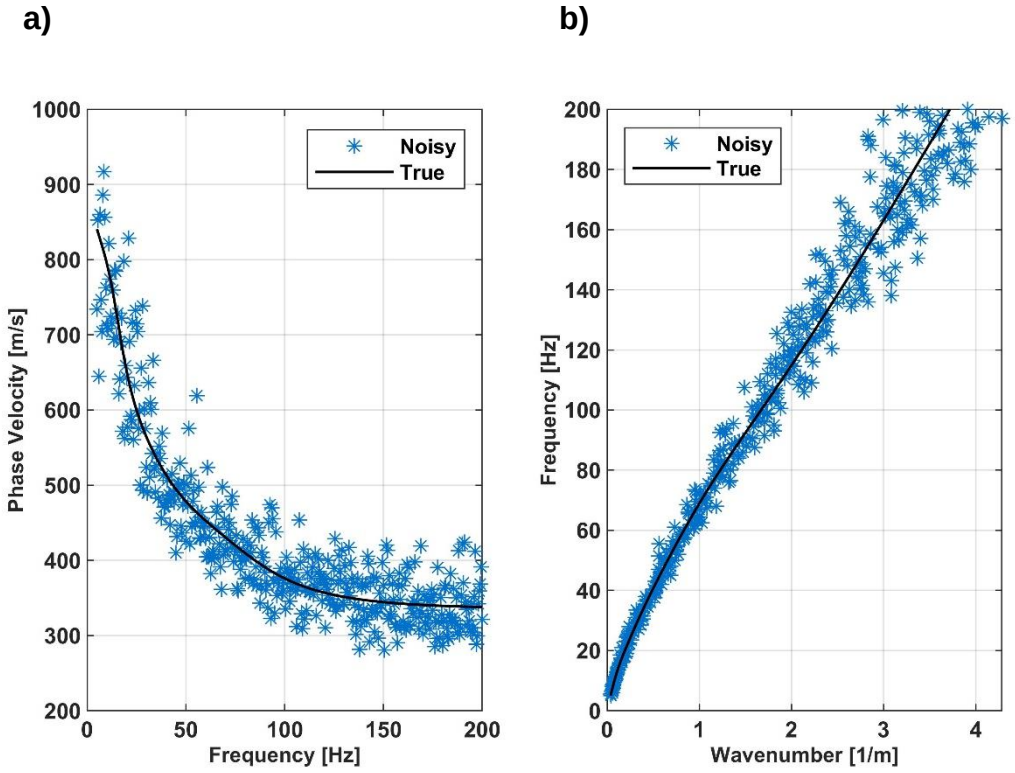

Source: Prepared by the author

Figure 80 – Distribution of α – 9.5% noise

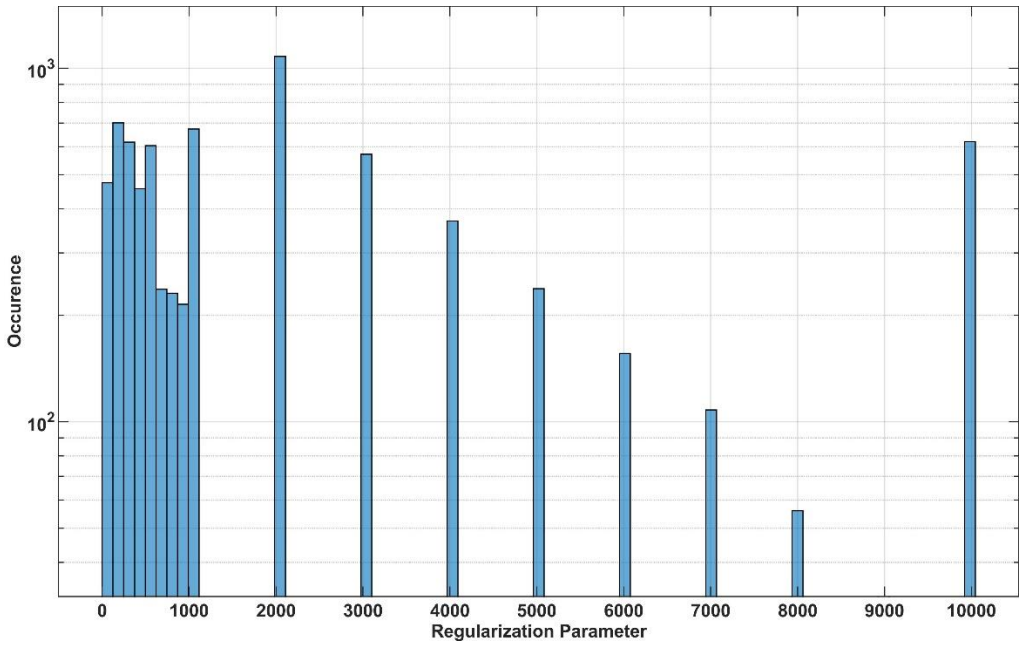

Source: Prepared by the author

Figure 81 - (a) Synthetic Profiles (b) Simulated Profiles – 9.5% noise

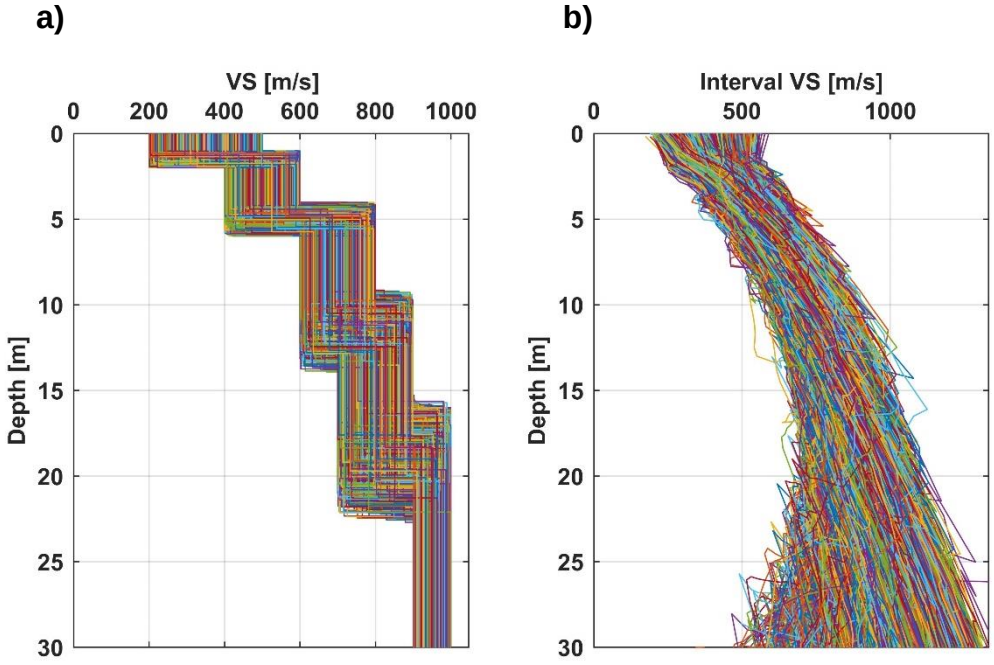

Source: Prepared by the author

4.3.21 Noise Level: 10%

When 10% noise (Figure 82a and Figure 82b) was applied, the optimum regularization parameter was still 2000 (Figure 83). The synthetic profiles (Figure 84a) and the estimated interval VS (Figure 84b) had an average error of 9.2%.

Figure 82 - 10% noise (a) True and Noisy DC (b) True and Noisy f-k

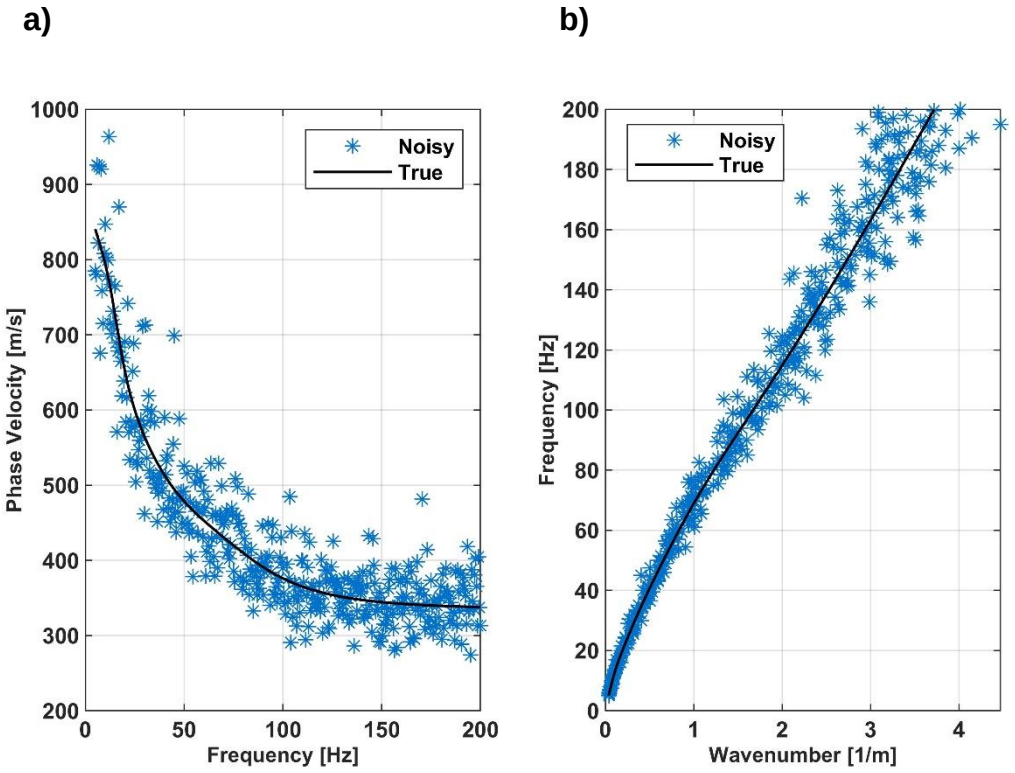

Source: Prepared by the author

Figure 83 - Distribution of α – 10% noise

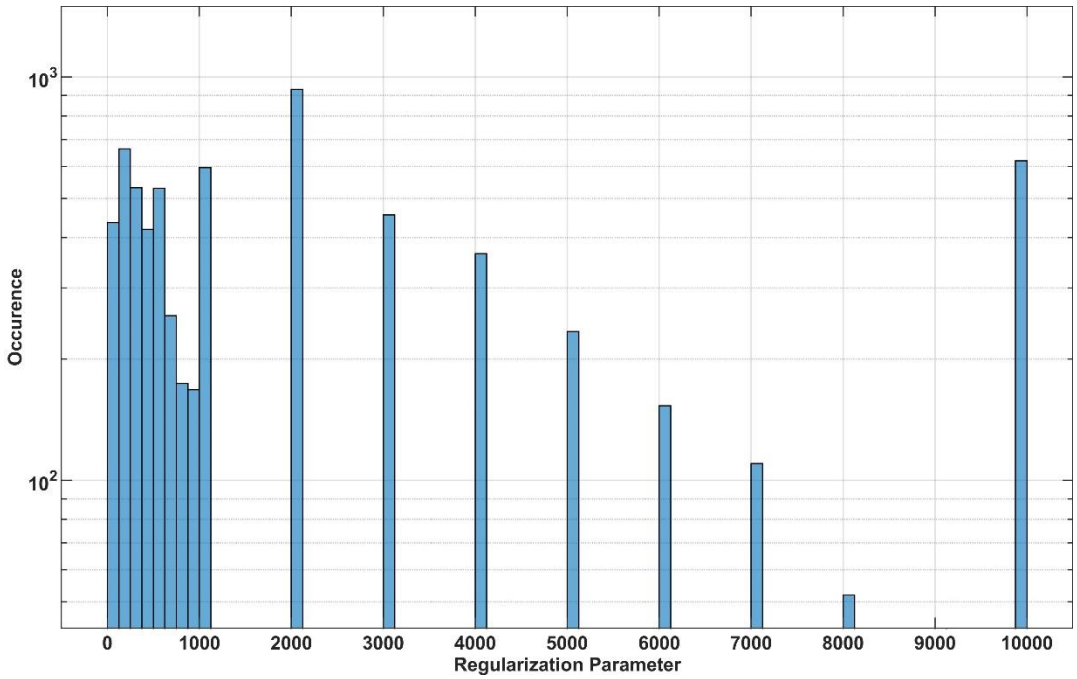

Source: Prepared by the author

Figure 84 - (a) Synthetic Profiles (b) Simulated Profiles – 10% noise

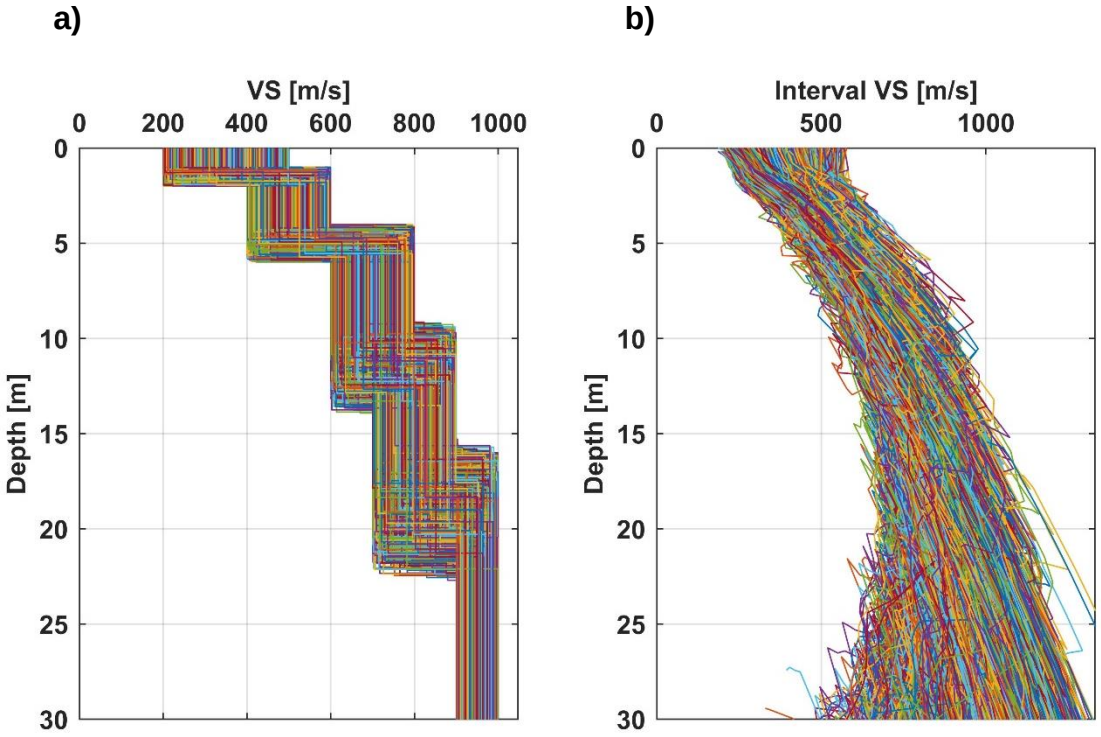

Source: Prepared by the author

4.3.22 The relationship between α and the noise level

After finishing the simulation, the optimum regularization parameters were plotted as a function of the noise level (Figure 85).

Figure 85 – Regularization Parameter vs Noise Level

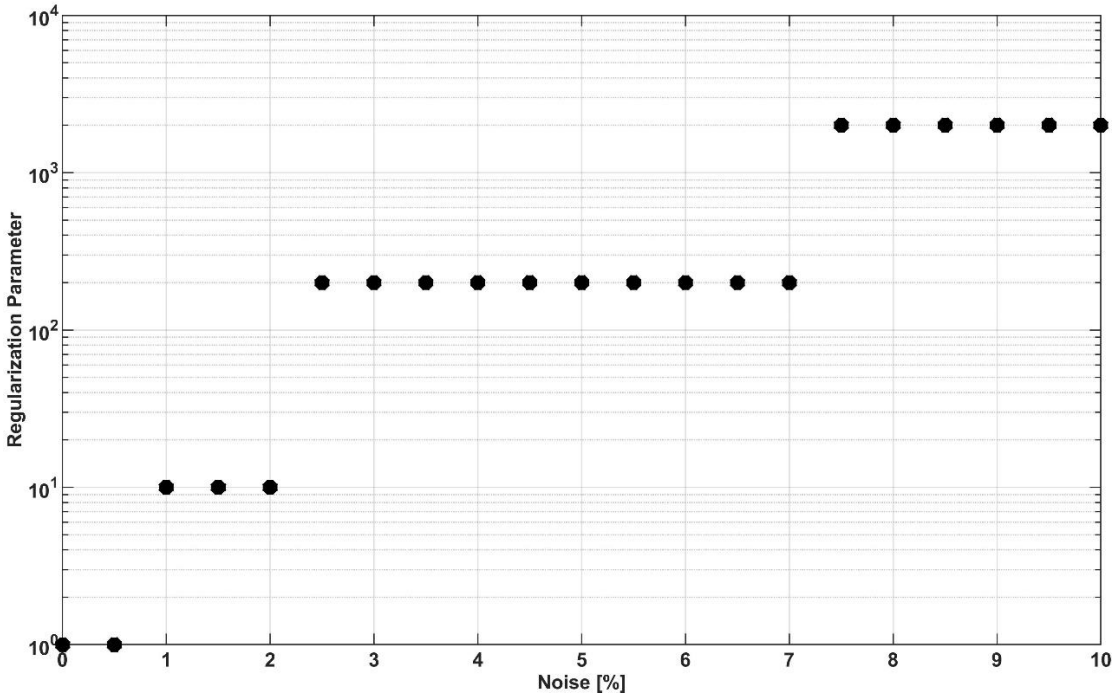

Source: Prepared by the author

The overall trend appointed four distinct values of α, increasing as the noise increases. For each one of them, considering a constant noise level for comparison, the derivative trend has a distinct intensity of smoothness.

For α=1 (Figure 86), although the regularized trend oscillates as much as the not regularized, its overall trend has been damped, with no sharp edges.

Figure 86 – α=1: True, regularized and not regularized derivative trendlines

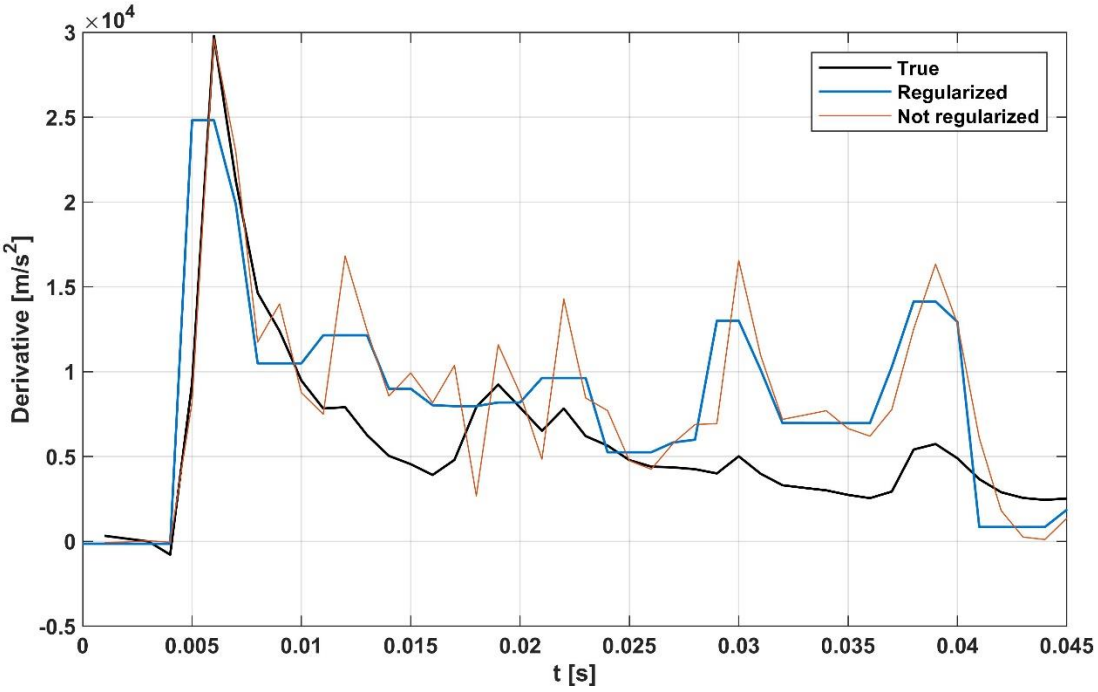

Source: Prepared by the author

For α=10 (Figure 87), as expected, the regularized trendline oscillates less than for α=1, approximating its trend to the true one.

Figure 87 - α=10: True, regularized and not regularized derivative trendlines

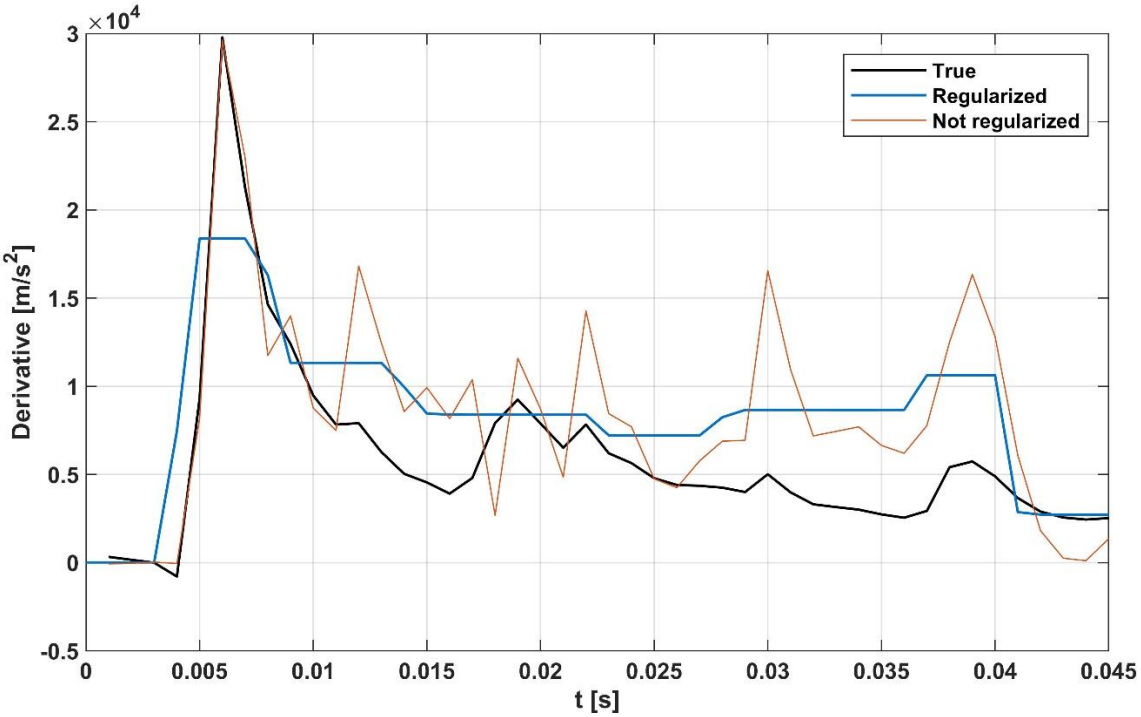

Source: Prepared by the author

For α=200 (Figure 88), the regularized trendline oscillates way less than for α=10, with little oscillation along the time.

Figure 88 - α=200: True, regularized and not regularized derivative trendlines

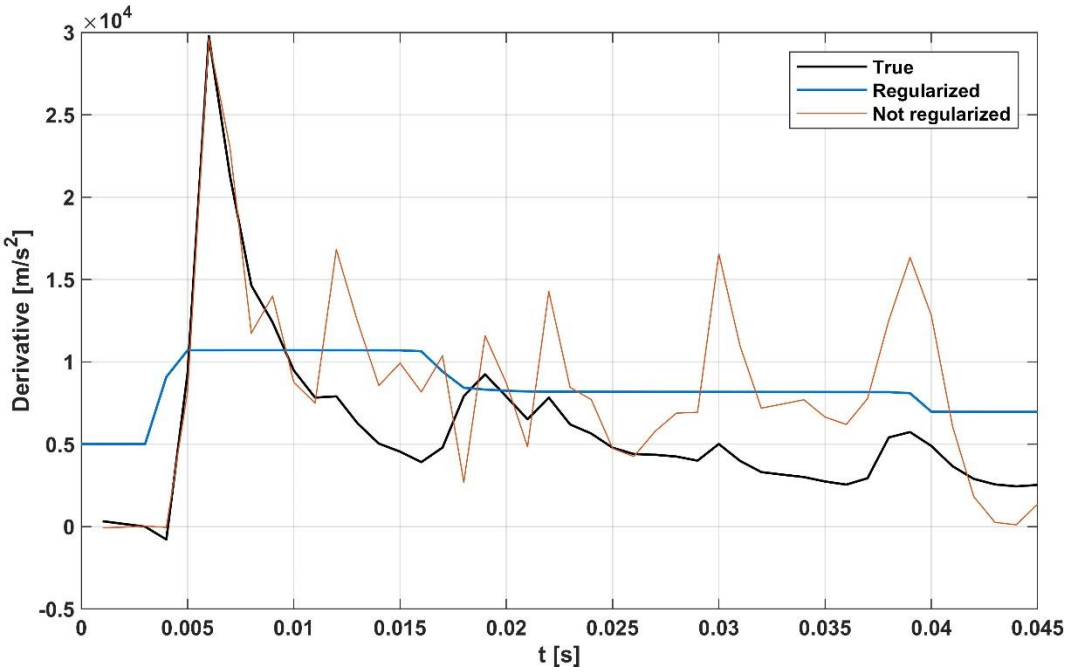

Source: Prepared by the author

For α=2000 (Figure 89), the regularized trendline becomes completely flat.

Figure 89 - α=2000: True, regularized and not regularized derivative trendlines

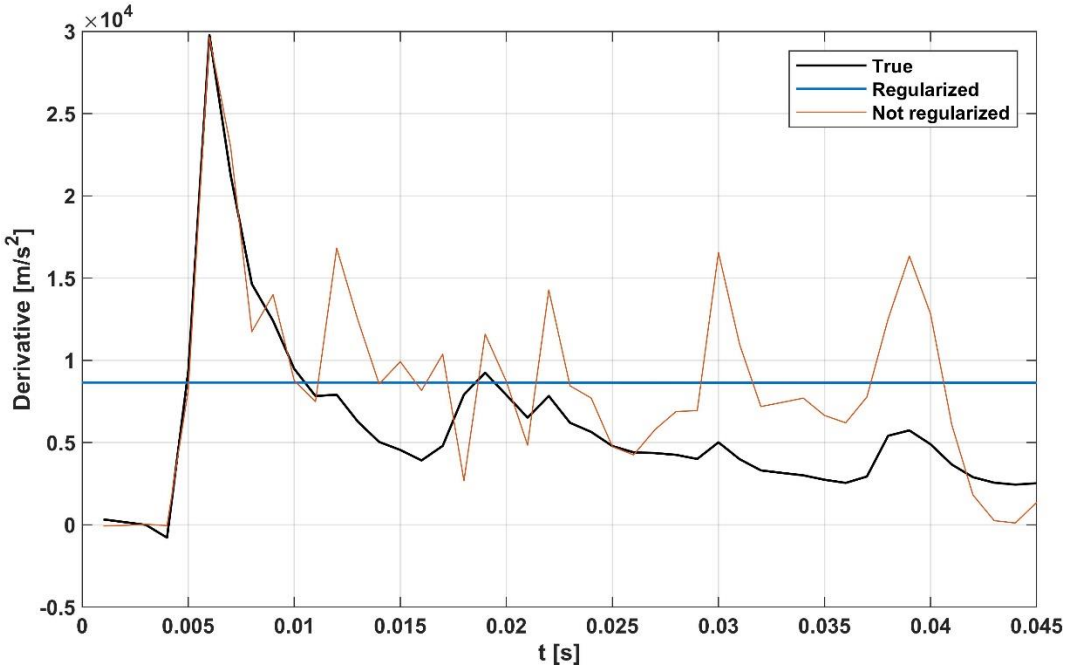

Source: Prepared by the author

5 DISCUSSION

Such approach was possible due to the fact that the initial data was well known – synthetic profiles were perturbated with a certain level of noise in order to generate field-like data. We were careful to add the disturbance in the f-k domain, in order to approximate the process as much as possible to an actual workflow with real data, where the process begin with the f-k analysis of acquired seismograms.

We were able to avoid the inversion procedure by adopting the W/D method, a vanguard process that establishes a direct correlation between wavelength and depth. Although it can be applied without inversion, at least one reference VS or Vsz profile must be known a priori in order to calculate the W/D relationship, to be later used in all the remaining DCs to assess the equivalent time-average velocity in sites with no strong lateral variations.

In this project there was no necessity to evaluate if the W/D attained was suitable or not for that specific profile, due to sharp lateral variations, because a new one was calculated at each loop, using its own synthetic VS, not being applied for other loops to estimate their time-average velocity, justifying the absence of a clustering method to group the DCs.

Even though many profiles were removed from the dataset it is important to highlight the expressive number of profiles successfully converted in interval VS 1D models, assuring a representative number of profiles in which the final result was based on. In fact, a significant number of profiles was essential to ensure that random outliers would not spoil the results.

The best regularization parameter was given by the minimum average error down to the settled investigation depth for each profile down to a certain investigation depth. The profiles were disturbed in different levels, and for each noise level the best α with the highest frequency was considered the optimum value for that noise level, being then applied to all profiles to estimate the interval VS.

When the regularization parameter increases, the derivative trendline becomes too flatten, not following the true derivative movement, over-regularizing it, approximating the estimated VS interval to the time-average velocity, causing the layers resolution to fade away. Even though this is not the ideal scenario, in the distribution plots, for the lowest noise levels, we observe that for a few profiles the chosen α was the maximum one – but due to the high number of models those outliers did not mask the outcome.

Even though high α values did not affect the whole group for low noise levels, as the noise increased, they became more recurrent. In addition to that, we also notice the general trend of optimum values switching up to higher values with the disturbance of the data. As the noise intensity increases, the expected optimum regularization parameter also tends to increase and as it increases, the smoothness of the derivative boosts dramatically, compromising the definition of the layers.

The quality of the results did not depend solely on the optimum α chosen; the noise level was a fundamental factor defining the final outcome. As it can be seen in the DCs, the adopted noise levels were in fact very high. Acquired data with that much of disturbance does not generate a good outcome without suppressing part of it before the processing phase.

The ideal scenario would be, undoubtedly, to determine the best regularization parameter for each DC acquired, but that is an impossible task to perform with raw data. The idea of linking the noise level and the regularization parameter could be extrapolated to support the decision making of best value for field data.

6 CONCLUSION

The characterization of the subsurface through surface wave analysis is traditionally given by three stages: data acquisition, extraction of dispersion curves and inversion. Even though such procedure is consolidated, the inversion procedure does not necessarily return an unique solution because the dispersion curve alone does not contain sufficient information to determine a model.

The wavelength-depth on the other hand avoids extensive inversion processes and gives rise to model uniqueness, and despite of being a vanguard method, it has proved itself to be effective not only in this project, but in several applications on synthetic and field data. It is indeed a powerful tool to convert dispersion curve into time average velocity, requiring only a sample of a shear wave velocity corresponding to one of the dispersion curves.

The 1D VS models had been disturbed with different noise levels and for each level total-variation regularization was employed in order to estimate the noisy data derivative (of the time-average velocity with respect to time) that best suited each simulated interval VS in comparison with the original VS model. This procedure, repeated for all profiles in the same noise level, resulted in an optimum regularization, i. e., the regularization parameter that suited the best the highest number of profiles for that noise level.

The optimum regularization parameter when subsequently applied to all noisy profiles presented a great output for lower levels of noise, with good resolution of layers that eventually faded away as the noise increased. For higher noise levels, the disturbance was excessive to generate any reliable result, causing the optimum regularization parameter to increase, over-regularizing the simulated profiles, approximating the overall shape to the time-average trend, and therefore losing the resolution of layers.

REFERENCES

ABBISS, C. P. Shear wave measurements of the elasticity of the ground. **Geotechnique**, [*s. l.*], v. 31, ed. 1, p. 91-104, 1981.

BOIERO, D. **Surface Wave Analysis for Building Shear Wave Velocity Models**. 2009. 244p. Ph.D. Thesis, Politecnico di Torino, Torino, Italy, 2009.

BRAILE L.W. **Seismic Waves and the Slinky**: A Guide for Teachers. Department of Earth, Atmospheric, and Planetary Sciences Purdue University. West Lafayette, IN , Available in: <https://web.ics.purdue.edu/~braile/edumod/slinky/slinky.htm>. Access in: 16/10/2019.

BROWN, L. T.; DIEHL, J. G.; NIGBOR, R. L. A simplified procedure to measure average shear-wave velocity to a depth of 30 meters (VS30). **12 Wcee 2000: 12th World Conference on Earthquake Engineering**: Bulletin of the New Zealand Society for Earthquake Engineering, New Zealand, v. 33, 2000. 12th World Conference on Earthquake Engineering, Auckland, New Zealand, 2000.

CHARTRAND, Rick. Numerical Differentiation of Noisy, Nonsmooth Data. **International Scholarly Research Network**: ISRN Applied Mathematics, Los Alamos, v. 2011, p. 1-11, 2011.

FLORES-MENDEZ, Esteban *et al*. Rayleigh's, Stoneley's, and Scholte's Interface Waves in Elastic Models Using a Boundary Element Method. **Hindawi Publishing Corporation Journal of Applied Mathematics**, [*s. l.*], v. 2012, p. 1-15, 2012.

FOMEL, Sergey. Shaping regularization in geophysical estimation problems. **Geophysics**, United States, v. 72, n. 2, p. R29-R36, 2007.

FOTI, Sebastiano *et al*. Guidelines for the good practice of surface wave analysis: a product of the InterPACIFIC project. **Bulletin of Earthquake Engineering**, Netherlands, v. 16, ed. 6, p. 2367–2420, 2017.

FOTI, Sebastiano et al. Notes on fk analysis of surface waves. **Annali di Geofisica**, Italy, v. 43, n. 6, p. 1199-1209, 2000.

FOTI, Sebastiano. **Multistation Methods for Geotechnical Characterization using Surface Waves**. Advisor: Renato Lancellotta. 2000. 251 p. Thesis (PhD Degree in Geotechnical Engineering) - Politecnico di Torino, Turin, Italy, 2000.

HASKELL, N. A. The dispersion of surface waves on multilayered media. **Bulletin of the Seismological Society of America**, [Cambridge, MA]: n.43 , p.17-34. 1953.

KHOSRO ANJOM, F. *et al*. Application of a method to determine S and P wave velocities from surface waves data analysis in presence of sharp lateral variations. **GNGTS 2017 Conference Paper**, Italy, v. 36, p. 632-635, 2017. Intervento presentato al convegno 36th GNGTS national convention, 2017.

KHOSRO ANJOM, F. et al. Full Waveform Matching Of Vp And Vs Models From Surface Waves. **Geophysical Journal International**, n.218, p.1873–1891, June 21st 2019.

MARASCHINI M., 2008. **A new approach for the inversion of Rayleigh and Scholte waves in site characterization**, PhD thesis, Politecnico di Torino.

NOVOTNY, O. **Seismic Surface Waves**: Lecture notes for post-graduate studies Salvador, BA ,Universidade Federal da Bahia Centro de pesquisa em geofísica e geologia, 1999.

ÓLAFSDÓTTIR, Elín Ásta. **Multichannel Analysis of Surface Waves**: Methods for dispersion analysis of surface wave data. Reykjavik, Iceland: University of Iceland, 2014. 76 p.

OLDENBURG, D. W.; LI, Y. **Inversion for Applied Geophysics**: A Tutorial. Near Surface Geophysics, [*s. l.*], n. 13, p. 1-86, 2005.

OROZCO, M.C. **Inversion Method for Spectral Analysis of Surface Waves (SASW)**. 2003. 311 p. Thesis (Degree Doctor of Philosophy in Civil and Environmental

Engineering) - Georgia Institute of Technology, Georgia, United States, 2003. Disponível em: https://smartech.gatech.edu/bitstream/handle/1853/5124/OROZCO_MARIA_C_200405_phd.pdf. Acesso em: 18 set. 2019.

RICHART, F.E.; HALL, J.R.; WOODS, R.D. Wave Propagation in an Elastic, Homogeneous, Isotropic Medium. *In*: RICHART, F.E.; HALL, J.R.; WOODS, R.D. **Vibrations of Soils and Foundation**: PRENTICE-HALL INTERNATIONAL SERIES IN THEORETICAL AND APPLIED MECHANICS. [*S. l.*: *s. n.*], 1970. cap. 3, p. 60-80.

RUDIN, L.; OSHER, S.; FATEMI, E. Nonlinear total variation based noise removal algorithms. **Physica D**, Netherlands, v. 60, p. 259-268, 1992.

RYDEN, Nils; PARK, Choon Byong. Fast simulated annealing inversion of surface waves on pavement using phase-velocity spectra. **GEOPHYSICS**, United States, v. 71, n. 4, p. R49–R58, 2007.

SOCCO, L. V.; COMINA, C.; ANJOM, F. K. Time-average velocity estimation through surface-wave analysis: Part 1 — S-wave velocity. **GEOPHYSICS**, United States, v. 82, n. 3, p. U49–U59, 2017.

SOCCO, L. V.; COMINA, C.; ANJOM, F. K. Time-average velocity estimation through surface-wave analysis: Part 2 — S-wave velocity. **GEOPHYSICS**, United States, v. 82, n. 3, p. U61–U73, 2017.

SOCCO, L. V.; MABYALAH, G. Robust static estimation from surface wave data. **SEG Technical Program Expanded Abstracts 2015**, New Orleans, p. 5222-5227, 2015. Society of Exploration Geophysicists New Orleans Annual Meeting, 2015, New Orleans.

SOCCO, L.V. ; BOIERO, D. Improved Monte Carlo Inversion of Surface Wave Data. **European Association of Geoscientists & Engineers, Geophysical Prospecting**, Torino, Italy, n.56, p.357-371 , 2008.

SOCCO, L.V.; COMINA, C. Approximate Direct Estimate of S-wave Velocity Model from Surface Wave Dispersion Curves. **Near Surface Geoscience**: European Association of Geoscientists and Engineers, Turin, Italy, p. 6-10, 2015. Near Surface Geoscience 2015 - 21st European Meeting of Environmental and Engineering Geophysics.

SOCCO, L.V.; STROBBIA, C. Surface-wave method for near-surface characterization: a tutorial. **European Association of Geoscientists & Engineers**: Near Surface Geophysics, Torino, Italy, v. 2, p. 165-185, 2004.

SOCCO, Laura Valentina; BOIERO, Daniele. Improved Monte Carlo inversion of surface wave data. **Geophysical Prospecting**: European Association of Geoscientists & Engineers, [*s. l.*], v. 56, p. 357–371, 2008.

STRUTT, J. On Waves propagated along the Plane Surface of an Elastic Solid. **Scientific Papers Cambridge Library Collection - Mathematics**, Cambridge, p. 441-447, 2009.

WANG, Q. Propagation of a Shear Direction Acoustic Wave in Piezoelectric Coupled Cylinders. **Journal of Applied Mechanics**, New York, v. 69, p. 391-400, 2002.

Universidade de São Paulo

Engenharia de Petróleo – Escola Politécnica

Número USP: 9017186 **Data: 31/10/2019**

Optimized Regularization of Interval S-Wave Velocity Estimation from Seismic Surface Wave Data

Ana Paula Gomes

Orientador: Prof. Dra. Laura Valentina Socco

Supervisor: Prof. Dr. Cleyton de Carvalho Carneiro

Artigo Sumário referente à disciplina PMI3349 – Trabalho de Conclusão de Curso da Engenharia de Petróleo II
Este artigo foi preparado como requisito para completar o curso de Engenharia de Petróleo na Escola Politécnica da USP. Template versão 2018v11.

Resumo

As ondas de superfície podem ser usadas para estimar modelos superficiais de velocidade de ondas de cisalhamento explorando sua natureza dispersiva: as curvas de dispersão locais (DCs, do inglês dispersion curves) estão sujeitas a uma dependência significativa da velocidade média quadrática ou de empilhamento Vsz. A relação entre o comprimento de onda da onda de superfície e a profundidade de investigação é usada para transformar diretamente DCs em Vsz, evitando o procedimento de inversão. Essa técnica, conhecida como método W/D, foi recentemente introduzida, mas a estimativa da velocidade intervalar de onda S (VS, do inglês shear-wave velocity) a partir de Vsz experimental, com ruídos de aquisição, usando uma equação do tipo DIX requer regularização dos dados. Um código MATLAB bem estruturado foi desenvolvido para simular VS em perfis sob diferentes níveis de ruído para testar e comparar o parâmetro de regularização que melhor se ajusta ao perfil de VS simulado com seu perfil original, na tentativa de correlacionar níveis de ruído e parâmetro de regularização.

Palavras-chave: Ondas de superfície, método W/D, parâmetro de regularização

Abstract

Surface waves can be used to estimate near-surface shear wave velocity (VS) models exploiting their dispersive nature: local dispersion curves (DCs) are subjected to a significant dependency to time-average velocity (Vsz) and the relationship between the wavelength of surface waves and the investigation depth is used to directly transform DCs into Vsz, avoiding the inversion procedure. Such technique, known as W/D method, has been recently introduced but the estimation of the interval VS from noisy Vsz using a DIX-type equation requires regularization of the data. A well-structured MATLAB code was developed to simulate the interval VS under different noise levels to test and compare the regularization parameter that best fits the simulated VS with its original profile, in an attempt to correlate noise levels and regularization parameter.

Keywords: Surface Waves, W/D method, Regularization Parameter

1. Introduction

In surface wave methods, after the acquisition phase, the data is processed to extract the dispersion curve and usually inverted to obtain the velocity model. The inversion process, however, does not ensure an unique solution, due to the fact that many models would fit the data to the same degree. The wavelength-depth (W/D) method is a new technique, first launched by Socco at al. (2015), that has been introduced recently for static corrections and time-average velocities estimation, avoiding extensive inversion processes by evaluating the time-average VS through simple data transform.

In addition, Khosro Anjom et al. (2019) developed a method to transform the estimated Vsz to interval VS using a DIX-type equation and imposing regularization - such approach is necessary because of the noisy invariably present in the input data. Therefore, it is essential to optimize the regularization parameter, a component that determines the regularization intensity, which, in this case, have not been fixed and depends on the noise level. Acting as a tradeoff, this parameter will control how much the noise will be smoothed: the higher the noise, the higher the parameter is expected to be.

To define what would be ideal value of the regularization parameter, at a certain noise level, a set of parameters is tested on synthetic data, and the simulated shear wave velocity (VS) compared with the equivalent synthetic profile to determine the parameter that fits the best; at the end, after repeating it for a considerable number of synthetic profiles disturbed at a certain degree, the parameter with the highest occurrence is taken as the optimum value for that noise level.

In this study, we adopt the W/D and the Total-Variation Regularization methods (KHOSRO ANJOM et al., 2019) instead of the classic inversion, in order to estimate a relationship between the noise level and the regularization parameter. A stochastic approach has been adopted with the purpose to generate 1D VS synthetic profiles, in which different levels of noise are added to the dispersion curves.

2. Background

2.1. Main types of elastic waves and their properties

Body waves and surface waves are two varieties of mechanical waves: the first travels through the earth's interior, while the second travels along the free-surface. Body waves are known as shear waves (S-waves) and compressional waves (P-waves) while Rayleigh and Love waves are the main types of surface waves.

Rayleigh waves propagate close to the surface, affecting a limited depth depending on the wavelength (SOCCO and STROBIA, 2004). Considering a point source, a high percentage of the radiated energy is transmitted as Rayleigh waves, making them prevalent in traces recorded on the surface. This makes the surface wave methods a powerful tool for near-surface characterization.

In heterogenous media Rayleigh waves become dispersive, which means that different phase velocities correspond to different frequencies or wavelengths, allowing Rayleigh waves to be used to study the medium in where they propagate. A dispersion curve depicts the distribution of phase velocities as a function of frequency or wavelength.

2.2. Wavelength-depth method

The wavelength to depth (W/D) method was first launched by Socco at al. (2015) as a method to calculate approximately time-average S-wave velocity (Vsz) models at any depth without the need to invert the data: a linear correlation is assessed to connect depth and wavelength, where Vsz is given by:

$$V_{sz} = \frac{\sum_n h_i}{\sum_n {h_i}/{V_i}}, \quad (1)$$

n is the number of layers below the depth z, hi and Vi are the thickness and the velocity of the ith layer, respectively. It initially requires a known Vsz profile for one of the DCs, which could be estimated through inversion or known from other independent surveys. This single profile is then used as a calibration velocity model for all the other dispersion curves: for each velocity value, the depth from the Vsz model is associated with the wavelength from the phase velocity model, allowing to collect points to develop the W/D relationship. Then, the W/D relationship can be used to transform all DCs to Vsz.

Once the Vsz values are known, it is possible to transform them into interval VS (V) models, through a DIX-type equation - V stands for the continuous local velocity profile. Starting from the Equation 1,

Khosro Anjom at al. (2019) developed a stable approach to transform Vsz into interval velocities (Vt), that led ultimately to the expression:

$$V_t = V_{sz} + t.\frac{dV_{sz}}{dt} \quad (2)$$

where t represents the one-way travel time. Small perturbations in the time-average velocity lead to large relative changes in the derivative estimation (KHOSRO ANJOM at al., 2019). Consequently, the derivative term must be evaluated through a different technique, mainly for noisy data.

2.3. Total-variation regularization

Regularization is an optimization methodology that controls the misfit between real and estimated values, reaching an optimum tradeoff through a term defined as regularization parameter. It was utilized by Chartrand (2011) to differentiate noisy data and it was chosen for this project due to the fact that unlike typical regularizations, it allows for discontinuities in the derivative, not smoothing it excessively while it suppresses the noise. The derivative is approximated by the solution u of the minimization of the following function (Equation 3):

$$F(u) = \alpha \int_0^T |u(t)'|dt + 0.5 \int_0^T |Au(t) - V_z(t)|^2 dt, \quad (3)$$

where $Au(t)$ defines the smoothed V_z and α is the regularization parameter, the terms controlling the balance between the two terms: the total variation of the first derivative u and the second term, which aims to minimize the distance between the smoothed and the input function, as a desirable balance between damping the oscillations while adjusting to the data.

3. Method

In forward modelling the theoretical DCs can be computed from 1D layered VS profiles, according to the method and MATLAB routine provided by Marashini (2008), for a fixed frequency band, using essential model parameters for each layer: thickness, density, Poisson's ratio. The adopted frequency band for this project was from 5 to 200 Hz.

In order to make the synthetic case realistic, it is necessary to disturb the data. DCs are transformed into f-k domain where random normal noise is added to the wavenumber, where the mean parameter is k and the standard deviation is proportional to the noise intensity.

The next step consists in assessing the W/D relationship, estimated using the true Vsz and noise-free DC, which is absolutely fundamental for this process in order to evaluate the noisy Vsz without the necessity to perform an inversion.

For the interval velocity estimation, Total-Variation Regularization is the chosen tool, since it provides a good approximation, avoiding too excessive smoothing, allowing for discontinuities. The MATLAB routine used to calculate the derivative was provided by Chartrand (2011). Through the regularization term a certain error threshold can be achieved, being the error given by:

$$\text{Error} = \frac{\sum \frac{|VS - VS\_est|}{VS}}{number\ of\ points}, \quad (4)$$

where VS is the real velocity at a certain depth and VS_est is the estimated VS, for a certain regularization parameter (α), at the same depth. Therefore, the α is directly linked with the fitting quality of the VS estimation, which means that for the minimum attainable error value, the correspondent α will be taken as the optimum one.

A code to search the optimum α was implemented in MATLAB, and for each profile, the best α value is retrieved. For a specific noise level, the program finds the α that best optimizes the interval VS for each VS profile generated. The α value with the highest occurrence is recorded as the best α that optimizes the interval VS estimation for that specific noise level. This procedure is repeated for different noise levels, from 0 to 10% in steps of 0.5%, and for each stage, the optimum α recorded. The α values were discretized in a logarithmic scale, from 1 to 10,000.

4. Results

The adopted dataset (Figure 2a) is composed by 10,000 1D VS models, generated with a stochastic approach based on a Monte Carlo procedure. Each single model was assumed to have 4 layers with constant mass density, being the 5th layer limited by an investigation depth, set at a depth of 30m. Table 1 summarizes the model parameters and their maximum and minimum adopted values.

Table 1 - Properties of the synthetic dataset: thickness, S-wave velocities, Poisson's ratio and mass density

		VS [m/s]		Thickness [m]		Poisson's Ratio		Mass Density
		min	max	min	max	min	max	[kg/m^3]
Layer	1	200	500	1	2	0.2	0.4	1800
	2	400	600	3	4			
	3	600	800	5	8			
	4	700	900	6	9			
	5	900	1000	n/a				

After running the simulation to evaluate the optimum α for each noise level, the correlation between them (Figure 1) was assessed. Such values were then applied to all profiles disturbed by the equivalent noise level. Table 2 summarizes the average error for some noise levels.

Table 2 - Average error generated at a certain noise level by adopting the optimum α

Noise [%]	Optimum α	Average error [%]
0	1	2.2
1	10	4.8
3	200	6.4
7.5	2000	8.5
10	2000	9.2

Regarding the resolution of the layers, the simulated profiles for no noise (Figure 2b) depicted the synthetic data impressively, for 1% noise (Figure 2c) the resolution is also excellent, with 3% noise (Figure 2d) only the shallow layers were successfully simulated, and for 7.5% noise (Figure 2e) and 10% noise (Figure 2f), the profiles were over-regularized, with no layers definition.

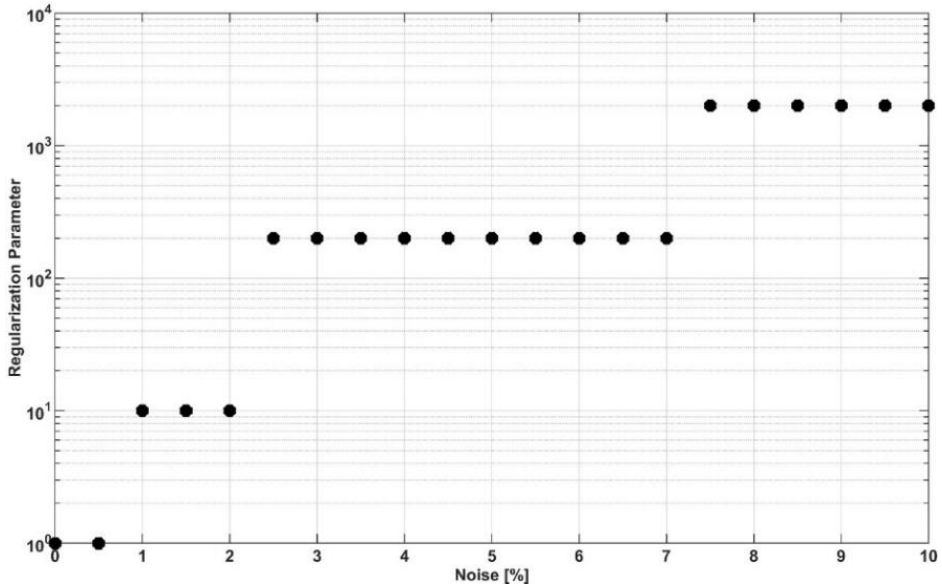

Figure 1 - Regularization Parameter vs Noise Level, prepared by the author.

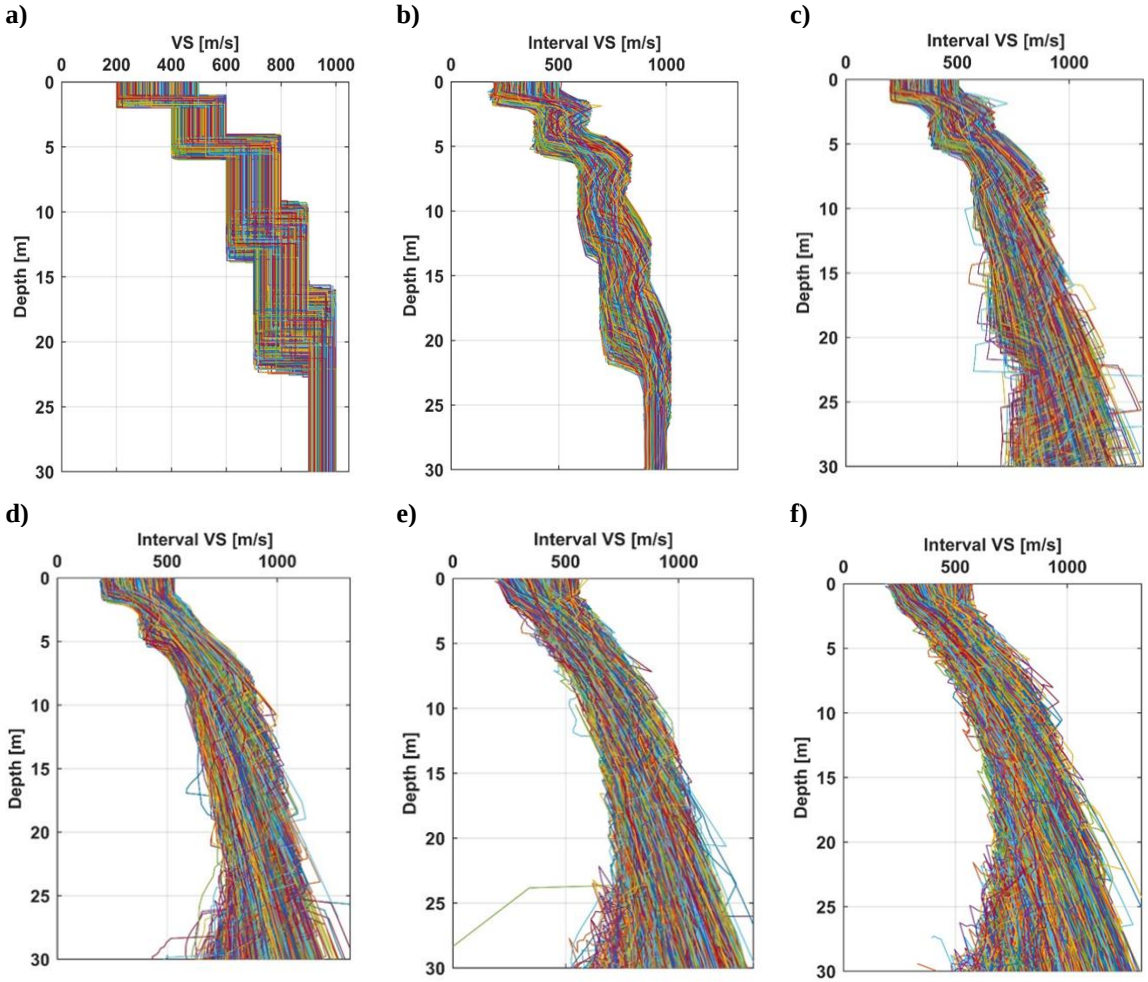

Figure 2 – (a) Synthetic profiles (b) Simulated profiles – no noise (c) Simulated profiles – 1% noise (d) Simulated profiles –3% noise (e) Simulated profiles –7.5% noise (f) Simulated profiles – 10% noise, prepared by the author.

5. Discussion

When the regularization parameter increases, the derivative trendline becomes too flatten, not following the true derivative movement, over-regularizing it, approximating the estimated VS interval to the time-average velocity, causing the layers resolution to fade away. Even though this is not the ideal scenario, in the distribution plots, for the lowest noise levels, we observe that for a few profiles the chosen α was the maximum one – but due to the high number of models those outliers did not mask the outcome.

Even though high α values did not affect the whole group for low noise levels, as the noise increased they became more recurrent. In addition to that, we also notice the general trend of optimum values switching up to higher values with the disturbance of the data. As the noise intensity increases, the expected optimum regularization parameter also tends to increase and as it increases, the smoothness of the derivative boosts dramatically, compromising the definition of the layers.

The quality of the results did not depend solely on the optimum α chosen, the noise level was a fundamental factor defining the final outcome: the adopted noise levels were in fact very high. Acquired data with that much of disturbance does not generate a good outcome without suppressing part of it before the processing phase.

The ideal scenario would be, undoubtedly, to determine the best regularization parameter for each DC acquired, but that is an impossible task to perform with raw data. The idea of linking the noise level and the regularization parameter could be extrapolated to support the decision making of best value for field data.

6. Conclusion

The 1D VS models had been disturbed with different noise levels and for each level total-variation regularization was employed in order to estimate the noisy data derivative (of the time-average velocity with respect to time) that best suited each simulated interval VS in comparison with the original VS model. This procedure, repeated for all profiles in the same noise level, resulted in an optimum regularization, i. e., the regularization parameter that suited the best the highest number of profiles for that noise level.

The optimum regularization parameter when subsequently applied to all noisy profiles presented a great output for lower levels of noise, with good resolution of layers that eventually faded away as the noise increased. For higher noise levels, the disturbance was excessive to generate any reliable result, causing the optimum regularization parameter to increase, over-regularizing the simulated profiles, approximating the overall shape to the time-average trend, and therefore losing the resolution of layers.

7. References

CHARTRAND, Rick. Numerical Differentiation of Noisy, Nonsmooth Data. **International Scholarly Research Network**: ISRN Applied Mathematics, Los Alamos, v. 2011, p. 1-11, 2011.

KHOSRO ANJOM, F. et al. Full Waveform Matching Of Vp And Vs Models From Surface Waves. **Geophysical Journal International**, n.218, p.1873–1891, June 21st 2019.

MARASCHINI M., 2008. **A new approach for the inversion of Rayleigh and Scholte waves in site characterization**, PhD thesis, Politecnico di Torino.

SOCCO, L.V.; COMINA, C. Approximate Direct Estimate of S-wave Velocity Model from Surface Wave Dispersion Curves. **Near Surface Geoscience**: European Association of Geoscientists and Engineers, Turin, Italy, p. 6-10, 2015. Near Surface Geoscience 2015 - 21st European Meeting of Environmental and Engineering Geophysics.

SOCCO, L.V.; STROBBIA, C. Surface-wave method for near-surface characterization: a tutorial. **European Association of Geoscientists & Engineers**: Near Surface Geophysics, Torino, Italy, v. 2, p. 165-185, 2004.